Precision Control of Cylindrical Stamp Contact in a Continuous Roll-to-Roll Microcontact Printing Machine

by

Adam M. Libert

B.S.E. Mechanical Engineering and Applied Mechanics
University of Pennsylvania, 2012

Submitted to the Department of Mechanical Engineering
in Partial Fulfillment of the Requirements for the Degree of
Master of Science in Mechanical Engineering

at the

Massachusetts Institute of Technology

June 2014

Signature redacted

Signature of Author.....
Department of Mechanical Engineering
May 20, 2014

Signature redacted

Certified by.....
David E. Hardt
Ralph E. and Eloise F. Cross Professor of Mechanical Engineering
Thesis Supervisor

Signature redacted

Accepted by.....
David E. Hardt
Ralph E. and Eloise F. Cross Professor of Mechanical Engineering
Graduate Officer

Precision Control of Cylindrical Stamp Contact in a
Continuous Roll-to-Roll Microcontact Printing Machine

by

Adam M. Libert

Submitted to the Department of Mechanical Engineering
on May 20, 2014, in Partial Fulfillment of the
Requirements for the Degree of Master of Science in
Mechanical Engineering

ABSTRACT

Microcontact printing is a form of soft lithography that uses a molded elastomeric stamp to print patterns with micron and sub-micron scale features. This is an effective low-cost technique for replicating master patterns onto substrates. However, the traditional embodiment of using a planar stamp with a planar substrate is limited in both scale and speed. In order to achieve higher production rates, the lab scale plate-to-plate microcontact printing method must be developed into a roll-based manufacturing process. The marriage of the precision of microcontact printing with the speed of traditional press printing will fill a niche in manufacturing capabilities. Large area, high rate patterning of micron and sub-micron scale features will help to enable the economic manufacturing of a wide range of emerging technologies. Specifically, this continuous microcontact printing process could be used to make flexible displays, thin film photovoltaic cells, transparent conductors, desalination membranes, and other large-scale surface modifications.

This thesis details the development of a precision roll-to-roll microcontact printing machine. This pilot-scale web-handling machine serves as the platform for research on the continuous microcontact printing process. Specific consideration is given to the design of a precision print head that is capable of maintaining consistent contact pressure even while printing at high speeds. As well, a novel camera system is developed to achieve *in-situ* real-time inspection of the contact region between the stamp and the substrate. The visual data from this sensor is used as feedback for the controller, enabling the print head to maintain the desired evenly distributed pressure along the entire stamp width. Results show that the closed-loop control of print contact is able to compensate for eccentricities and disturbances in the system, significantly decreasing variation in print pressure. These tests show promise for the usefulness of this novel process control technique, rather than traditional downstream sensing. As well, this pilot-scale machine succeeds in serving as a platform for continuous roll-to-roll microcontact printing research that will help to guide the scale-up of the process into a high rate manufacturing technique.

Thesis Supervisor: David E. Hardt
Title: Ralph E. and Eloise F. Cross Professor of Mechanical Engineering

ACKNOWLEDGEMENTS

This thesis is dedicated to my grandfather, Mitchell Marcus. A 1941 graduate of MIT, Mitchell proudly sported the Brass Rat for the rest of his life, from when he was working as a young wind tunnel engineer in Dayton, Ohio to many years later when he would take me and my brother to see the Space Shuttle launches in Cape Canaveral. It is undoubtedly to Mitchell that I owe my love and passion for engineering, and it's quite an amazing privilege to be at MIT, studying and working in the very same buildings that he did years ago. I cannot express how grateful I am to him, and to the rest of my family, for encouraging me and supporting me in my journey to be an engineer.

I would like to thank Professor David Hardt, my advisor, who has always willingly shared with me his many years of thoughts and experiences. Whether it's a story about the carpentry of colonial New England, or specific advice on how to decrease the response time of a system with noisy sensor data, conversations with Dave are never without their fare share of fun and education.

MIT is a place where you can learn as much from your peers as you can from your teachers. I would not have been able to complete my thesis without the constant support from the 35-135. It's amazing how much this community knows, not just about engineering, but also about life and love and everything in between. I think no challenge is too great for the teamwork of 135.

Unfortunately, two years is not enough time to fully experience MIT. This school is magical in how much it has to offer. I hope to find more places like it, but either way, I'm sure I'll be back before long.

Finally, this project was funded and supported by the Center for Clean Water and Clean Energy, a joint program between MIT and KFUPM. It is my hope that this research will serve as building block on the way a future with cleaner energy.

CONTENTS

Table of Contents

FIGURES

CHAPTER 1

INTRODUCTION

Microcontact printing was developed in the early 90's by Whitesides and Kumar at Harvard University [1]. In this embodiment of the process, polydimethylsiloxane (PDMS) resin is poured over a master template wafer that was patterned using a conventional lithographic process. The cured PDMS stamp is peeled back from the master and inked with alkanethiols. The inked stamp is brought into contact with a gold film substrate, and the alkanethiols transfer to the substrate where contact is made, in a pattern replicate of the master wafer template. These alkanethiols form a self-assembling monolayer (SAM) on the surface of the gold film, which is then used as a resist in a wet etching process. This process was able to reproduce patterns with features as small as 1 μm, and within a year of these results, Whitesides was able to pattern features down to 200 nm in size [2], though with limited quality. The process was further developed by Biebuyck et al. to reliably cast and print geometry with features below 100 nm [3]. A review of microcontact printing achievements and limitations is available [4], [5].

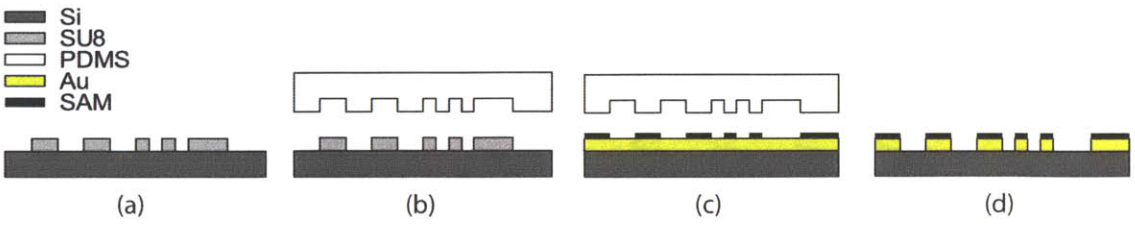

Figure 1.1: Traditional plate-to-plate microcontact printing process: (a) A master template is formed with conventional lithographic techniques. Typically, this is formed as a pattern of SU8 photoresist on a silicon wafer. (b) PDMS resin is cast poured onto the master template. Once cured, it is peeled from the template and shown to have reproduced the template's features. (c) The PDMS stamp is inked with alkanethiols, and brought into contact momentarily with a gold-coated wafer substrate. These molecules diffuse onto the gold surface and self-assemble into a monolayer. (d) The SAM acts as a protective mask for when the substrate is etched, leaving just the desired pattern of gold remaining.

1.1 Inks

The purpose of microcontact printing is to reproduce a master pattern on a substrate. A patterned stamp is used to deposit ink onto the substrate where contact is made. Because the printing relies on ink transfer from the stamp to the substrate, the process is highly dependent on characteristics of the stamp, the ink, and the substrate. Compatibility between all three materials is crucial for successful printing.

1.1.1 Molecular Inks

Microcontact printing is most commonly performed with self-assembling monolayer (SAM) inks. A self-assembling monolayer is an organized assembly of molecules that form on a surface via adsorption. These single-molecule-thick layers occur when the organic molecules contain a functional head group that has a particular affinity for the target surface. These head groups cause the molecules to self organize and anchor themselves in a single monolayer thick structured domain on the surface. The head group has an attached molecular chain that forms a tail, with a functional group at the end. These tails also neatly self-organize, protruding from the surface, and the functional groups at their ends can be changed to vary the interfacial properties of the monolayer. The organization of this layer is depicted in Figure 1.2.

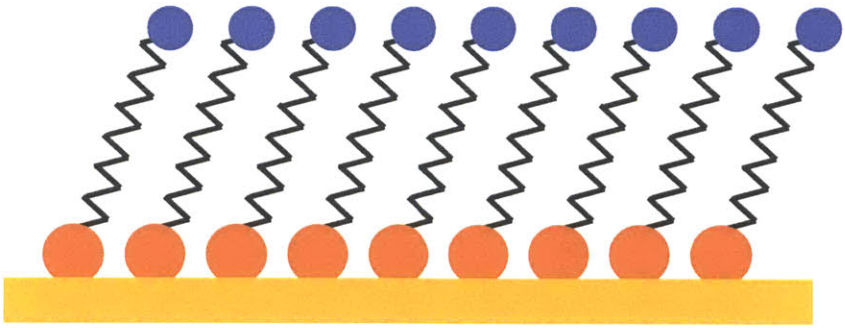

Figure 1.2: Simplistic representation of SAMs on a gold substrate. Typically, alkanethiols are used in microcontact printing, due to the molecule's head group (orange) showing a strong affinity for gold substrates (yellow). The tails (blue) are functionalized for a variety of purposes, but most commonly, they are able to protect the gold substrate from an etching bath, resulting in a selectively etched patterned surface.

Alkanethiols are specific molecules commonly used to form SAMs. When brought into contact with gold substrates, alkanethiols self-organize into a protective monolayer that can be used to protect the gold from wet etchants. Typically, a PDMS stamp is wetted with a solution of alkanethiols in ethanol or other solvent. This stamp is allowed to dry before being brought into contact with the substrate, during which time the alkanethiols transfer via a diffusion process. This means that, in most cases, the alkanethiols are deposited exactly and only where contact is made between the stamp and the substrate. Once the alkanethiols are on the gold surface, they self-assemble into a monolayer within minutes [6].

The alkanethiols have been shown to quickly transfer to the substrate, with good pattern reproduction achieved with a stamp contact time of only 1 ms [7]. This is one of the benefits of using SAMs in microcontact printing, as the short requisite contact time allows for high-speed printing. As well, alkanethiols are a molecular ink that transfers via diffusion; there are no fluid dynamics effects that need to be considered. Finally, because alkanethiols diffuse through PDMS, a saturated stamp may allow for multiple prints before having to be re-inked [8]. For these reasons, alkanethiols have become commonly used in the process of microcontact printing on gold substrates.

There are a variety of other molecules that form SAMs on specific substrates. Geissler et al. demonstrate that eicosanethiols have a similar affinity to alkanethiols for gold, silver, copper, and palladium surfaces [9]. This was used to print metal nanowires on a 1 μm pitch. Lopez and Craighead manufacture surface-relief gratings on a 300 nm pitch via microcontact printing of octadecanethiols onto gold [10]. Delamarche et al. print hexadecanethiols onto copper films in order to achieve a selective etchant mask for TFT LCD gate layers [11]. Jeon and Nuzzo selectively deposit copper onto various substrates using chemical vapor deposition with printed alkylsiloxanes as the SAM mask [12]. These molecules were shown to assemble on substrates of aluminum, silicon, titanium nitride, and their oxides. As well, glasses, indium tin oxide (ITO), and plasma-modified polymide substrates are patterned with the same process. Octadecyltrichlorosilane is shown to assemble on ITO coated glass, which was used in a process to make OLEDs [13]. Hexadecanephosphonic acid [9] and alkanephosphonic [14], [15] acids are shown to form SAMs on aluminum and aluminum oxide surfaces. This is significant because it might allow for the printing of SAMs onto aluminized PET film substrate in the roll-to-roll

microcontact process, rather than having to use alkanethiols on expensive gold film substrate. This aluminum-coated film is made via the physical vapor deposition process, and is commonly used in a variety of industries.

More information on SAMs and their use in microcontact printing can be found in the review paper [16].

1.1.2 Liquid Inks

Microcontact printing is also used to print liquid inks. In the field of printed electronics, conductive substrates with printed SAM masks are selectively etched to form the desired conductive traces. Instead, conductive liquid inks are directly printed onto non-conductive substrates in the desired trace pattern, as shown in Figure 1.3. In the printed electronics industry, PET films have emerged as common substrates due to their low cost, high clarity, and ease of handling. The use of liquid inks allows for numerous other materials to be used as substrates in the microcontact printing process. Kaufmann and Ravoo provide a review of the use of polymer inks in microcontact printing, as well as a review of the use of polymer substrates in microcontact printing [17].

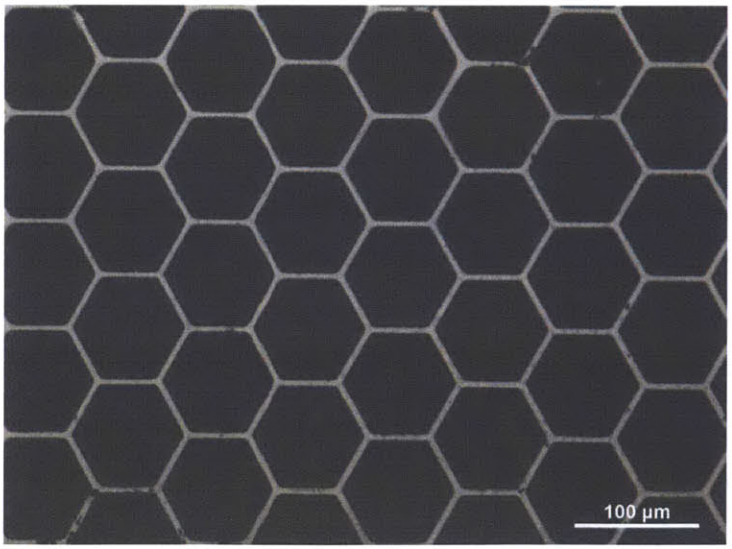

Figure 1.3: Hale's microcontact printing of liquid ink onto polymer substrate [18]. A PDMS stamp was used to transfer Cabot CSD-66 silver nanoparticle ink to a cyclic olefin copolymer substrate. The lines that form the hexagons are approximately 5 µm in width. Such a pattern is discussed in the literature for its properties as a conductive grid with a high percentage of optical transmission, potentially useful in photovoltaic cells.

Due to the fluid dynamics involved, the process of printing liquid inks with PDMS stamps is neither as well understood nor as robust as the SAM printing process. There are many more factors that come into play, such as the surface energies of the stamp and the substrate, the composition of the ink, the inking technique, the geometry of the features, etc. The variables and sensitivities of the liquid ink transfer process are studied in Hale's thesis work [18]. Some of the printed results are shown in Figure 1.3 and Figure 1.4. With a robust model for ink transfer at the micron scale, the direct printing of conductive patterns on polymer substrates could be scaled up into a high-rate manufacturing process.

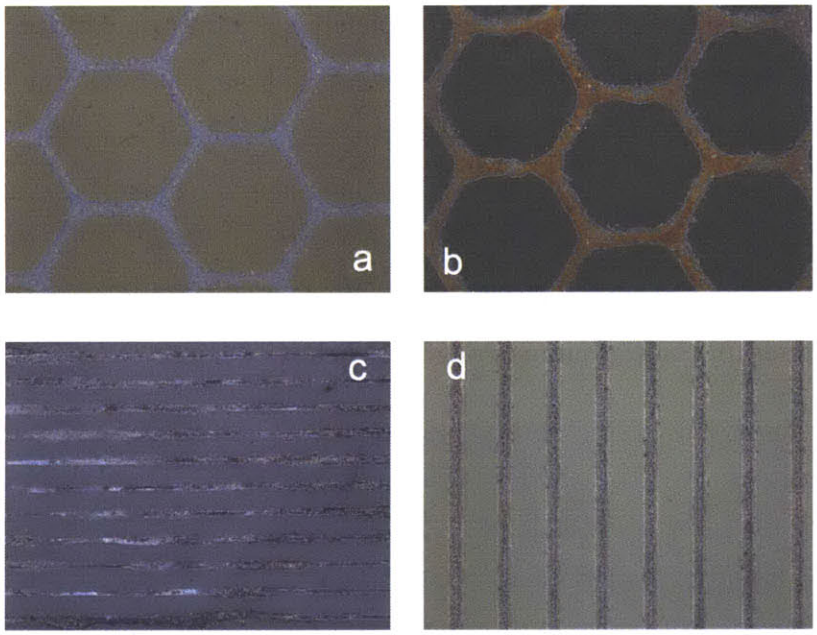

Figure 1.4: Liquid inks are not as simple to print as SAMs. For example, some of the liquid inks used in Hale's thesis have tendencies to exhibit clumping, which negatively impacts printing results [18]. The Nanomas MES-40 ink used in (a)-(d) is made from 40% solids loading of silver nanoparticles in a mesitylene solvent. (a)-(b) 5 μm line width hex pattern (c) 20 μm line width (d) 50 μm line width

1.2 Stamp

Typically, the stamps used in the microcontact printing process are cast out of polydimethylsiloxane, a silicon-based organic polymer. Commercially available Dow Corning Sylgard 184 PDMS is a thermoset silicone elastomer that is formed from the mixing of a base and a curing agent. The pre-cured fluid is poured onto a master pattern and is able to closely conform to its geometry. Typically, the masters are made from silicon wafers patterned with the

negative of the desired geometry in a conventional lithography process. Drawing a vacuum on this casting helps to degas the liquid and improve results in casting more intricate features, though it is not necessary for casting larger features. As this liquid cures into a solid, the cross-linking process does not cause any significant shrinkage or distortion. These characteristics enable the high fidelity replication of complex geometry with sub-micron features.

PDMS is also a good material for stamps because of its ability to make complete contact with substrates with surface asperities. Because SAMs only transfer from the stamp to the substrate where contact is made, this complete contact is necessary for reliable feature replication. Petrzelka refers to the ability of a stamp to completely conform to a surface, even over small asperities, as *conformal contact* [19]. This phenomenon is illustrated in Figure 1.5. The characteristic of PDMS that makes it good for conformal contact is its high ratio of surface energy to elastic modulus. This ratio is defined as the material radius of curvature [20], which, for PDMS, is on the order of 10 nm. The significant surface energy of the PDMS enables the stamp to conform around asperities on this scale, allowing PDMS stamps to make conformal contact with substrates that have a surface roughness below 10 nm.

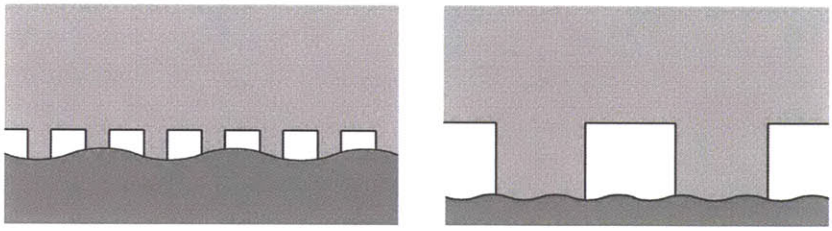

Figure 1.5: Conformal contact is achieved when the stamp conforms to surface asperities of the substrate [19].

Though PDMS has a lot of characteristics that make it a good material to use as a stamp, it also has a variety of traits that are problematic. The high ratio of surface energy to elastic modulus can cause elastic collapse, where features spontaneously adhere to each other, as shown in Figure 1.6. This effect is pronounced in features closely spaced together or with large aspect ratios. PDMS is a soft elastomer, making it very sensitive to contact stresses and allowing it to easily deform. Finally, PDMS is prone to swelling when exposed to organic solvents [21]. This limits material compatibility to select inks and can cause large area deformations that decrease absolute accuracy.

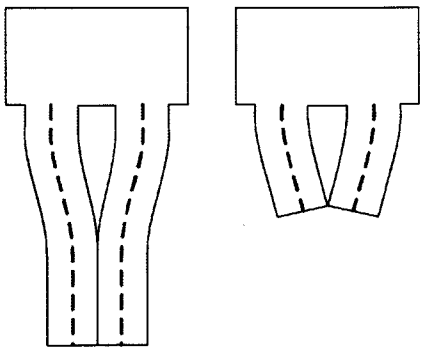

Figure 1.6: Petrzelka discusses two types of lateral collapse, in which the high surface energy of the PDMS stamp causes neighboring features to stick to each other [19].

1.2.1 Flat

Microcontact printing has traditionally been a plate-to-plate process. In this method, the PDMS stamp is casted from a planar, featured silicon wafer, as seen in Figure 1.7. This plate stamp is then inked and brought into contact with a flat substrate, transferring the ink to that surface, as shown in Figure 1.8. Though it has been shown to be able to reproduce patterns with great fidelity even at feature sizes of less than 100 nm, this plate-to-plate process is inherently limited and does not allow for printing larger areas than the size of the master wafer. In order to allow microcontact printing to scale to large areas and high rates, a continuous process must be developed to replace this existing method of batch processing.

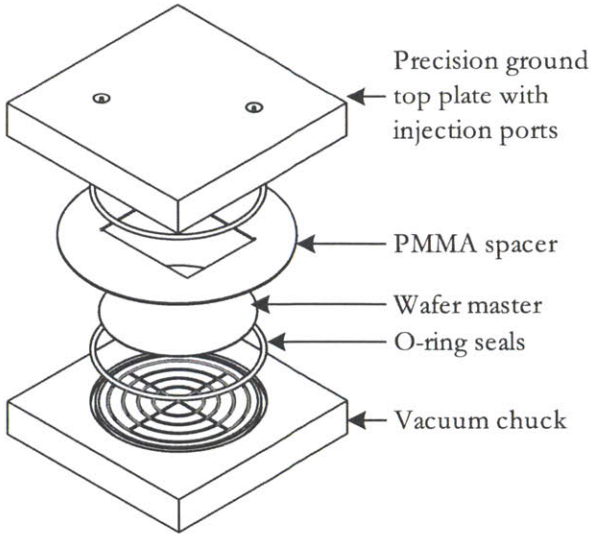

Figure 1.7: The mold created by Petrzelka to cast planar PDMS stamps from patterned master wafers [19]. These stamps were used in a plate-to-plate printing setup. As well, some of the stamps formed this way were wrapped around a print roll for roll-to-plate microcontact printing.

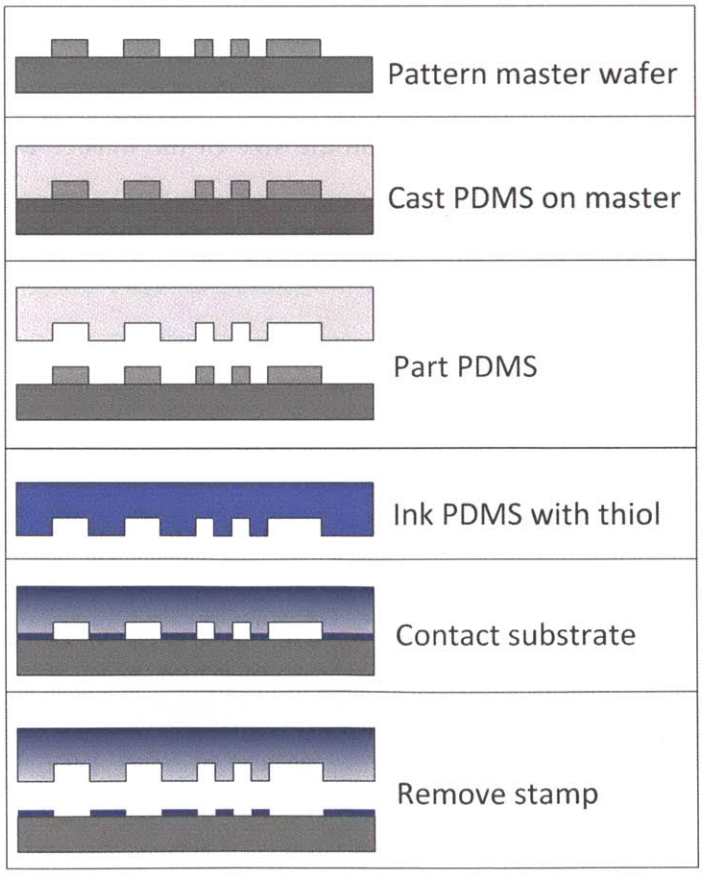

Figure 1.8: A summary of the traditional microcontact printing process [19].

An appropriate continuous manufacturing method to aspire to is roll-to-roll processing. These processes start with a large roll of a thin flexible material, often plastic film. This flexible substrate, called the web, is fed from roll to roll throughout the web-handling machine. Figure 1.9 shows a large roll-to-roll printing facility for manufacturing newspapers. A web-handling machine can be designed to have one singular purpose, or it can have many sequential stations each serving their own purpose, before the finished substrate is finally sliced up into sections, rolled up again, or passed on to the next step of manufacturing in some other way. Compared to the batch processing method, which normally involves a discrete number of sheets in each step of the process, the roll-to-roll web-handling method allows for a higher speed and more continuous process. Not only does this lend itself to more favorable economics, but it also helps with improved process control because it has fewer start-stop transients.

Figure 1.9: The ultimate goal is to determine how microcontact printing could be scaled up into a high-speed large-area roll-to-roll manufacturing process, such as the shown newspaper printing press.

1.2.2 Wrapped Stamps

In order to bring microcontact printing to a roll-to-roll basis, the first challenge is to transform the tooling from flat to round. Xia et al. made the first steps in transferring to a round tool by simply wrapping a flat wafer-casted PDMS stamp around a hand-held roller [22], as shown in Figure 1.10. Inking this roller with SAMs and rolling it over a flat wafer substrate yielded good results, showing that microcontact printing could be successfully achieved on a roll-to-plate

basis. Though this was a necessary step on the way to continuous manufacturing, it is requisite to replace the rigid plate substrate with a thin flexible web in order to make the full transition to a continuous roll-to-roll process.

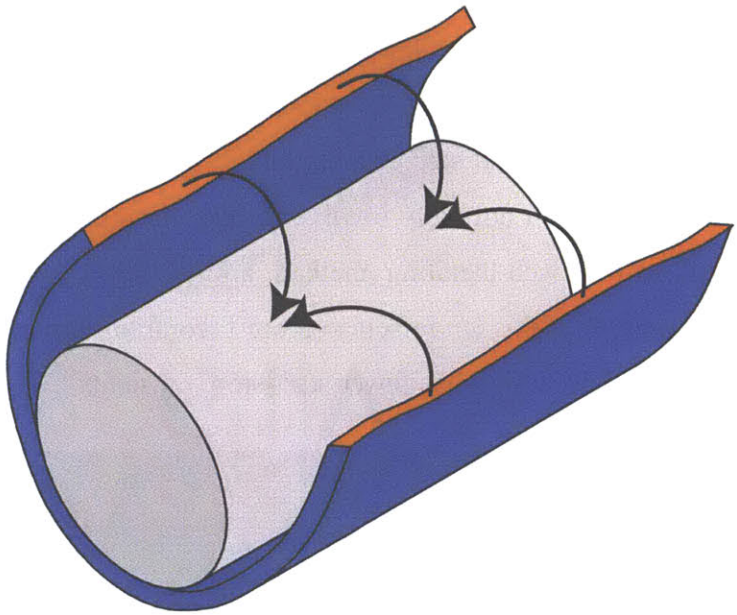

Figure 1.10: A planar stamp is wrapped around a print roll to enable roll-to-plate microcontact printing. Often, the stamp is held in place simply by its large surface energy. For more permanent and precise adhesion, the use of cyanoacrylate glue has been considered, and prior art has also shown PDMS stamps to be plasma bonded to glass cylinders, as in [23].

Rogers et al. proposed a process in which a flat PDMS stamp is plasma-bonded to a glass cylinder and printed on a flexible substrate [23], [24]. The Rogers group then worked on porting microcontact stamp-making techniques to a flexographic printing setting by investigating the fabrication of large area stamps [25]. Flat 12" by 12" PDMS stamps were cast with a mylar backing on a patterned surface, and demonstrated to be able to print features down to 1 μm. These stamps were proposed for printing on flexographic presses with flexible substrates at high speeds. The marriage of microcontact printing and flexography was referred to as microflexography. However, this printing technique was never tested.

Roll-to-plate and roll-to-roll microcontact printing processes require a cylindrical stamp for the print roll. For this purpose, nearly every machine in the literature uses a flat-casted stamp that is then wrapped around a cylinder [22], [23], [25]–[27]. Typically, these stamps are cast from

patterned silicon wafers and then cut down into a rectangle before being mounted on a roll, so as to give a clean and prismatic stamp profile. However, wafer sizes are limited, so this process will not be able to scale. There are methods for casting larger area microcontact printing stamps [25], but these result in low absolute accuracy and have not been fully developed. In addition, any method that involves the wrapping of a flat-casted stamp around a cylinder will result in residual stress and persistent pattern deformation. Though a stamp can be cut to proper size for wrapping, there will always be a discontinuity at the seam, where the ends of the stamp meet. Such a seam is depicted in Figure 1.11. This seam will result in a significant once-per-revolution disturbance that might preclude any reliable printing of micron-sized features. Finally, the stamp accuracy can only be as good as the mounting process. None of the mounting processes in the literature will be sufficiently accurate for mounting of large stamps without causing any pattern distortions or thickness variations.

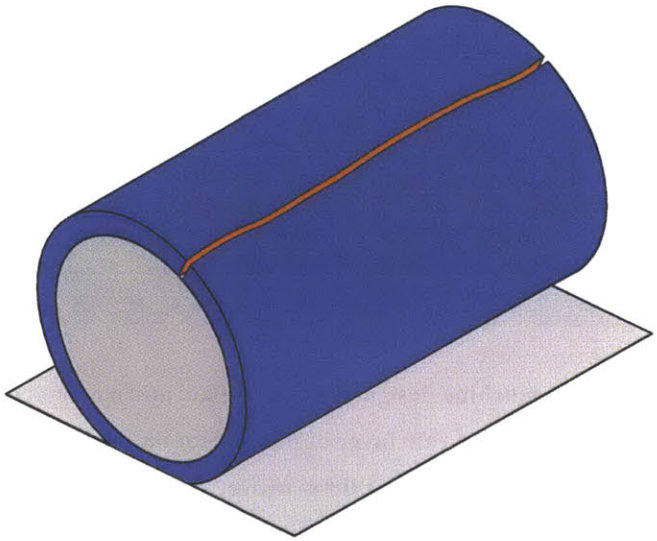

Figure 1.11: Roll-to-plate microcontact printing has traditionally been accomplished with planar stamps that are wrapped around a print roll. However, this technique will invariably present a gap or seam where the two ends of the wrapped stamp meet (orange). Such a seam results in a once-per-revolution impulse disturbance to the system, often orders of magnitude greater than the height of the stamp features.

1.2.3 Cylindrical Stamps

One of the key enabling technologies necessary to achieve precision roll-to-roll microcontact printing is the ability to cast a continuous cylindrical stamp and accurately mount it onto a roll. To address this challenge, Petrzelka developed a centrifugal casting machine that allowed for the

casting of continuous cylindrical stamps [19]. These stamps are cast on the inside of a rotating cylinder onto a layer of photoresist that has been patterned by a direct-write laser. These cylindrical stamps have no seam and no feature distortion. The casting machine and stamp are shown in Figure 1.12 below.

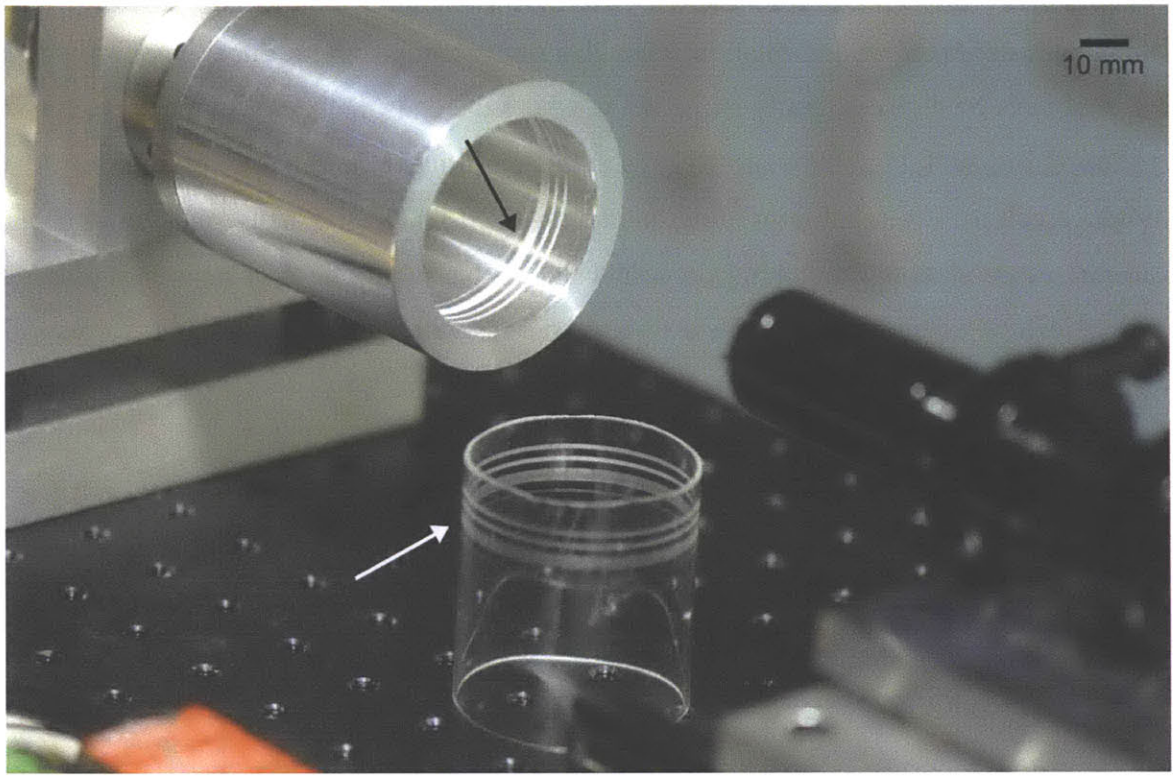

Figure 1.12: The centrifugal casting machine designed by Petrzelka, and a cylindrically cast stamp [19]. This machine works by using a laser to pattern a thin layer of photoresist on the inside of a rotating drum. PDMS resin is then poured into the spinning drum, and the centrifugal force causes the resin to evenly spread throughout the interior surface of the drum. Once the resin is cured, the cylinder is stopped and the stamp is removed. Note the seamless nature of this stamp, and the ability it affords for continuous printing.

Because the PDMS is so sticky and difficult to slide onto a roll, a special bushing was developed to provide an air cushion for the stamp to slide on over the surface of the roll. When the stamp is in place, the air supply is cut off and the stamp collapses onto the roll as the fluid film dissipates. The bushing is removed from the roll, leaving just the cylindrical stamp mounted in a stress-free state, but fixed in place by the large work of adhesion. A demonstration of this mounting technique is shown in Figure 1.13.

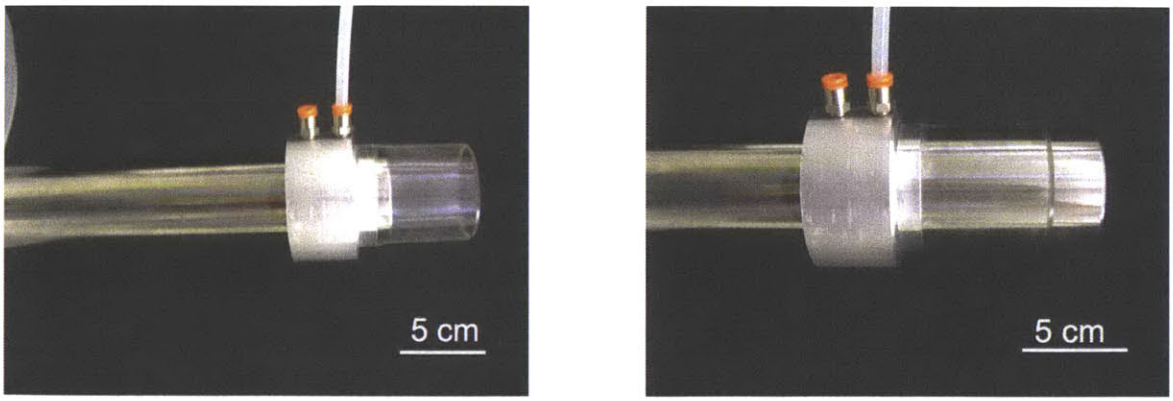

(a) (b)

Figure 1.13: The air bushing designed by Petrzelka to enable mounting of cylindrical stamps on metal rolls [19]. Because of the high surface energy of PDMS, it is too sticky to slide over a metal roll without assistance. This device forms a thin air film cushion between the stamp and the roll, allowing the stamp to be easily slid into place. When the air supply is turned off, the air film collapses and the stamp contracts onto the surface of the roll evenly.

1.3 Precision Printing

It is possible to obtain satisfactory patterns from microcontact printing with solely low-cost materials and techniques. However, in order to scale microcontact printing into a large-area high-rate manufacturing process, a reliable and repeatable process must be developed. The machine used for the purpose will likely have to have some precision designed and controllable elements in order to ensure consistent quality printing results.

1.3.1 Stamp Defects

The success of the microcontact printing process is contingent upon the complete and conformal contact of the stamp with the substrate. This requires a great enough print pressure to ensure that there are no gaps between the stamp and the substrate. However, too great of a print pressure will lead to stamp defects that can significantly affect the integrity of the transferred pattern. Examples of defects introduced by excessive print pressure include roof collapse, in which the roof of the stamp between features bulges outward to make contact with the substrate, and feature buckling, wherein features with large aspect ratios buckle under load. These are illustrated in Figure 1.14. Other potential printing defects include sidewall collapse, in which the sidewalls of the features bulge significantly, and lateral collapse, wherein closely packed features

stick to each other due to the large surface energy of PDMS. The effects of such failures are shown in Figure 1.15.

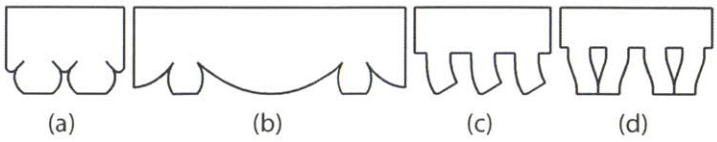

Figure 1.14: Petrzelka discusses four prominent failure modes of fragile PDMS stamps: (a) bulging features and sidewall collapse, (b) roof collapse in sparsely patterned areas, (c) buckling of features, (d) lateral collapse due to the high surface energy of PDMS [19].

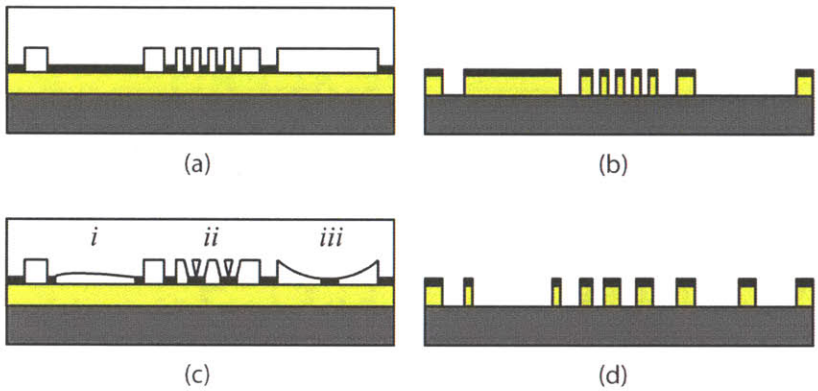

Figure 1.15: An illustration of how the various failure modes of PDMS stamps can affect the printed results: (a) a stamp in conformal contact without any significant defects, (b) a high-fidelity replication of the intended pattern, (c) a stamp showing three significant failure modes: (i) air trapping (ii) lateral collapse (iii) roof collapse, (d) The printed result from the poor stamp contact is significantly different than the master pattern.

There have been many papers on the stability of PDMS stamp features [28], [29]. Sharp et al. investigate the theory behind these printing defects and formed models that help to guide the stamp design process [30]. Still, due to the high surface energy and low stiffness of PDMS, microcontact printing stamps often have very narrow process windows for complete conformal contact.

In order to increase the robustness of the process to these failure modes, various materials stiffer than standard PDMS have been used to form the stamp. Schmid and Michel demonstrated the use of a special formulation of hard PDMS that was about four times stiffer than the regular formation, but at the expense of being more brittle [31]. A UV curable hard PDMS formulation

by Rogers allowed for quicker curing times and alleviated thermal shrinkage issues that result from the usual thermal cure process for regular PDMS [32].

The original microcontact printing process by Whitesides experimented with using standard photolithographic plate material, but these were relatively imprecise and only able to pattern features down to 200 μm [1]. Finally, the potential for using block polymer elastomers as microcontact printing stamps was investigated by Trimbach et al [33]. These stiff thermoplastics are formed using a hot-embossing process that requires high temperatures and pressures, but can handle 10-15 times the load of traditional PDMS stamps before structural collapse occurs. These stiffer stamps are more robust to structural failure, but they have not been widely adopted in microcontact printing because their high stiffness also results in a decreased ability to achieve conformal contact.

1.3.2 Sensing and Metrology

In the course of their work investigating the failure modes of PDMS stamps, Sharp et al. present methods for observing the stamp and the contact pattern during deformation during deformation using an inverted microscope shown in Figure 1.16 [30]. This laid the groundwork for directly observing stamp behavior in situ.

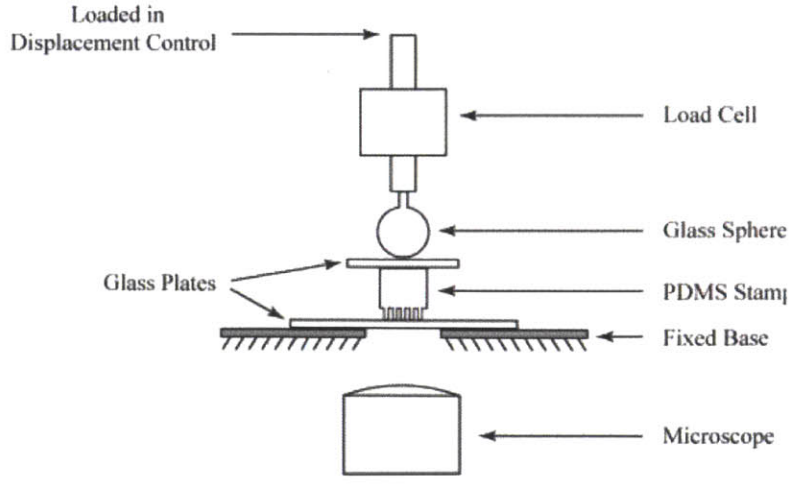

Figure 1.16: Sharp et al. present a method of in situ observation of stamp deformation. The system utilizes an inverted microscope to view the contact. The stamp is placed pattern-side down and loaded through a glass sphere to permit coaxial illumination. Redrawn with permission from Effect of Stamp Deformation on the

The idea for imaging the stamp at the point of contact is employed by Petrzelka to evaluate different methods for controlling the print head in a roll-to-plate configuration. He implements a Furthermore, the work suggests that direct sensing and control of the contact may be a viable method for scalable process control.

1.3.3 Printing Machines

Precision printing machines have been designed to actuate standard PDMS stamps in such a way that conformal contact is achieved without causing any feature collapse or defects. These machines, especially in the manufacturing setting, must allow for the precise control of contact pressure in the print region.

Kendale developed an automated plate-to-plate printing machine that used precision actuation of a hard-backed stamp to print onto silicon wafers [34]. A schematic of this machine is shown in Figure 1.17. By controlling the displacement and special orientation of the stamp plane, it is possible to control the deformation of the stamp features. Similarly, Burgin et al. built a contact aligner that enabled the careful control of the forces exerted on the substrate during the printing process [35]. This printing machine enabled the printing of sub-micron features and suggested that a similar design would work even for larger scale plate-to-plate machines.

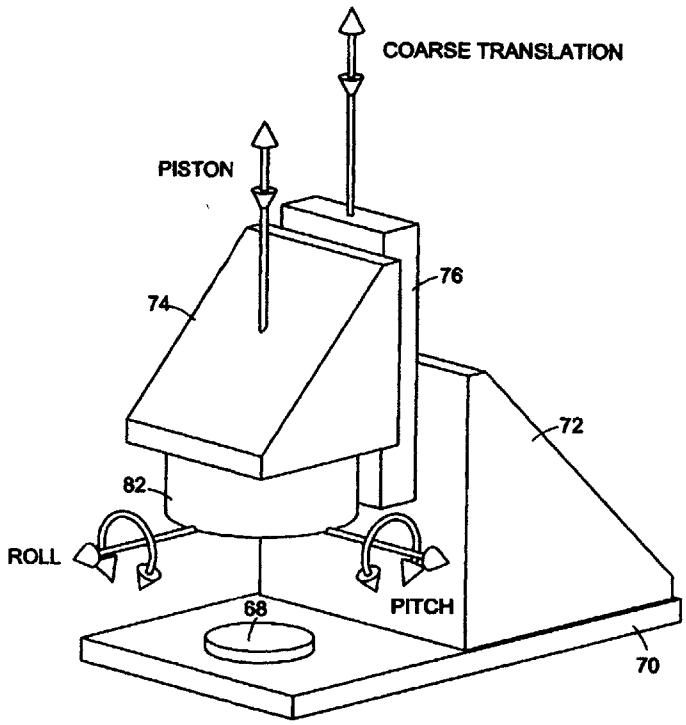

Figure 1.17: An illustration from the U.S. Patent filing of Kendale's planar microcontact printing machine [36], [37]. This machine precisely controls the roll, pitch, and height of the stamp to enable precise plate-to-plate printing. Though this form of displacement control might work for smaller wafers, it cannot be scaled up to a large area or continuous process.

Petrzelka built a precision roll-to-plate microcontact printing machine, pictured in Figure 1.18, that enabled control of either the displacement or force boundary conditions on the stamp [36]. This printing process is quite different from plate-to-plate printing, as there is only a narrow region of stamp-substrate contact at any given point of time. This contact propagates as the stamp is rolled over the substrate. The Petrzelka machine showed that the precise control over the contact forces was the key to roll-based microcontact printing, and that *in-situ* inspection of the print region could be a robust form of real-time process control. This precision roll-to-plate printing machine validated the potential for successful roll-to-roll printing and served as the inspiration for this thesis.

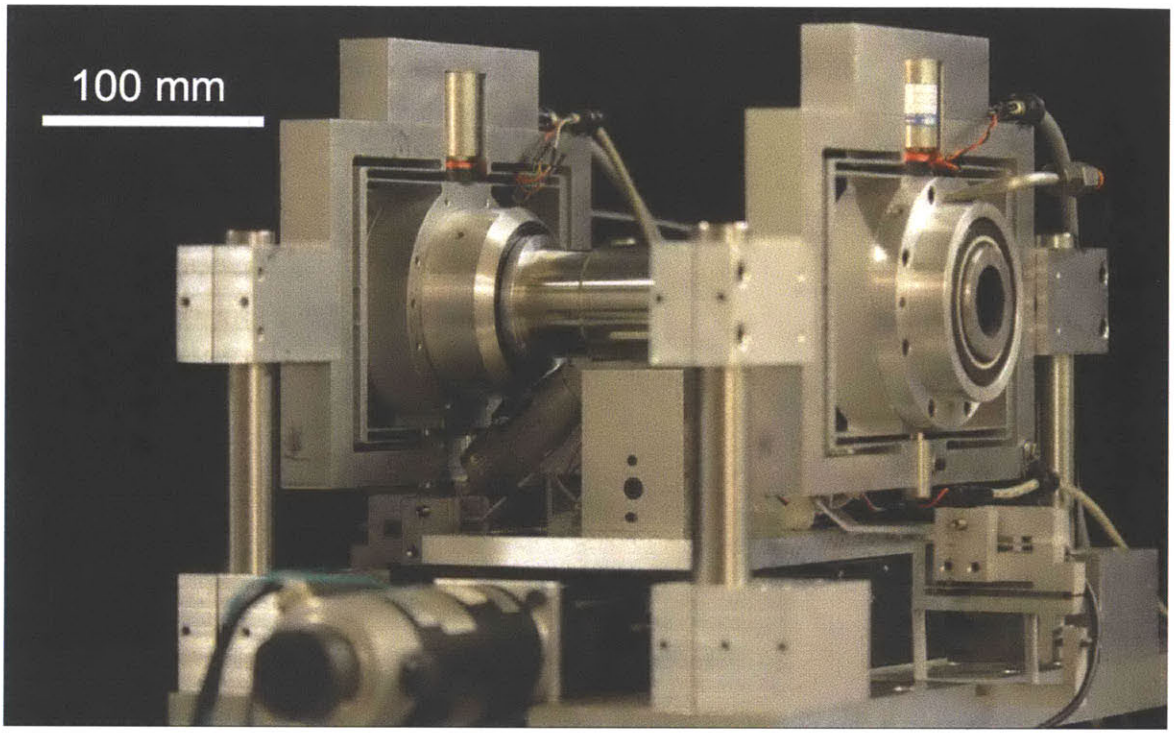

Figure 1.18: The roll-to-plate microcontact printing machine developed by Petrzelka [19]. This machine utilized parallel kinematic flexure stages to give control over the height and tilt of the print roll. A linear positioning stage below the print roll was designed to carry a wafer or glass microscope slide substrate. As well, an optical prism could be mounted on the linear positioning stage, allowing for real-time *in-situ* visualization of the contact region between the round stamp and flat substrate.

To investigate the feasibility of roll-to-roll microcontact printing, Stagnaro developed a web-handling machine for the continuous printing of alkanethiols on gold foil [26]. This pilot-scale machine was possibly the first to combine the material system and printing methods of microcontact printing with the roll-based processing techniques used in the manufacturing industry. It demonstrated the successful printing of etch-resistant SAM patterns with 40 μm features at speeds of up to 400 feet per minute. These results show the potential for high-speed roll-based microcontact printing. However, the machine was limited in its ability to control force at the contact region. The print force was indirectly controlled by manually adjusting micrometer heads, which compressed a compliant layer of foam on the impression roll against the print head. This gave little ability to control the contact between the stamp and the substrate, which would prevent this machine from being able to print more intricate and fragile patterns. As well, the use of a planar casted stamp limited the repeatability of the printing, as the mounting process was

very dependent on the operator skill [27]. Overall, the Stagnaro machine, pictured in Figure 1.19, showed promise for roll-to-roll microcontact printing, but also demonstrated the need for a more precisely controllable print head.

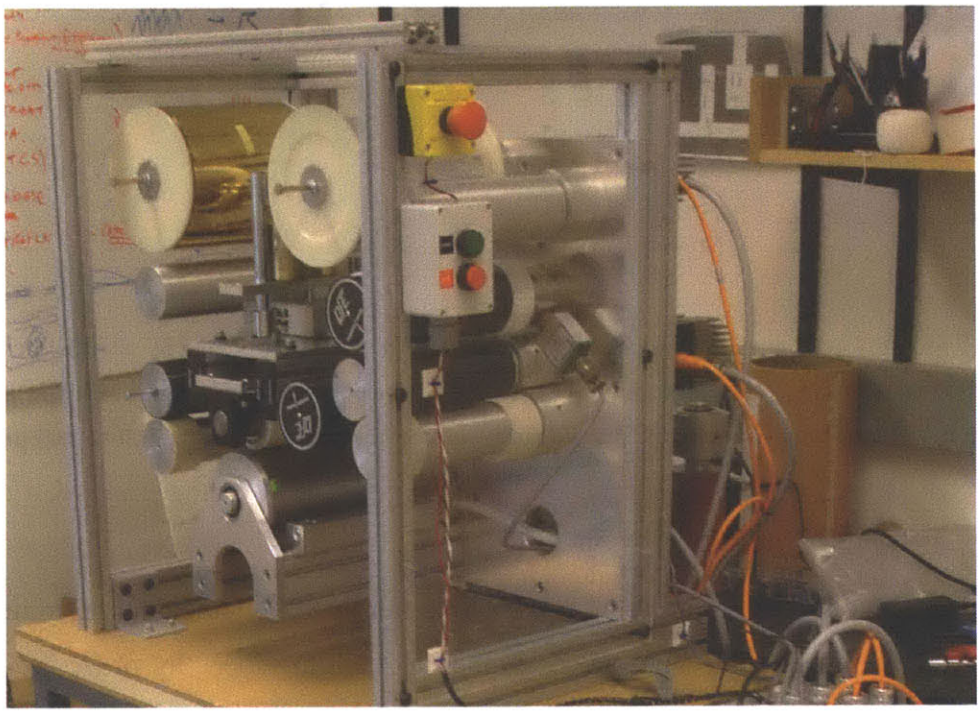

Figure 1.19: The roll-to-roll microcontact printing machine developed by Stagnaro. This machine achieved successful pattern transfer at web speeds of up to 400 feet per minute, but also demonstrated the need for a precision print head and a continuous stamp.

Baldesi continued work on this project and made a precision positionable print head for Stagnaro's roll-to-roll microcontact printing machine [38]. This print head was designed to have actuation in five axes, allowing for the precise setting of the print head location relative to the impression cylinder. However, the positioning was achieved through the manual actuation of micrometer heads. This design, shown in Figure 1.20, was an improvement over the original print head and allowed for the stage to be set in the proper location at the beginning of each print run. However, Baldesi concluded that automated actuators and a closed-loop controllable print head would be necessary for any further development of the process.

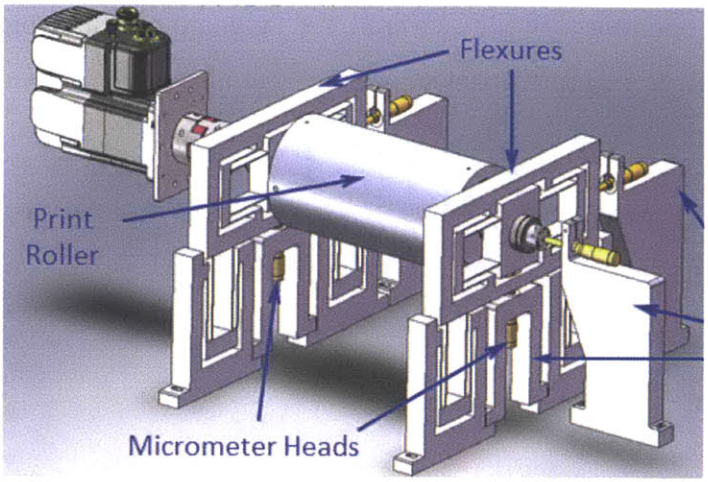

Figure 1.20: The print head developed by Baldesi [38]. The print roll is supported by parallel flexure stages with micrometer positioning. This gave manual control over five degrees of freedom, but it was determined that an active closed-loop controllable print head would be necessary for future roll-to-roll printing.

1.4 Thesis Contributions

The individual components of a precision controllable roll-to-roll microcontact printing machine have each been demonstrated, but never synthesized all together. In order to show that microcontact printing can be scaled up into a high-speed manufacturing process that allows for the continuous printing of micron-sized features, a roll-to-roll web-handling machine with an actively controllable print head must is designed. This machine utilizes a novel *in-situ* inspection technique to image the region of contact between the stamp and the substrate. This enables the camera to measure the distribution and magnitude of the contact pressure in real time. These measurements are used as feedback in the control system, enabling direct control of the stamp contact pressure and balance. As well, these measurements are used to verify a model of the roll-to-roll contact mechanics that is found to accurately describe the behavior of the stamp.

This thesis contributes with the creation of a precision roll-to-roll microcontact printing machine, the implementation of a novel inspection technique that enables closed-loop process control, and the development of an accurate model of roll-to-roll stamp contact mechanics. With these contributions, this thesis lays the groundwork for the investigation of how microcontact printing can be scaled up in a manufacturing process that enables the high-speed printing of patterns with micron-scale resolution.

CHAPTER 2

DESIGN

This chapter details the design of a precision controllable roll-to-roll microcontact printing machine. This pilot scale web-handling machine is designed to serve as the platform for many years of research on the continuous microcontact printing process. All the design and manufacturing work to create this machine was done in-house. This saves on budget, but more importantly it allows for full knowledge of and control over the design, form factor, functionality, integration, and workings of the machine. This is especially important considering the unpredictable and iterative nature of research.

The photo of the microcontact printing machine is shown in Figure 2.1, and Figure 2.2 clearly diagrams the layout of the various critical sub-systems.

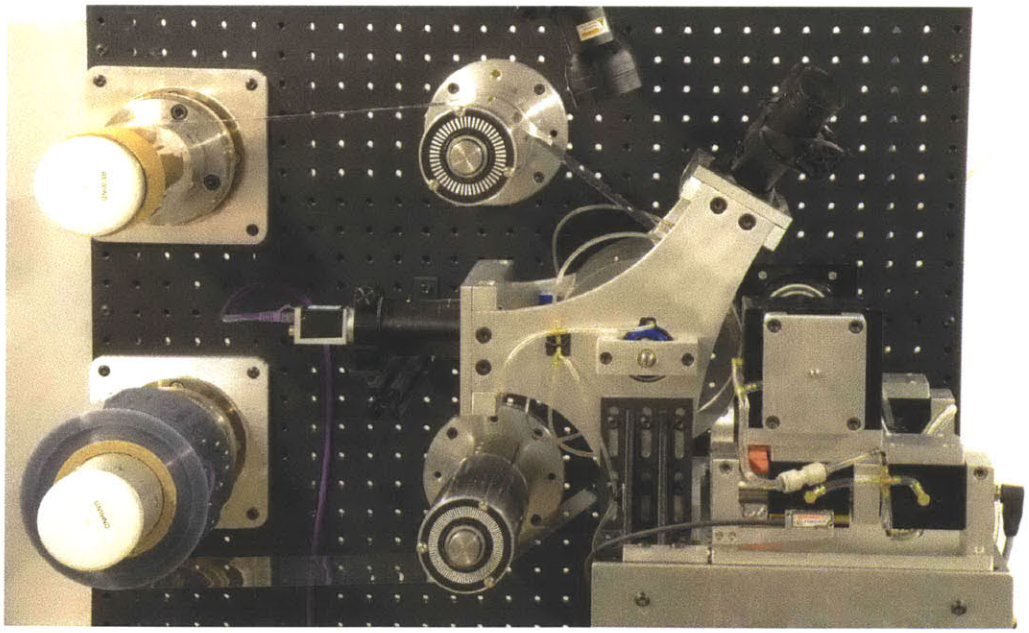

Figure 2.1: A close-up photo of the critical components in the roll-to-roll microcontact printing machine. These components are discussed in detail throughout this thesis.

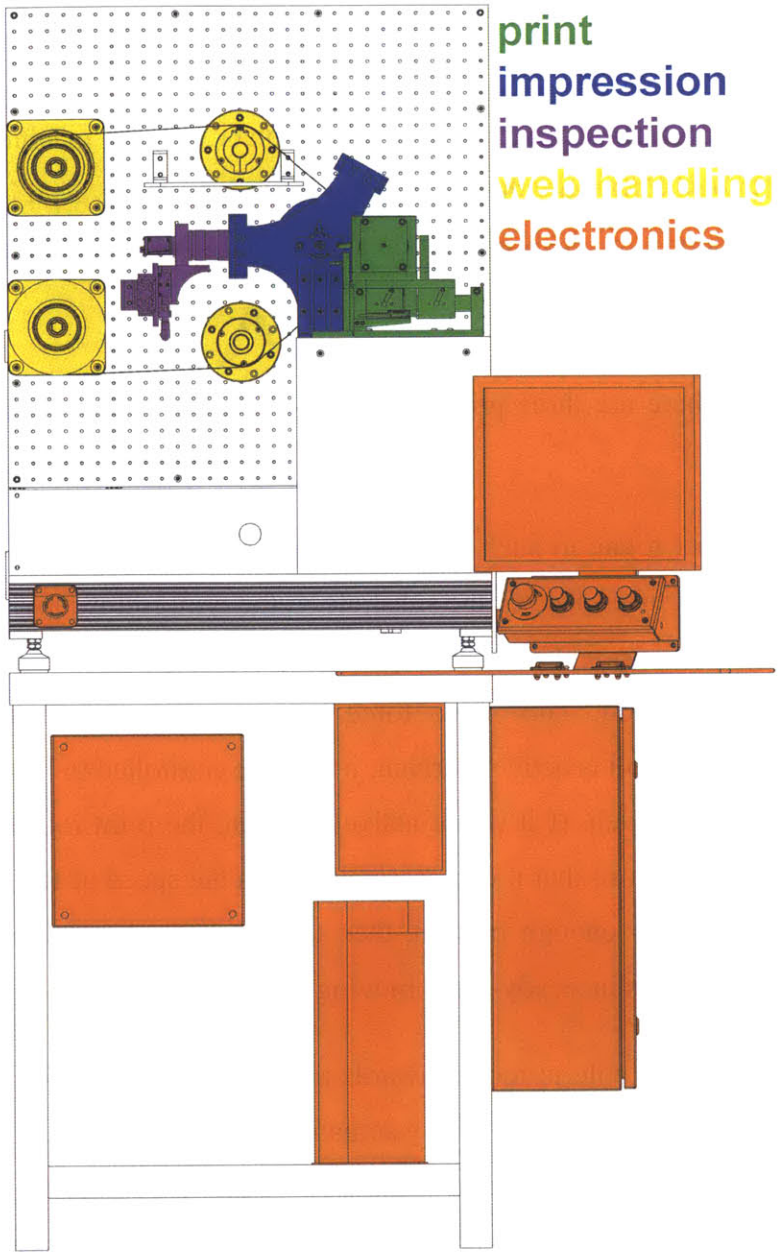

Figure 2.2: Diagram of sub-systems: (green) The print head is arguably the most critical part of the machine, as it is what actuates the stamp and controls print pressure. The precision of the printing process can be no better than the precision of the print head. (blue) The impression cylinder has the job of presenting the substrate to the print head in a reliable and repeatable manner. (purple) The novel inspection technique uses a camera to look through the back of the impression cylinder at the print region. This allows direct closed-loop control of the print contact. (yellow) The web-handling components are meant to transport the substrate through the system in such a manner to provide an ideal printing surface. (orange) The electrical cabinet contains all of the critical electronics for the system and the human machine interface (HMI) is the terminal that allows the operator to interact with the machine.

2.1 Print Head

The print head is the most critical part of the microcontact printing machine. Petrzelka [19], Stagnaro [26], and Baldesi [38] show that a precision controllable print head is a prerequisite for high-speed microcontact printing. This chapter details the design of such a print head.

2.1.1 Functional Requirements

It was determined that there are three primary degrees of freedom that the printing process is sensitive to.

1. The print roll must rotate in such a way that the tangential speed of the stamp features equals the linear surface speed of the substrate. If the print roll is moving slower or faster than the web, the stamp features will experience significant shear force, due to their no-slip boundary condition. This shear force leads to their deformation, smearing, or buckling. If the print roll is actively driven, it must be controlled to have the same surface speed as the moving web. If it is not actively driven, the print roll must have minimal friction and low inertia so that it can passively match the speed of the web when brought into contact. With low enough friction, then there will not be a significant shear force interaction if the web is in steady-state, moving at a constant speed.

2. The print roll must be able to move towards the impression cylinder in such a way that their axes of rotation remain parallel. By actuating this degree of freedom, it is possible to control the displacement of the stamp. The use of a position controller or force controller will have a significant effect on the characteristics of the printing process.

3. The print roll must be able to slew in such a way that one side of the print roll can move forwards or backwards relative to the other side. This angular rotation is important in correcting for any taper in the stamp and for imperfect alignment between the print roll and the impression cylinder.

These axes are illustrated in Figure 2.3.

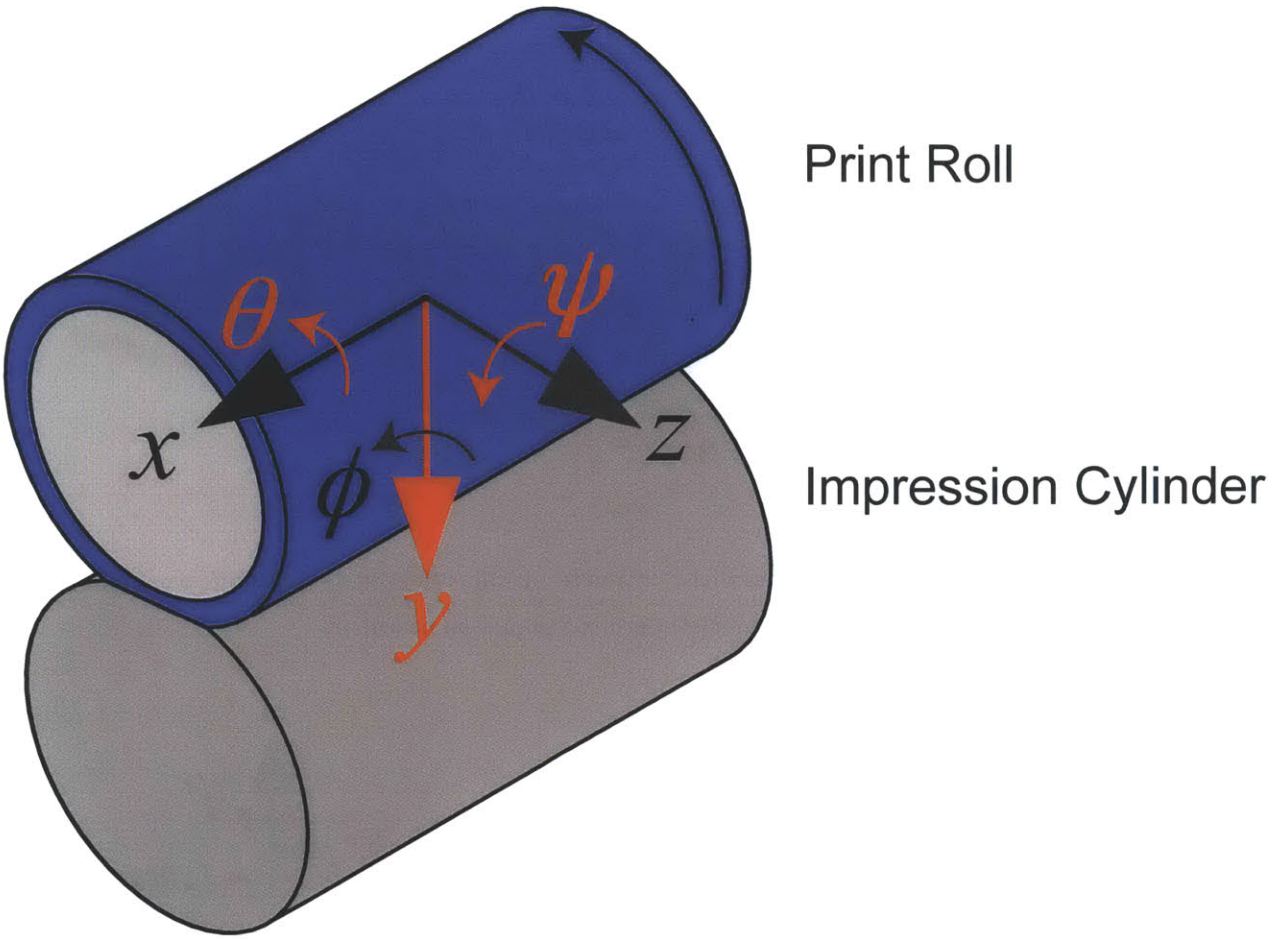

Figure 2.3: Print head degrees of freedom: The roll-to-roll microcontact printing process is sensitive mainly to the y direction movement of the print head, which controls print pressure. As well, the print roll must rotate in the θ direction with the same tangential velocity as the impression cylinder to avoid any shear or slip from occurring. Angular slew in the ψ direction helps to correct for stamp taper or machine misalignment.

Because of the delicate nature of PDMS stamps with micron-sized features, the print head must be able to actuate any of these degrees of freedom repeatably in the sub-micron range with sub-Newton forces. Any significant friction or hysteresis in the system will make it difficult to precisely control the interaction between the stamp and the substrate. Therefore, each of the degrees of freedom of the print head makes use of frictionless flexures or incredibly low friction air bearings.

2.1.2 Construction

The construction of the print head is presented from Figure 2.4 through Figure 2.11.

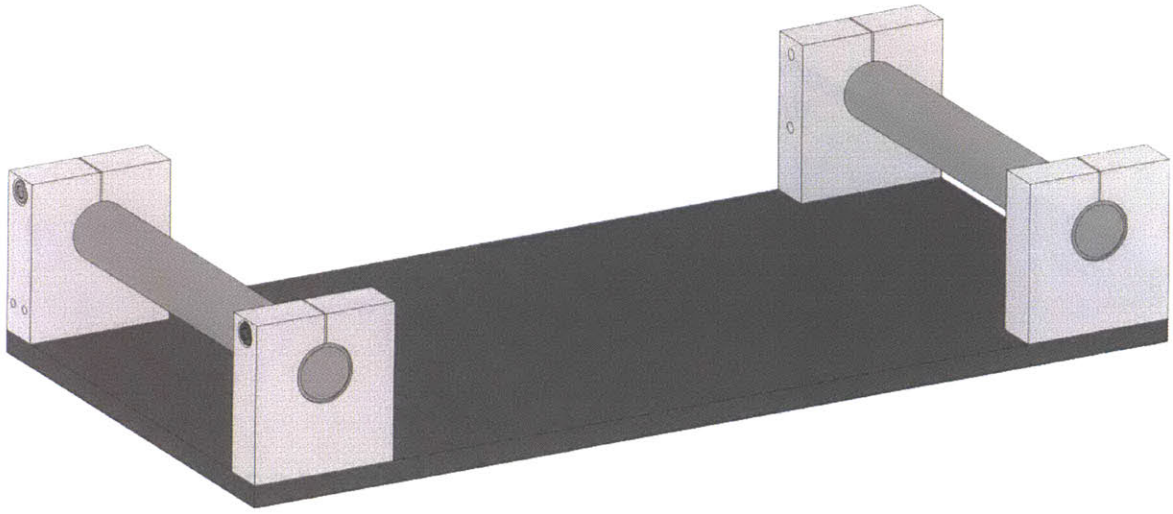

Figure 2.4: Print head construction: Two parallel 1" diameter stainless steel guide rod shafts were mounted off of a 3/8" thick precision ground aluminum baseplate.

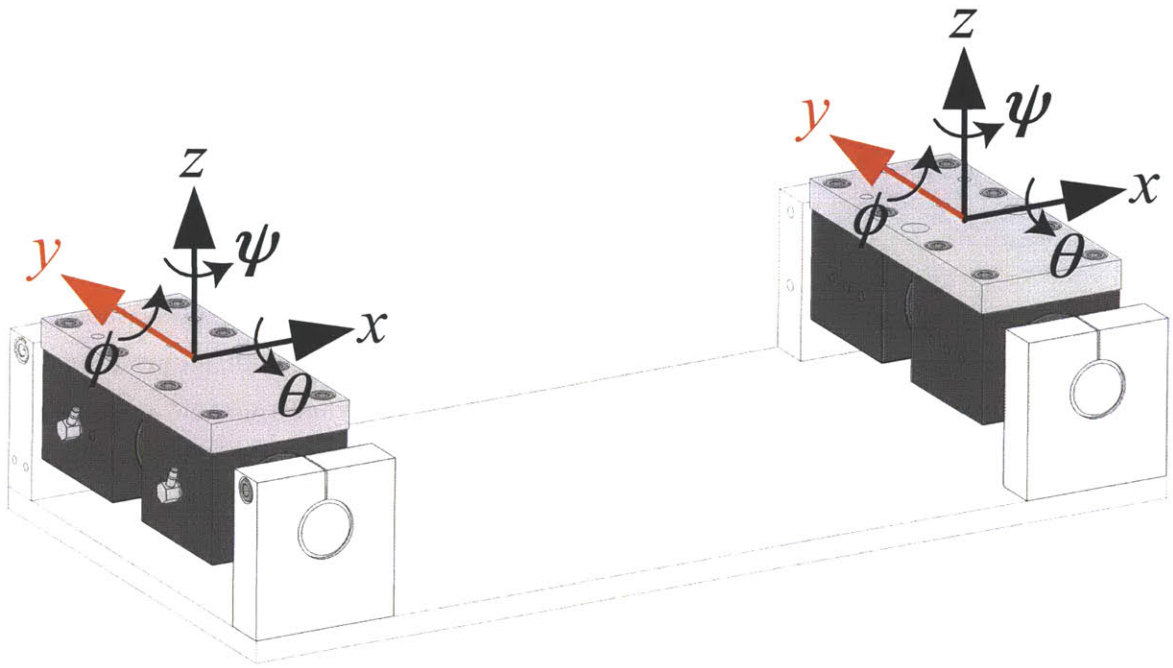

Figure 2.5: Print head construction: On each guide rod, there is a linear stage. Each stage consists of two collinear 1" air bushings mounted in aluminum pillow blocks that are connected by a ½" thick aluminum plate. These near-frictonless stages allow either side of the print head to move forwards and backwards with a total travel of 1".

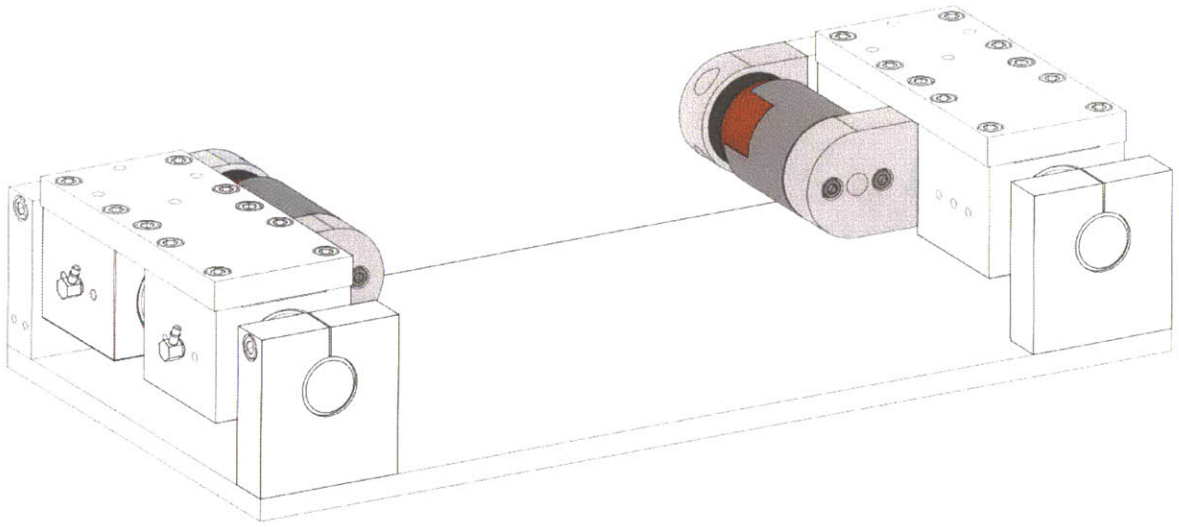

Figure 2.6: Print head construction: Each linear stage is actuated with a voice coil. The coil side of the voice coil is mounted to the stationary guide rod mount, while the magnet side of the voice coil is mounted to the linear air bearing stage. There is no contact between the two parts of the voice coil, so there is no mechanical friction due to this actuator.

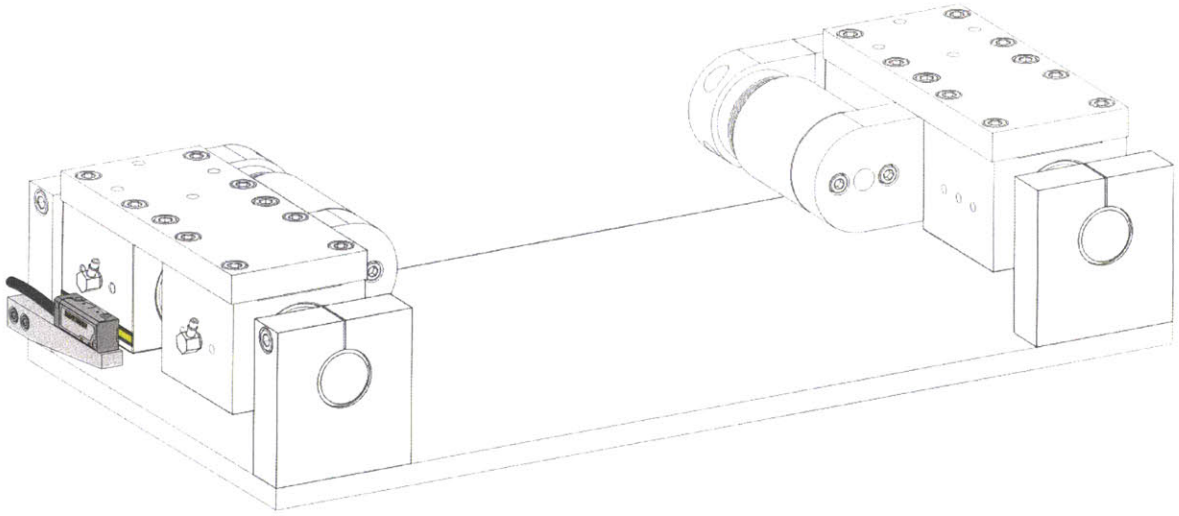

Figure 2.7: Print head construction: Each side of the print head was instrumented with linear optical encoders, able to measure movement with 10nm resolution. The read-head is fixed to the guide rod mounts, while the scale is glued onto the front air bushing pillow block.

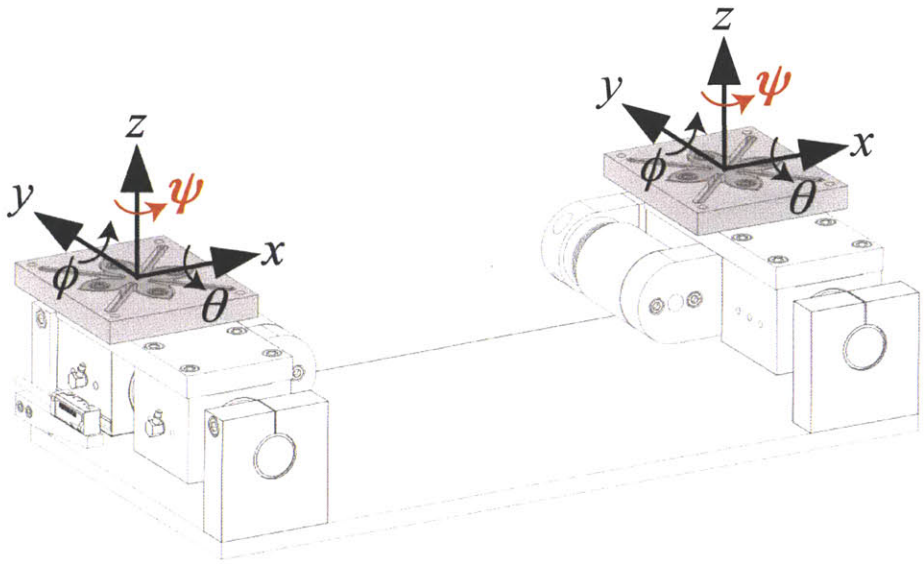

Figure 2.8: Print head construction: Rotational flexures were mounted on each linear stage to allow for the small degree of rotational movement that is necessary for the print head to be able to compensate for any misalignment in the system or taper in the stamp. Flexural bearings were chosen for this purpose because they are frictionless, though they do introduce a non-linear rotational stiffness.

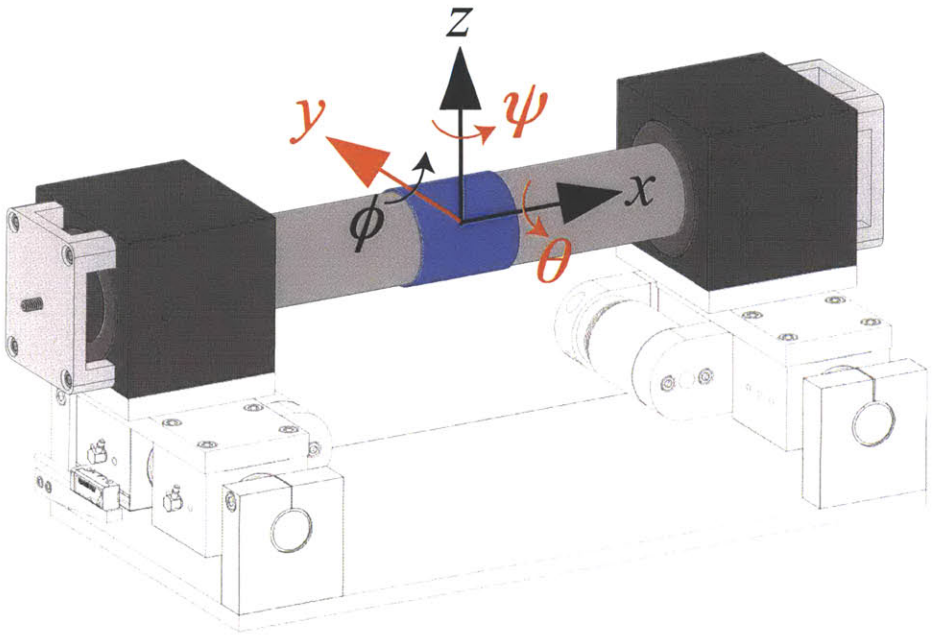

Figure 2.9: Print head construction: The 2" diameter 440C stainless steel print roll is supported radially by air bushings that allow it to rotate with nearly zero friction. The print roll is constrained from lateral movement in the *x* direction by opposing flat round puck air bearings, mounted on ball joints. The thrust bearing on the inboard side of the machine is fixed, while the thrust bearing on the outboard side of the machine is spring pre-loaded.

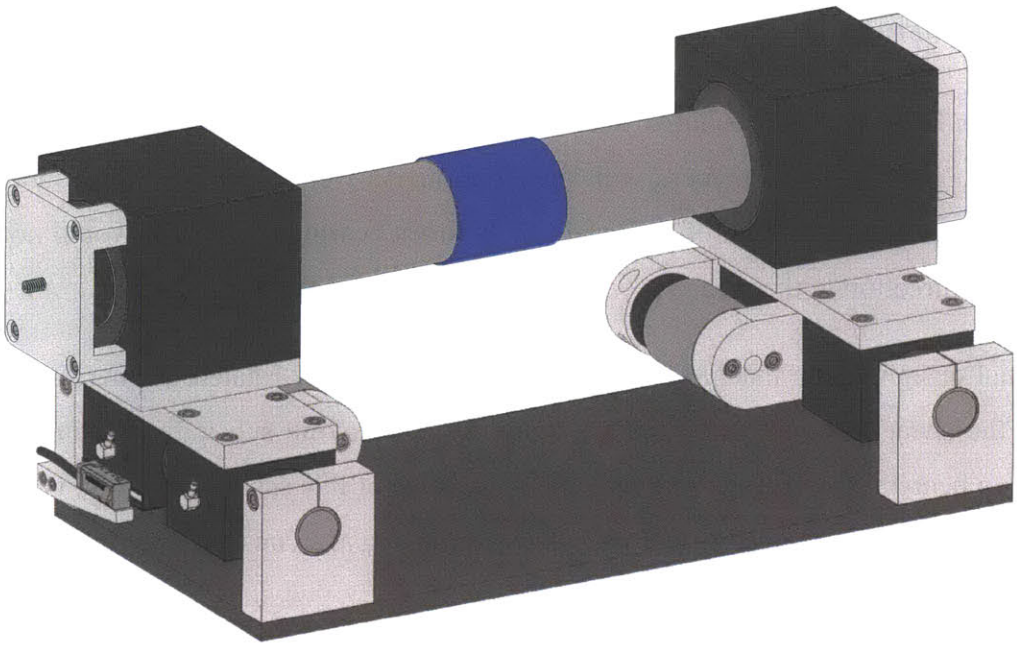

Figure 2.10: Print head construction: Diagram of the complete print head assembly. Altogether, the print head is able to actuate the stamp in the y and ψ axes, while the θ axis is free to rotate.

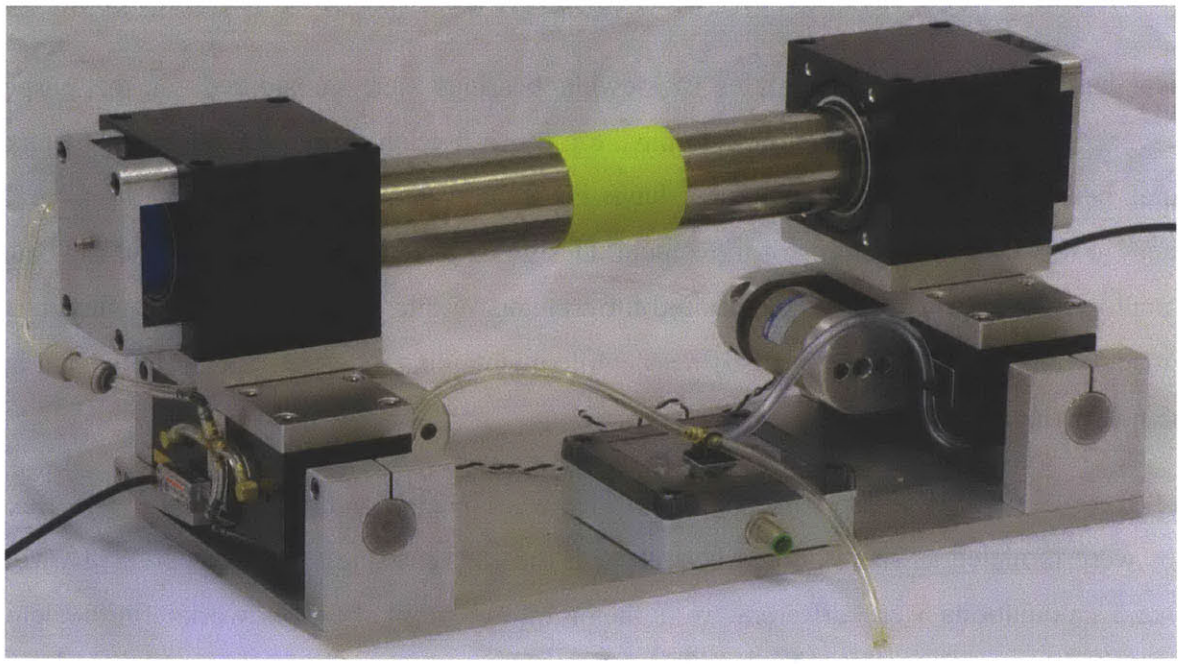

Figure 2.11: Print head construction: Photo of the complete print head assembly. Note the addition of the voice coil electrical distribution box and the air hoses used to supply the air bearings with pressurized air. These hoses were chosen to be soft and compliant, and they were routed in a way that their stiffness would have the least effect on the print head.

2.1.3 Air Bearings

New Way Air Bearings' air bushings were selected to support each end of the roll because of their ability to provide high stiffness with low friction. As well, New Way flat round puck air bearings were used at either end of the print roll as thrust bearings, so that it would not move in the transverse direction to the web.

In this initial design of the machine, the print roll is not actively rotated. Rather, it is passively driven by the shear force imparted on the stamp by the moving substrate. Because the roll is supported on near-frictionless air bearings, the magnitude of this shear interaction is expected to be small if the system is at steady-state with the web moving at a constant speed.

2.1.4 Slewing bearings

In order for the print head to slew in such a way that could compensate for any stamp taper or stage misalignment, rotational bearings were required between the linear stages and print roll. The ideal bearing would have both zero friction and zero stiffness in the ψ rotational direction.

Typical ball and crossed roller styles of slewing bearings were considered for the purpose. However, sample bearings were found to have too much friction or too low stiffness. Instead, a flexural bearing was designed. Flexures have no friction and can be designed to have low stiffness in the desired directions of movement. Designing a slewing flexure also had the benefit that it allowed for a custom fit to the desired form factor. Within this form factor, the flexure was designed to have minimal rotational stiffness, while maintaining a high stiffness of the print head in the y direction.

The flexure design was first done by hand with basic beam-bending equations. The flexure blades were modeled as fixed-guided beams, with the ends rotating about the center. However, the hand calculations were different by a factor of two from the Solidworks finite element analysis simulation. It was hypothesized that this was because the movement of the blades is not exactly fixed-guided, but rather the ends of the blades are able to rotate slightly, as defined by their circular movement path. This difference is depicted in Figure 2.12.

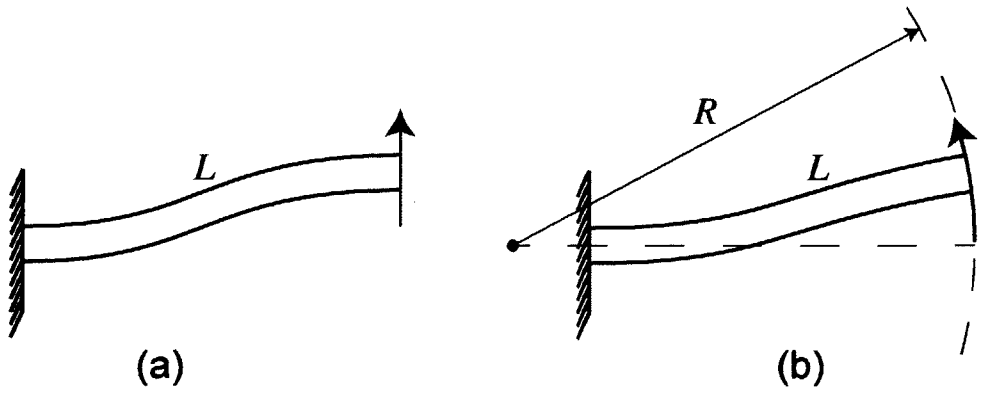

Figure 2.12: Slewing flexure design: Beam-bending equations were used to design the flexure. Originally, the flexure was modeled as a set of four fixed-guided beams as shown in (a). However, it was quickly apparent that this was not an accurate model, so (b) was used instead.

To reconcile this difference, Chapter 4 of *MEMS Vibratory Gyroscopes: Structural Approaches to Improve Robustness* was consulted [39]. The desired flexure design matched closely with the in-plane torsional flexures used in some MEMS gyroscopes. The torsional spring constant of the flexure is shown as Equation 4.13 in the book and copied as Equation (2.1). This equation describes the torsional spring constant of an in–plane torsional flexure when the beam is located inside the mass.

$$K_{zz} = 4\frac{EI_y}{LN}\left[3\left(\frac{R}{L}\right)^2 - 3\frac{R}{L} + 1\right] \tag{2.1}$$

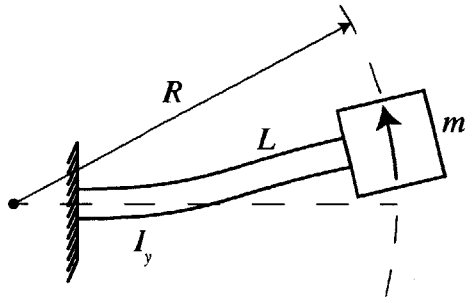

Figure 2.13: The in-plane torsional flexure from [39]

The flexure was designed to have a maximum stress of one-third the yield strength of 6061-T6 aluminum. This was chosen to avoid the formation of any micro fractures in the material. As well, because aluminum does not have an endurance limit, designing for a low maximum stress allows this flexure to safely be used without worry for fatigue failure. Hard stops were included

to protect the flexure in case of any over-travel. This monolithic flexure was waterjet cut out of 6061-T6 aluminum, though the manufacturing tolerances of this process limited the ability to accurately achieve the desired geometry. The flexure geometry is shown in Figure 2.14 and its location is shown in Figure 2.15.

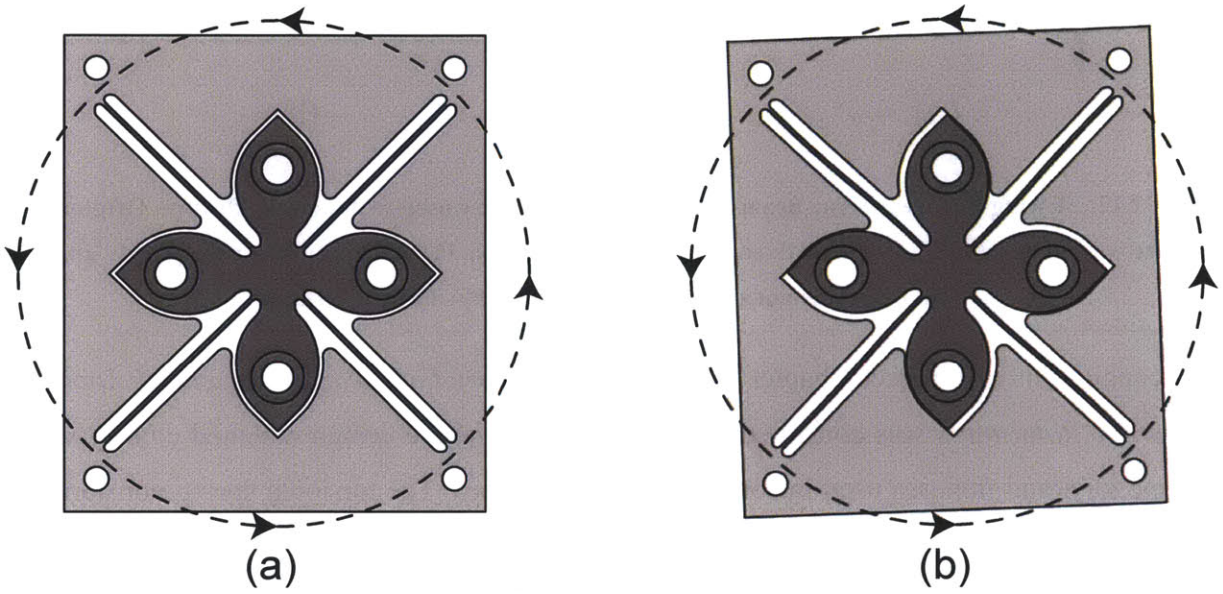

Figure 2.14: Slewing flexure design: The light gray portion of the flexure rotates in plane around the dark gray portion, which is grounded. The flower shape results from the in-cuts used to increase the flexure blade length, and therefore decrease the overall stiffness of the flexure. Note that the tips of the flower will make contact with the surrounding material, which serves as a hard stop to prevent over-rotation and damage to the flexure blades. (a) shows the flexure in the undeformed state, while (b) shows the flexure rotated to the hard stop.

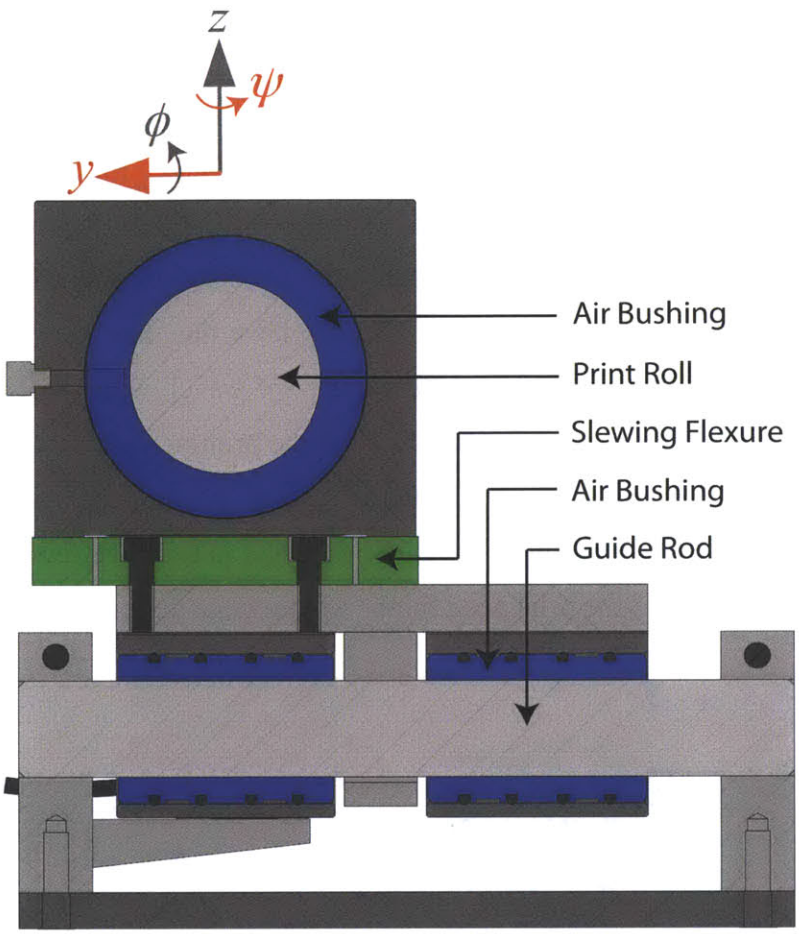

Figure 2.15: Slewing flexure design: The slewing flexure is sandwiched between the print head's linear stage and the print roll pillow block. This flexure allows the relative rotation of these components, which enables one side of the print head to advance in front of the other in order to compensate for any taper in the stamp or misalignment in the machine.

2.1.5 Actuators

H2W Technologies NCC05-18-060-2X voice coils are attached to each side of the print head stage for force actuation. Voice coils were appropriate for this application for a variety of reasons. Because there is no contact between the coil and the magnet, the voice coils are free from mechanical friction. Voice coils have no backlash, cogging, or noise, which gives them the ability to actuate with nearly unlimited force resolution. They are high-bandwidth, with electrical time constants on the order of 0.4 ms. Finally, voice coils are able to output large forces. Because they are mainly thermally limited, they are also able to safely output bursts of extremely large

forces for limited periods of time, which could be useful in controlling for a large impulse disturbance to the system. A photo of one of the installed voice coils is shown in Figure 2.16.

The voice coils are easily interfaced and controlled with DAC and a linear amplifier. The linear amplifiers used to drive the coils are the H2W Technologies LCAM 5-15. One linear amplifier is interfaced with each coil. These voice coils each have a resistance of 11.5 ohms and a motor constant of 29.56 N/amp. The actuators are designed to have this motor constant remain as flat and constant as possible throughout the specified 0.5" of travel. With the machine's 24-volt supply, each voice coil is able to apply a 60 N force to the print head, for a total maximum print force of 120 N. Outfitting the machine with a higher voltage power supply will allow for larger coil forces. Though the desired printing force is not expected to exceed a few Newtons or tens of Newtons, aggressive control of the print head might require large actuator efforts.

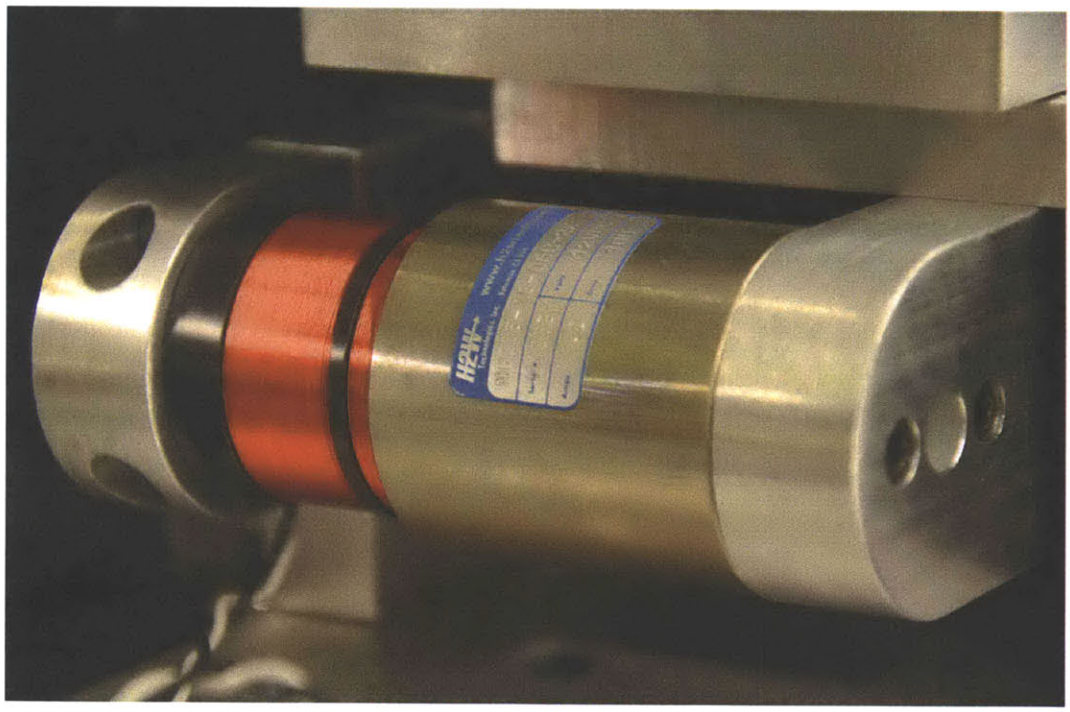

Figure 2.16: One of the voice coils used to actuate the print head

2.1.6 Displacement Sensors

The displacement of each stage is measured with Renishaw TONiC RGSZ 10nm linear optical encoders. These encoders give quadrature readings at 10 MHz, which are fed into the National

Instruments CompractDAQ's NI-9401 high speed digital input module. The CompactDAQ system's onboard counters are used to record the position of the stage.

One encoder readhead is mounted on each side of the print head. The encoder scales are affixed to the front linear air bushing pillow blocks. The encoder readheads must be carefully aligned with the scales during the mountain process in order to give a reliable measurement. Once the encoder is properly aligned, the bolts are firmly tightened down to keep it in place. One of the installed encoder setups is shown in Figure 2.17.

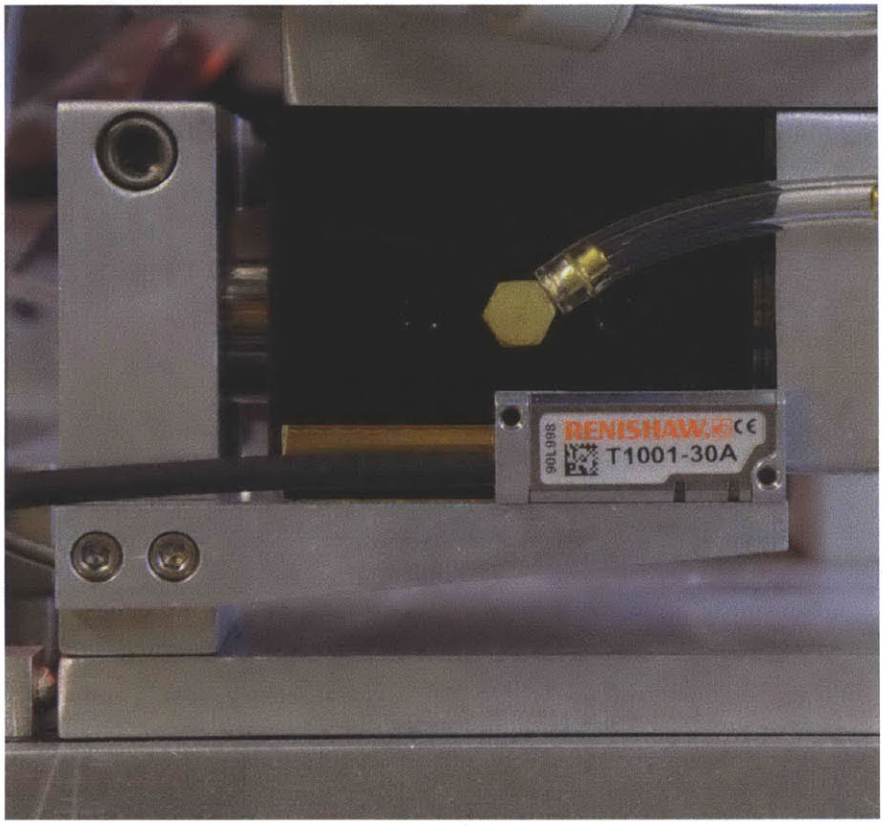

Figure 2.17: Renishaw linear optical encoder and gold scale (partially obscured by read-head cable)

2.1.7 Kinematic Mounts

The machine is designed for the print head assembly to be entirely self-contained and work as a standalone unit. This is useful in the event that experiments on the print head are to be conducted separately from the rest of the machine. The print platform allows for the easy mounting and removal of the print head. As well, multiple print heads can be tested and quickly swapped out for one another.

In order to ensure that the print head is properly aligned with the impression roll, a kinematic hard stop was designed. This hard stop uses three spherical steel balls to make three points of contact with the print head base plate and exactly constrain the three degrees of freedom in that plane. Such a kinematic mount allows for repeatable sub-micron alignment of the print head with respect to the impression cylinder. One of these hard stops is pictured in Figure 2.18.

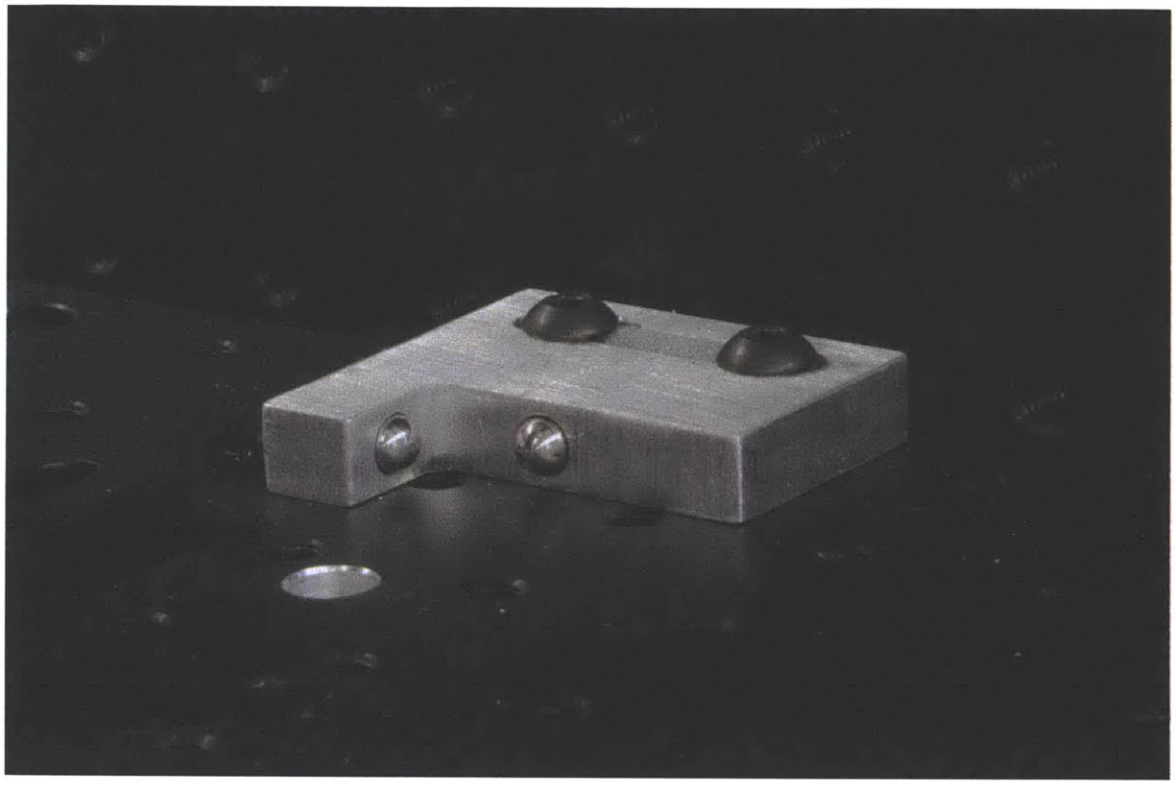

Figure 2.18: One of the kinematic hard stops used to for the repeatable positioning and alignment of the print head assembly

2.1.8 Inking

This iteration of the print head does not have an inking system in place. However, space was left on the linear air bearing connecting plates for the addition of an inking system, and mounting holes were machined into the print roll's air bushing pillow blocks. An inking system could consist of a roller on air bearings being passively pressed up against the back of the print roller with pre-loaded springs. By setting the preload on the springs, it would be possible to control the inking pressure. The inking roller might have an ink tray and doctor blade attached to it. However, if the inking roller imparts any significant torque on the passively driven print roll,

then this could cause deformation, smearing, or buckling of the stamp's features. If this is observed, then the print roll will likely have to be actively driven and controlled to have the same surface speed as the moving web. This can be done by replacing the print roll's outboard thrust bearing mount with a motor mount and using a speed-controllable motor with a flexible shaft coupling.

2.2 Impression Assembly

The impression cylinder is a critical component in any roll-to-roll printing process. It is the part of the machine that carries the web through the printing interaction and provides a reliable, stable backing for the print head. This allows the print roll to make a strong impression on the substrate, which is where the name comes from. An illustration of this interaction is depicted in Figure 2.19.

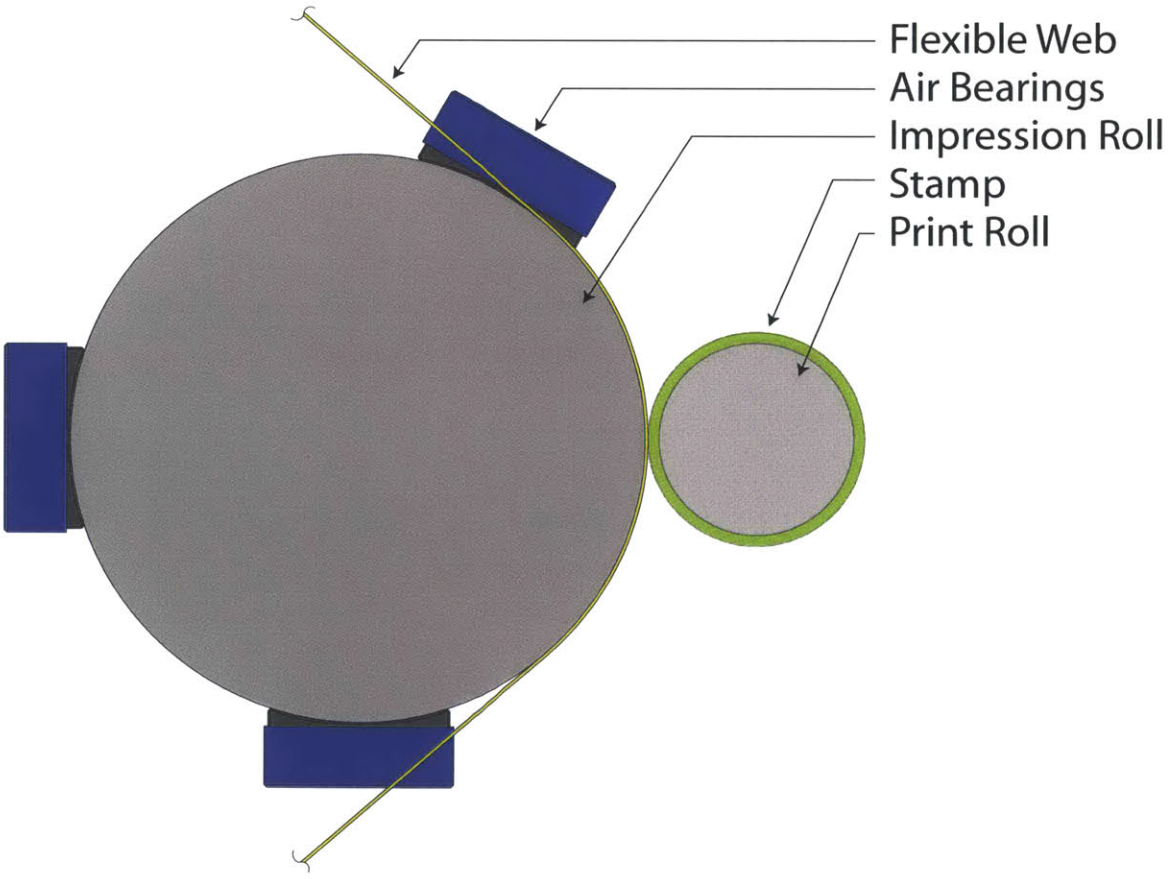

Figure 2.19: Diagram of the interaction between the print roll and the impression roll

Depending on the specific printing process and the desired results, the surface of the impression cylinder may either be made of a very stiff material or a more compliant one. Because the substrate is sandwiched between the surface of the impression cylinder and that of the print roll, the surface properties of the impression cylinder greatly affect the printed results. Typically, a harder impression surface gives higher precision and cleaner printed edges, while a softer impression surface allows the substrate to conform to the print roll surface, which can widen the process window at the expense of accurate registration.

The axis of the impression cylinder is usually fixed in place with precision bearings that do not move in the machine frame. This allows the impression cylinder to serve as a datum for all the other rolls in the machine. They must be aligned to have parallel axes to this roll for good web tracking. As well, the print roll must be the one to move relative to the impression cylinder in order to control print pressure.

A photo of the impression cylinder mounted on the print platform is shown in Figure 1.18.

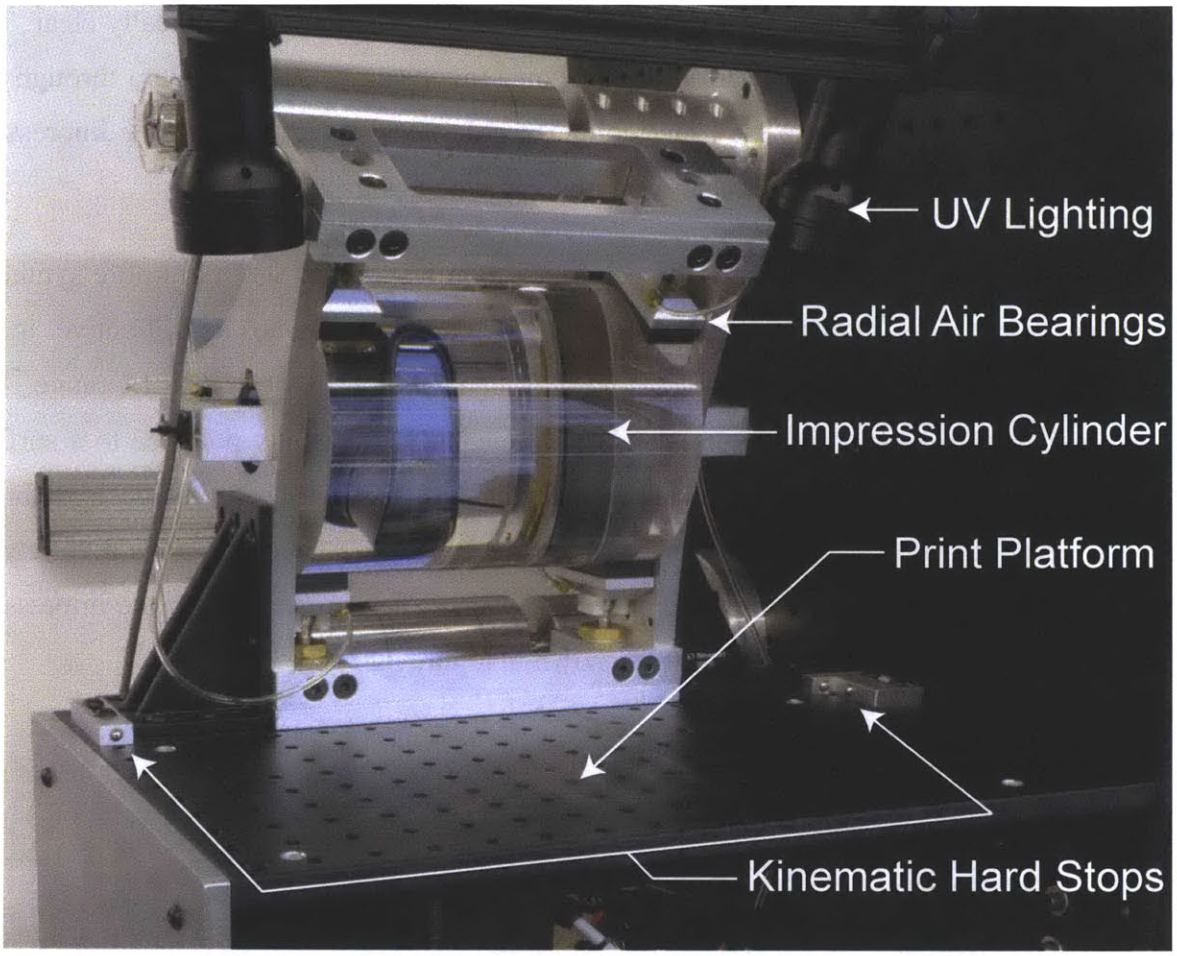

Figure 2.20: The impression roll assembly installed on the print platform. The clear impression cylinder is held in place by air bearings, which are mounted in the impression roll frame.

2.2.1 Impression Cylinder

It is critical that the impression roll be as close to an ideal cylinder as possible. The tensioned flexible web is wrapped around the impression roll, so it will take on the shape of that surface. Any large- or small-scale deformations in the impression cylinder can transfer to the substrate, which will lead to a less ideal printing surface. The printing process is especially sensitive to any eccentricity or total indicated runout (TIR) of the impression cylinder, as the print roll has to precisely track this movement in order to prevent oscillating regions of high and low print pressure. For these reasons, it is desirable to have an impression cylinder with as smooth and round a surface as possible.

Another requirement of the impression cylinder for this machine is that it be optically clear. The novel *in-situ* inspection technique used in this machine involves focusing a camera through the opposite side of the cylinder onto the print region. In order to visualize through the impression roll, it must be made of an optically transparent material with a polished surface.

The impression cylinder was made by Hellma Optics from j-plasma's SQ1 ultra-pure synthetic fused silica. This glass is recommended for optical elements due to its refractive index homogeneity, stability under thermal stress, and high transmission in the UV to IR range. The specified cylinder size was 6" in diameter and 8" in length. It is optically polished to a surface finish of 0.5 nm RMS. This clear glass cylinder, or cylindrical lens, allows for the desired ability to inspect the print region from the opposite side of the cylinder. As well, it gives a variety of options and configurations for lighting and alternative camera setups. A photo of the impression roll assembly installed on the print platform is shown in Figure 2.23.

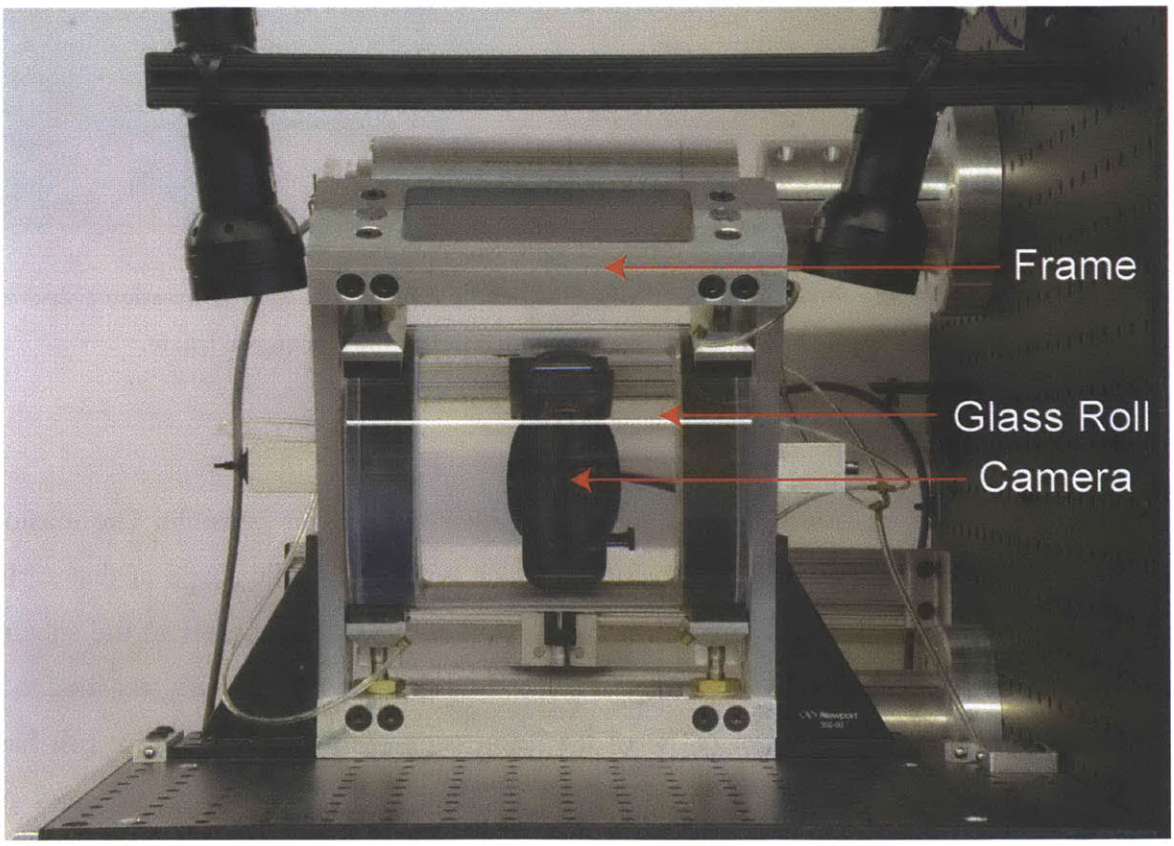

Figure 2.21: The impression roll assembly (gray) is installed on the print platform (black). The clear impression roll is held in place by air bearings.

2.2.2 Inspection

The impression assembly frame was designed with cutouts to allow for visual inspection and lighting of the impression cylinder. The novel inspection technique developed by Petrzelka [19] to visualize the contact region in a roll-to-plate microcontact printing machine in illustrated in Figure 2.22.

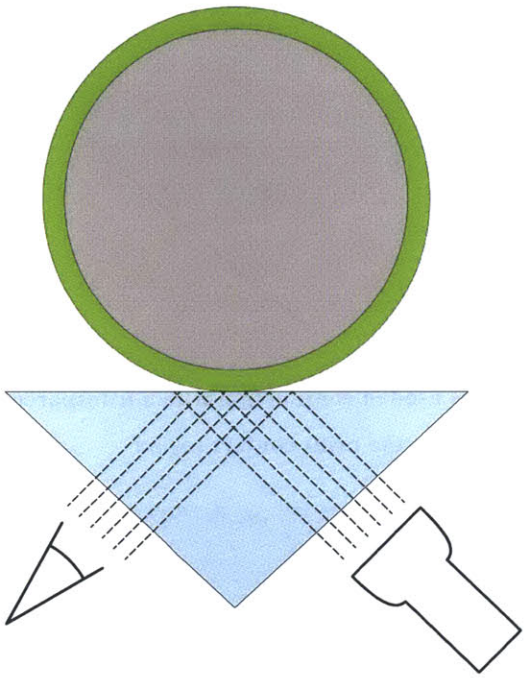

Figure 2.22: Petrzelka used a glass prism to view the contact region in a roll-to-plate setup

Inspired by the success of Petrzelka's method for controlling the printing process via direct visualization of the contact region, a similar imaging technique is implemented in this roll-to-roll machine. The camera used for sensing contact was mounted directly behind the impression cylinder, looking through the center of it to the print contact region. Lighting is provided by UV flashlights mounted above the impression cylinder, also aimed at the print contact region. A diagram of this camera setup is presented in Figure 2.23, and a photo of its implementation is shown in Figure 2.24. Details on the inspection system can be found in [40].

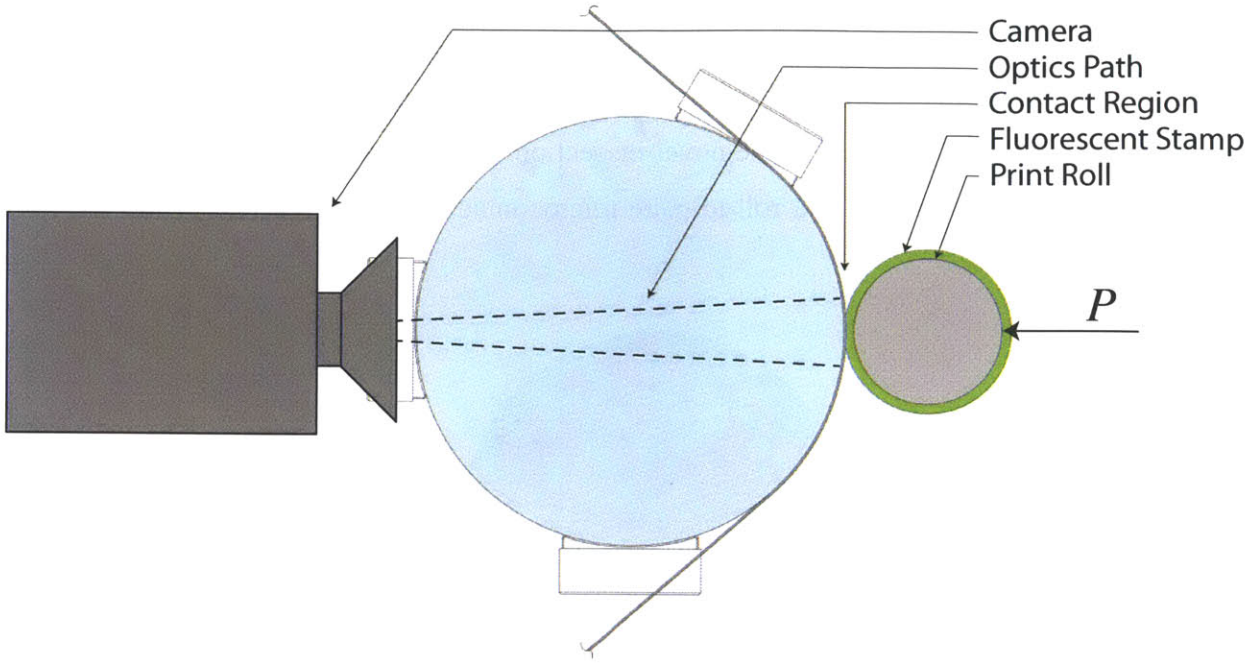

Figure 2.23: Diagram how a camera is used in conjunction with a transparent impression cylinder to inspect the print contact region

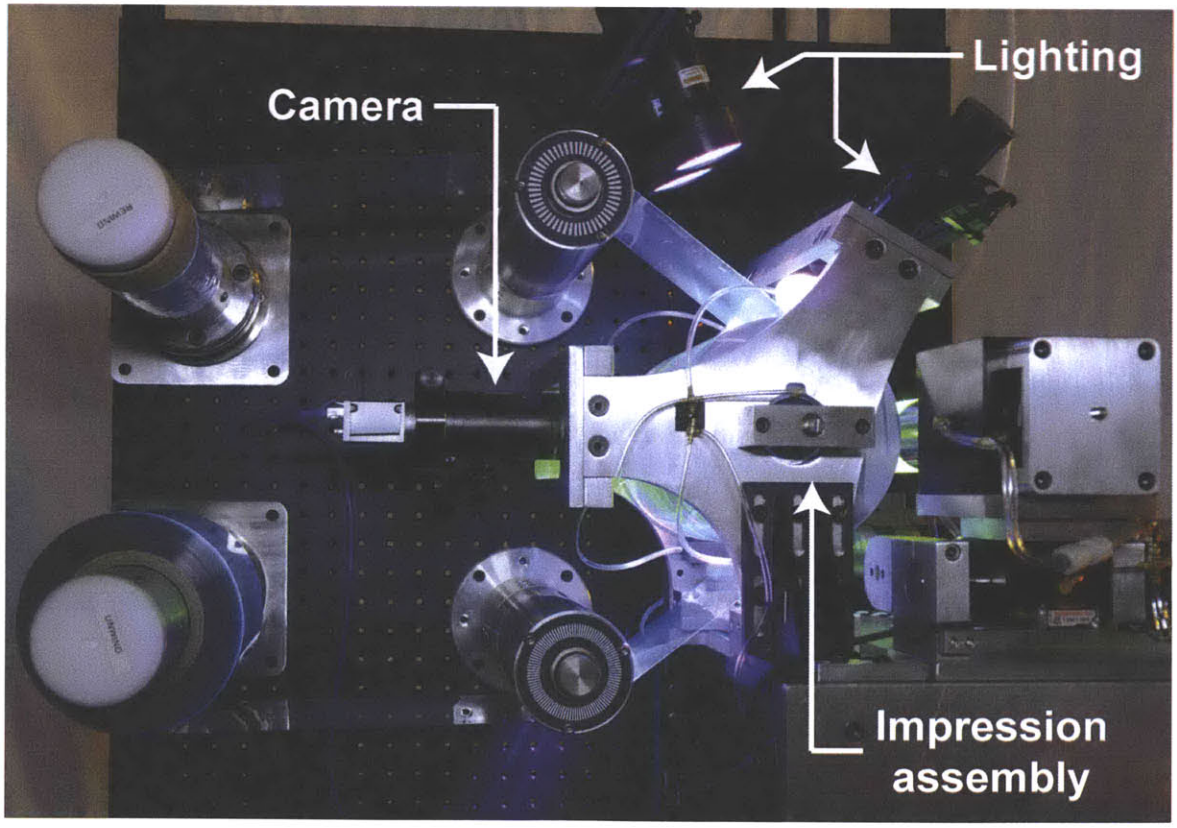

Figure 2.24: Impression roll camera and lighting system implemented on the roll-to-roll machine

2.2.3 Bearings

In order to hold the impression cylinder in place, yet allow it to freely rotate, a selection of bearing options was investigated. The impression roll bearings were to be of high stiffness and low friction. As well, because neither the impression cylinder nor the print cylinder were to be stepped, the impression roll bearings were required to leave clearance for the print roll to come into contact with the substrate. The bearings chosen were New Way Air Bearings' 30 mm x 60 mm concave radial segment air bearings. The radius of these bearings is cut and ground to match that of the impression cylinder. Figure 2.25 shows a photo of these bearings.

Figure 2.25: New Way radial segment air bearings with a 3" radius

The air bearings have a porous carbon surface that allows air to pass through, creating a thin high-pressure air film that the impression cylinder can float on. By having three segment bearings mounted around the cylinder at each end, it is possible to constrain four degrees of freedom. Using one of New Way's flat round puck style air bearings as thrust bearings at each end of the cylinder allows for constraint of the fifth degree of freedom, leaving the cylinder to just rotate in place. Air bearings have both high stiffness and exceptionally low friction.

The eight air bearings are mounted on ball-head screws, such that they can self-align to the cylinder. As well, these ball-head mounting screws have a very fine 0.5mm thread pitch, allowing for precise adjustments and positioning. This same action can be used to remove any slop in the mount and preload the bearings. One such screw and nut mount is shown in Figure 2.26.

Figure 2.26: New Way radial segment air bearing (blue) mounted on a fine pitch ball-head screw in a brass mounting nut (gold). The 3D printed retaining block (white) is used to keep the air bearing connected to the screw.

2.2.4 Frame

The ball-head mounting screws are held in brass nuts, which have nylon-tipped set screws to lock the bearings in position. These brass nuts were mounted in the impression assembly frame, which was designed and manufactured in-house. This frame sets the spacing of the bearings around the circumference of the impression cylinder, while leaving plenty of room for the substrate, inspection cameras, and lighting sources. This frame is pictured in Figure 2.27.

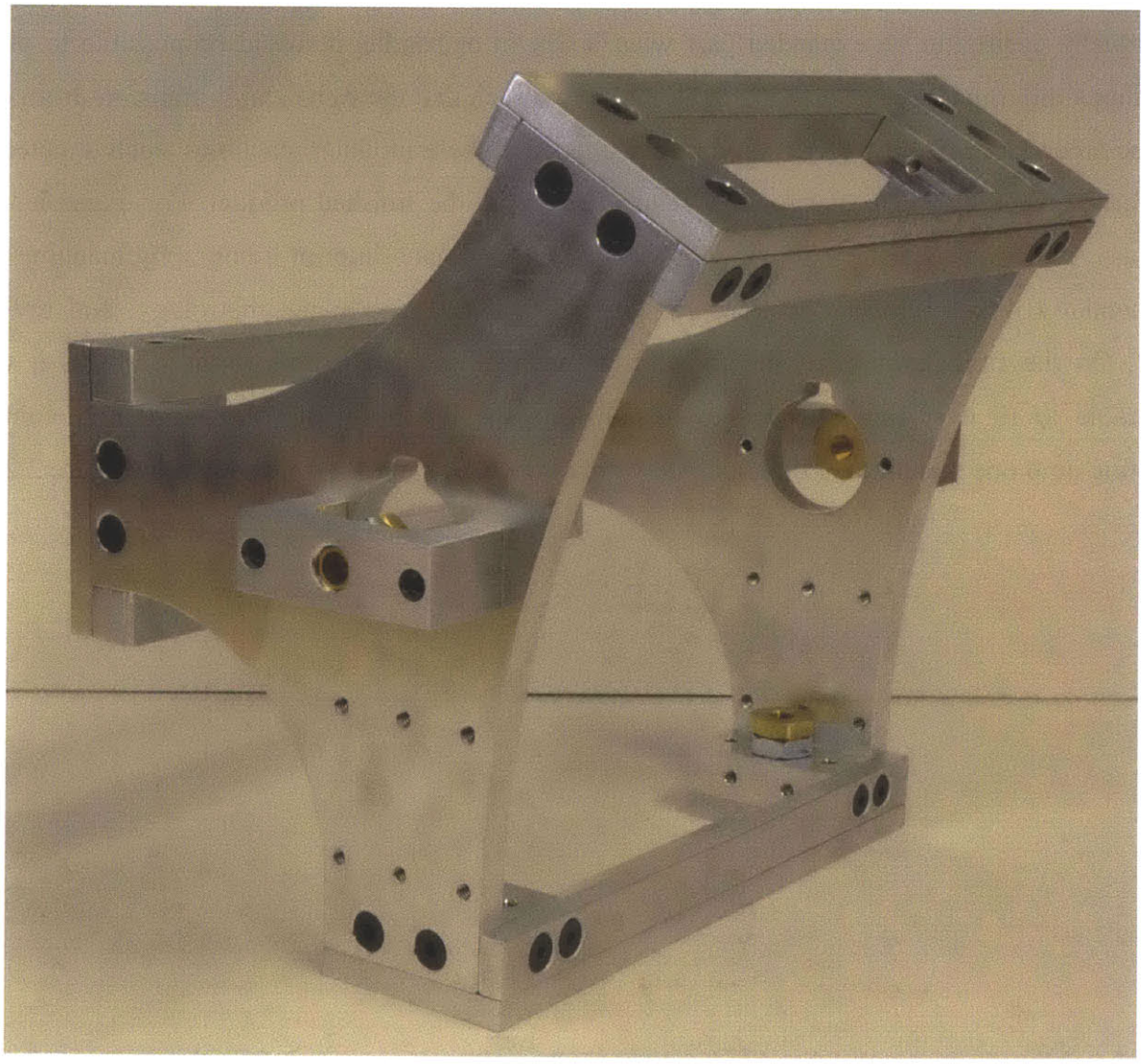

Figure 2.27: Impression roll assembly frame with air bearing mounting nuts installed

The frame is bolted to the print platform with 90-degree mounting brackets. The impression assembly and air bearings encapsulate the glass impression cylinder in such a way that it has high stiffness in all directions except for the low-friction rotation about its axis.

2.3 Structure

The machine was designed to be a bench top machine, with the potential to be moved around or placed on any lab table with a large enough footprint. If the capabilities of the machine are eventually desired to be expanded past what it can fit or handle, it would be possible to place another similar machine next to it and align the two such that the web cleanly transfers from one to the other. Conceivably, there could be a sequence of these modular machines, each devoted to performing one or two processes that help to make up the finished product. For example, the UMass Amherst Center for Hierarchical Manufacturing's nano-imprint lithography machine has sequentially linked machine sections for unwind, coating, embossing, metrology, and rewind [41]. On the first iteration of the roll-to-roll machine detailed in this thesis, though, it was desirable to fit everything needed to demonstrate the feasibility of roll-to-roll microcontact printing onto one machine. Orthogonal view drawings of this machine are shown in Figure 2.28.

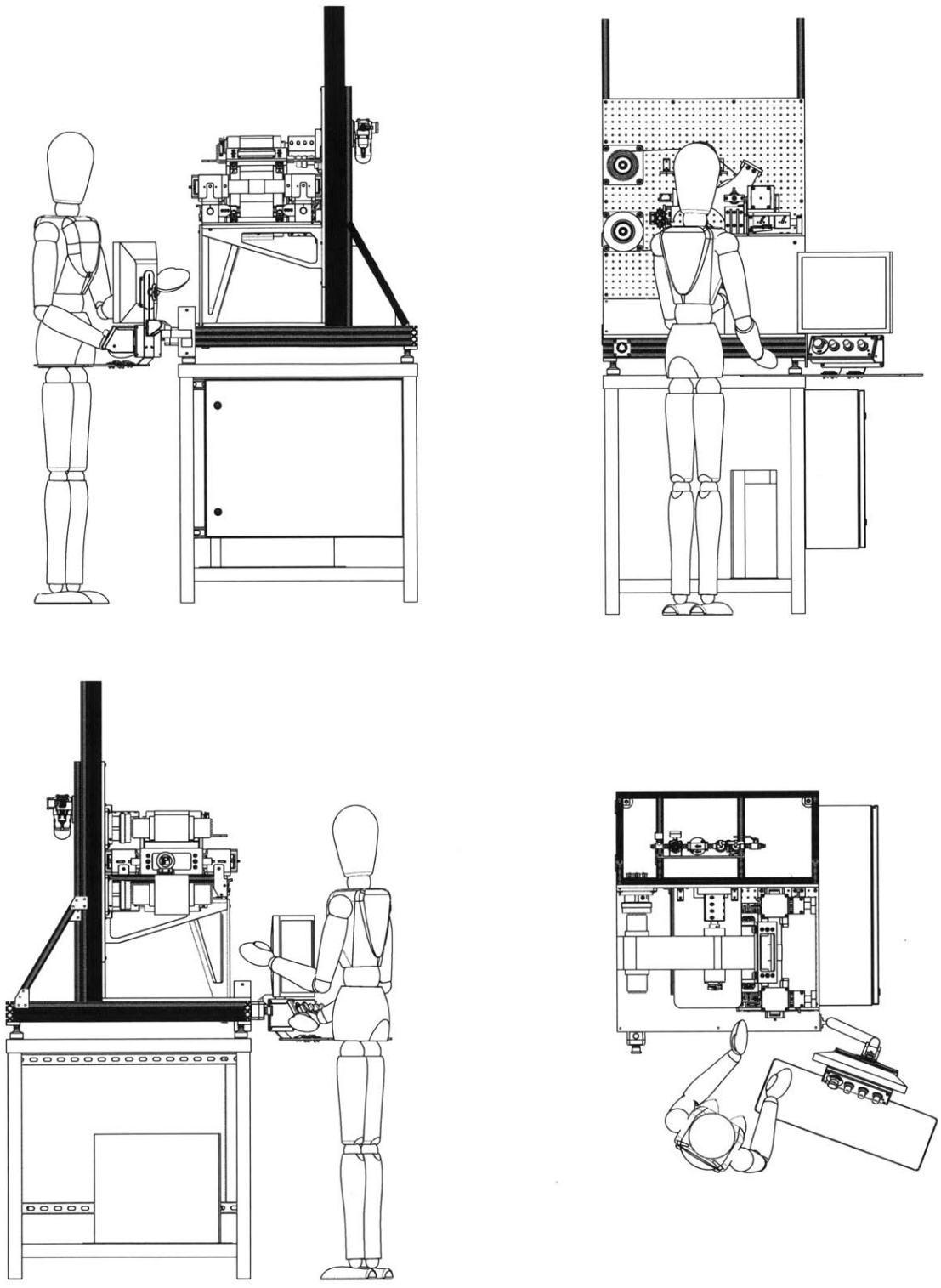

Figure 2.28: The machine structure with an operator mannequin for scale

2.3.1 Base

A heavy-duty machine table base was purchased to put the machine on. The machine table measures 30" x 30" and the machine sits entirely on top of it. For convenience, the electric cabinets and computer were mounted to the side of the machine table, and an operator interface was suspended on an arm at the corner of the table. Altogether, this forms one entirely self-contained standalone unit.

2.3.2 Frame

The structure of the machine is constructed from 80/20 aluminum T-slot extrusions. This type of framing system is commonly used to develop research scale roll-to-roll machines. It was chosen because of its modular nature, which easily allows for modifications and additions to the machine at later points in time. This is especially important for a research machine, for which there will be a lot of prototyping and development needs.

2.3.3 Backplane

Web-handling machines have many rollers that pass the substrate from process to process within the machine. In large machines with web widths up to 2 or 3 meters, these rolls are supported at each end by the machine frame. However, for smaller web-handling machines with more narrow webs, a cantilevered roll design is often employed. In this style of machine, the web is supported on rolls that are mounted to the structure at only one end. Often, there is a solid backplane to which these rolls can be bolted.

The cantilever style of design was chosen for the research machine because it allows for the operator to more easily see and access the web, as well as other machine components. A solid ½" thick aluminum breadboard was chosen to be the backplane of the machine. A Newport Optics Table was used for this purpose, as it is full of tapped ¼"-20 holes on a 1" grid. This allows for the machine's rolls and other components to be easily mounted. As well, it gives the ability to quickly change the configuration of the machine by simply moving components around on the breadboard. This optical breadboard backplane is shown in Figure 2.29.

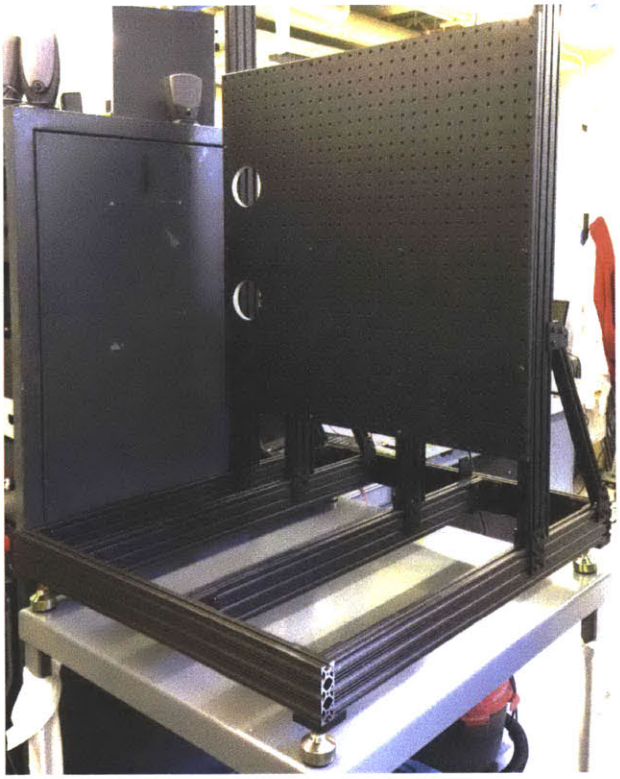

Figure 2.29: The optical breadboard backplane allows for components to be easily mounted and moved

2.3.4 Print Platform

A smaller optical breadboard was mounted perpendicular to the backplane, parallel with the ground. This print platform was designed to hold all the critical printing components. Its grid of mounting holes is also very convenient in allowing for the easy mounting of print components. In order to ensure proper alignment of the print head, kinematic hard stops are placed at two corners of the print platform to make three points of contact with the print head base plate. Figure 2.30 shows the print platform.

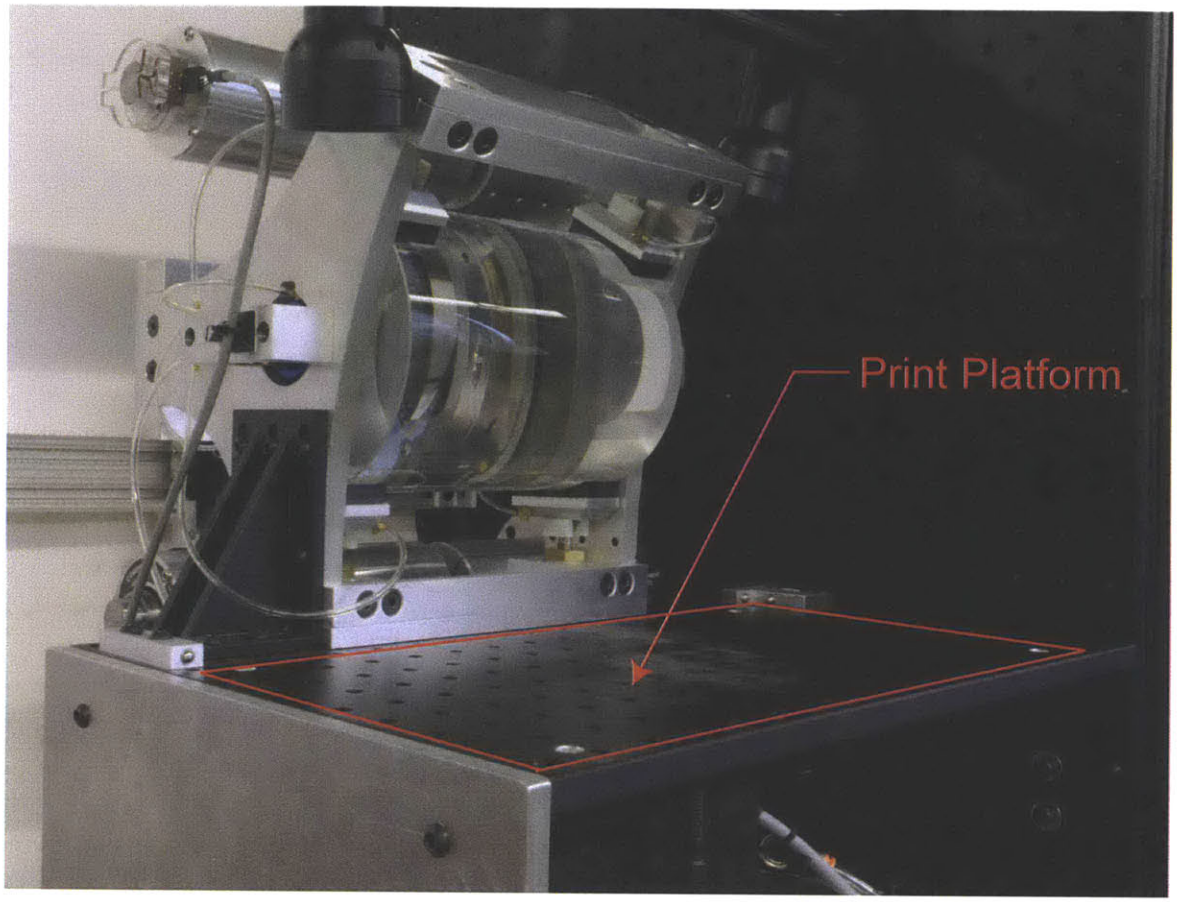

Figure 2.30: The print platform provides convenient mounting for the impression assembly (pictured) and the print head assembly (not pictured). Note the kinematic hard stops used for repeatable alignment of the print head.

2.3.5 Air Handling

On the rear of the machine, opposite from all the web-handling and print components, are mounted all of the air handling components. A two-stage filter, drier, and regulator are used to provide the clean, dry, regulated air that the machine's air bearings require. These are shown in Figure 2.31.

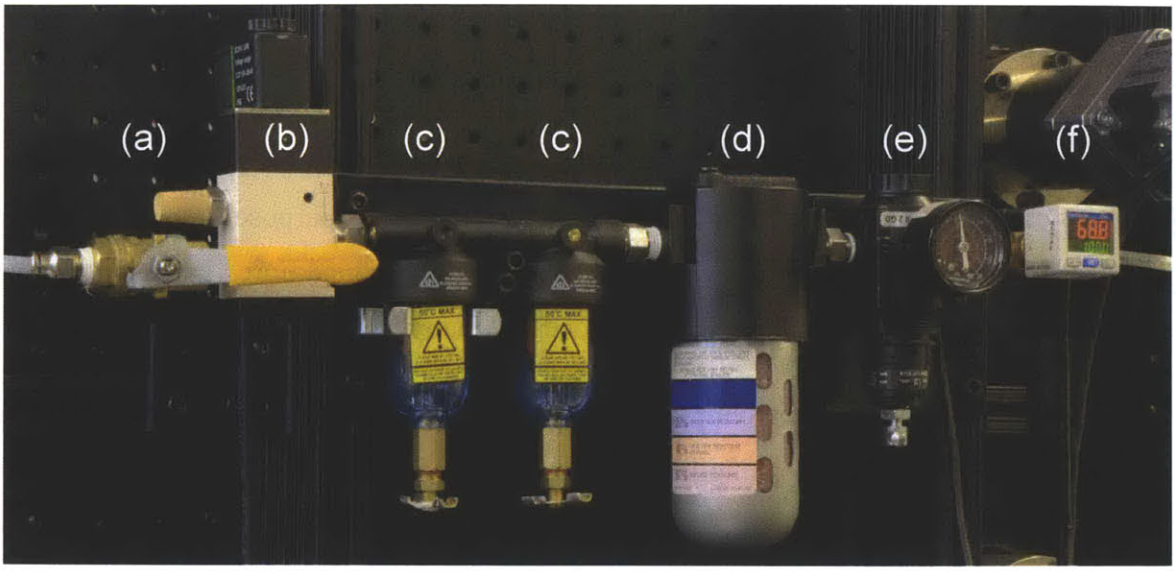

Figure 2.31: The air handling components mounted on the back of the machine. From input (building compressed air supply at ~100 psi) to output: (a) ball valve for manual shutoff of air (b) electrically actuated solenoid valve for automated shutoff, controllable by the LabView script (c) two stage coalescing filter to capture oils and particulates (d) desiccant-based air drier (e) air pressure regulator with analog gauge (f) air pressure transducer, used as an emergency shutoff switch in case the machine loses air supply

2.4 Web-handling Components

Taking inspiration from existing machines, a web-handling machine was designed specifically for the investigation of scaling microcontact printing to a roll-to-roll process.

2.4.1 Web-handling Overview

Most every web-handling machine starts with an unwind reel, which is a specialized roll meant to carry a large roll of raw web material. These rolls of material typically come on cores, which are rigid tubes of helix wound paper or plastic from 1" in diameter to 12" in diameter. Many material suppliers provide their webs on 3" ID paper cores, which the industry seems to be somewhat standardized around. Depending on the length of web contained, these material rolls can be just a few inches in outer diameter, or for more industrial and high-throughput processes like newspaper printing, the initial material rolls can be a few feet in diameter. In order to feed the web from these rolls into the web-handling machine, there exists a range of specialized 3" OD expanding reels specifically designed to chuck up raw material rolls. By using these safety

chucks, the operator is able to quickly change out empty cores for new rolls of material, or switch materials, provided they all come on the standard 3" core.

Most web-handling machines end in a rewinding process, with a rewind reel. This reel is often a safety chuck of similar design to the unwind chuck, except that its purpose is to wind the fully processed web material neatly onto an empty core. The fully wound cores can then easily be swapped for empty ones, ready to accept more processed material.

Both the unwind and rewind safety chuck reels are driven with servomotors. If the radius of the material roll is known, then controlling the rotational speed of the motor directly translates into controlling the web's linear speed. Or, still knowing the radius of the roll, control of the motor's torque is a stand-in for controlling the web's tension. Often, an ultrasonic distance sensor aimed at the center of the safety chuck is used to determine the radius of the roll at any given point in time. This lays the groundwork for controlling web tension and speed in a simple web-handling machine, as there are two safety chuck reels to control these two web characteristics.

The simplest web-handling machine might be one with just two rolls: an unwind stand and a rewind stand. If the radius of each roll is measured, then using torque control on one motor and rotational speed control on the other motor allows for accurate control of both the web's linear speed and tension. From this framework, specialized rolls and components can be added to the web path as necessary in order to accomplish the desired manufacturing process.

2.4.2 Functional Requirements

It was decided that the web-handling machine used to demonstrate scale-up of microcontact printing should be as simple as possible. Web-handling is something that is widely done in the industry and is not the focus of this research. Rather, the purpose of the web-handling machine is just to provide an ideal substrate for the roll-to-roll microcontact printing experiments.

For best printing results, it was determined that the substrate should move at as near a constant speed as possible. This will allow the rolls in the system to operate in a steady state, rather than having to accelerate or decelerate with any web speed transients. This is especially important in the case of a passively driven print roll, for which the print rotation comes simply as a result of shear force from stamp contact with the substrate. With a massive print roll, there can be some

significant torques required for any change in rotational speed. Therefore, if the web speed is changing significantly, there will be varying amounts of shear on the stamp's features. This shear could cause features to buckle or smear along the substrate.

As well, the web should have minimal movement in the transverse direction, perpendicular to the web's movement. This side-to-side shifting of the web could result in sheared features, or with a lower frequency of movement, wave-like deformations in the printed results rather than straight or aligned features.

Finally, it was determined that the web should have constant tension across the contact length of the stamp. If the tension were to vary in this region, then stamp features would be moving in shear relative to each other as the web stretches or contracts. This would result in smearing or other undesirable distortions in the printed result.

The functional requirements for the web-handling machine were formed around the desire to have the ideal printing substrate. The following sections detail the design choices used to ensure a robust and reliable web-handling system, so that the focus of the research can be on the printing rather than the mechanics of the web.

2.4.3 Five Roll Design Choice

The simplest web-handling machine that could be used in this microcontact printing machine would have simply an unwind reel, an impression cylinder, and a rewind reel. Though this three-roll system meets all three primary functional requirements, it introduces a few issues.

As web moves through the system from the unwind roll to the rewind roll, these rolls are decreasing and increasing in diameter, respectively. The rate of diameter change depends on the web speed, the thickness of the web, and the diameter of the roll at any given moment in time. This means that the total included angle of web wrap around the impression cylinder changes over time. As well, this means that the resultant force on the impression cylinder due to web tension would be varying in both direction and magnitude over time. Because the impression roll is held in place with bearings of finite stiffness, the variations in web wrap angle, resultant force direction, and resultant force magnitude could cause the impression cylinder to shift in position over the course of a long printing run.

The purpose of the impression cylinder is to provide an ideal backup datum for the substrate, so it was determined that the addition of an entry idler roll and an exit idler roll would be a cheap and simple solution for removing the effects of time-varying variables from the system. As the web leaves the unwind roll, it goes first over an idler roll before wrapping around the impression cylinder, and exits the impression cylinder to go over one more idler roll before being rewound. By fixing the placement of these idler rolls, the wrap angle, resultant force magnitude, and resultant force direction on the impression cylinder are all constant (the latter two with respect to web tension). As well, the inclusion of these idler rolls allows for a stationary web path between each of them and the impression cylinder, which could be very useful in the case of downstream inspection with a camera. This could be done by mounting the camera in such a way that it is focused on the surface plane of the web. Without these idler rolls, the web would move in and out of the focal plane of the camera as the unwind and rewind rolls change diameter. The comparison of the three-roll and five-roll layouts presented in Figure 2.32 and Figure 2.33.

The inclusion of an idler roll provided an easy place to mount a rotary position optical encoder, which, combined with the measured constant idler roll radius, would give a clear measurement of linear web position and speed. Finally, the idler roll mounts could be instrumented with strain gauges or replaced with application-specific load cells to measure the force on them, which would give a measure of tension in the web at each idler.

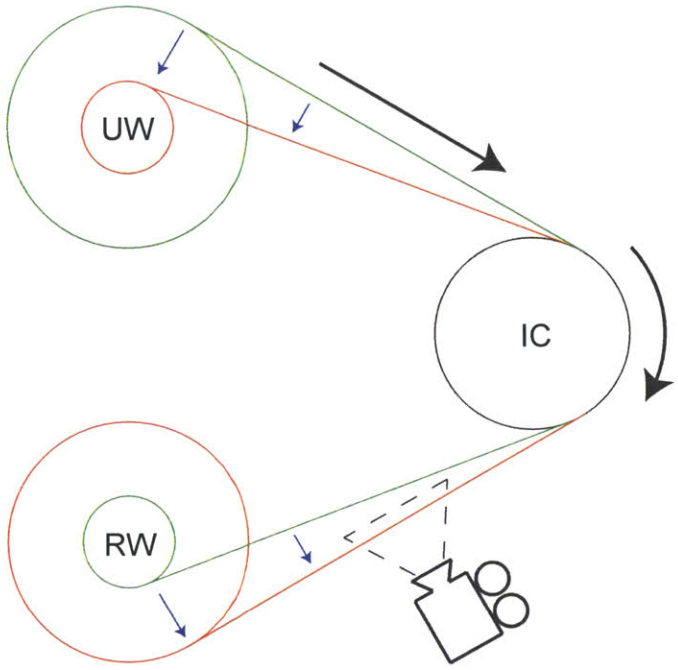

Figure 2.32: As the unwind roll (UW) decreases in diameter and the rewind roll (RW) increases in diameter, there are slight changes to the web path entering and exiting the impression cylinder (IC). Compare the initial state of the machine (green) to the final state of the machine (red). This changing web path makes it difficult for a camera to stay focused on the web, as it is moving in and out of the camera's focal plane.

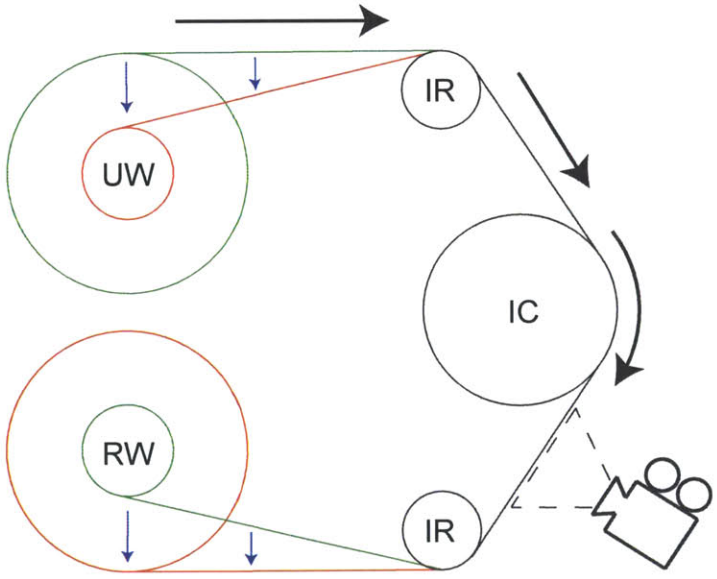

Figure 2.33: The inclusion of entry and exit idler rolls (IR) ensure that there is a consistent web path entering and exiting the impression cylinder (IC), regardless of the diameter of the unwind (UW) and rewind (RW) rolls. This gives the opportunity for an inspection camera to be placed downstream of the print region, with the web always remaining in focus.

2.4.4 Substrate Material Choice

There exist a wide variety of flexible substrates suitable for roll-to-roll processing. The most general requirement for a material to be compatible with a web-handling machine is that it must be thin, flexible, and available in long lengths on a roll. In the printed electronics industry, some of the most common substrates are paper, plastic film, and metal foil. There are many characteristics that make a material more or less suitable for a given web-handling machine or process. For this machine, the selection of substrate had to fulfill the following criteria.

1. The web must be available on 3" diameter cores so that it can be loaded onto the unwind reel safety chuck.

2. The web must be at least 60mm wide if the entire width of the stamp is to be printed, though stamps can be cut down to size if a more narrow web or print region is desired.

3. The web must be no wider than 5.5" so that it can fit on the machine, with the bottleneck being the spacing between the air bearings that hold the impression cylinder.

4. The web must be flexible enough to withstand a bend radius of 1.5" without any damage, as it will have to safely bend around the idler rolls with this radius. For most papers, films, and foils, this should not be an issue. However, there are some thin flexible glass substrates on the market, such as Corning's Willow Glass, that could be interesting to experiment with. A 1.5" bend radius is near the limit of what these thin glass substrates are able to safely handle.

As well, if the process of microcontact printing using a PDMS stamp with micron-sized features is to be considered, then some additional constraints are placed on the potential substrate choices.

5. The substrate must be very smooth. Though PDMS is elastic and can conform to substrate irregularities on some scales, a substrate with significant thickness variations or surface roughness will make it difficult for the stamp to achieve complete conformal contact. The magnitude of acceptable web thickness variation and surface roughness depends mainly on the stamp's geometry and material properties, but also on the performance of the print head controller.

6. The substrate must readily accept the ink used in the printing process. For example, if a self-assembling monolayer ink such as alkanethiols are used, then a gold film substrate is required to allow for molecular assembly. It is also possible to use plastic films with thin vapor-deposited metal coatings, onto which the molecular ink could assemble. Or, if a liquid ink is used, such as a typical flexographic ink, then the substrate must have a suitably high surface energy for ink adhesion.

Finally, if real-time *in-situ* visual inspection of the contact region is desired, then there exists one last requirement of the substrate:

7. The substrate must be optically transparent. Because the camera is on the opposite side of the substrate from the stamp contact region, the substrate must be optically clear in order for the camera to visualize the contact.

Considering all of these criteria, it was determined that the machine should be designed around polyethylene terephthalate (PET) film. PET is a thermoplastic polymer resin in the polyester family that is widely used due to its characteristic of being a good water and moisture barrier. For example, PET films can be found in food packaging. As well, it is a common substrate in the printed electronics and solar energy industry. The back of crystalline photovoltaic cells may be laminated in PET film, or the film may serve as the substrate for flexible thin film photovoltaic modules.

One of the benefits of using PET for roll-to-roll microcontact printing trials is that it is so widely used in the industry and well understood as a substrate. Because of this, it is also readily available from a multitude of suppliers and at a very low cost. As well, there are hundreds of different formulations of PET available in a variety of thicknesses and surface treatments, each made for a specific application. In this case, it was desirable to find a PET film with high optical transmission to promote visualization of the contact region and high surface energy to promote ink adhesion. Each of the major manufacturers of PET film seems to have a film or two specifically made for the purpose: DuPont Teijin's Melinex 454, Mitsubishi's Hostphan 4507, and SKC's SH82 are all marketed as "ultra-clear" films specially treated or coated for print adhesion.

Five rolls of Mitsubishi's Hostaphan 4507 film were procured for use with the machine. The purchased film was 0.002" thick, after an experimental roll of 0.005" thick PET proved to be much tougher and thicker than required. Each roll of film came with 1000 feet of 5" wide PET wound on 3" ID paper cores. One of these rolls is shown in Figure 2.34.

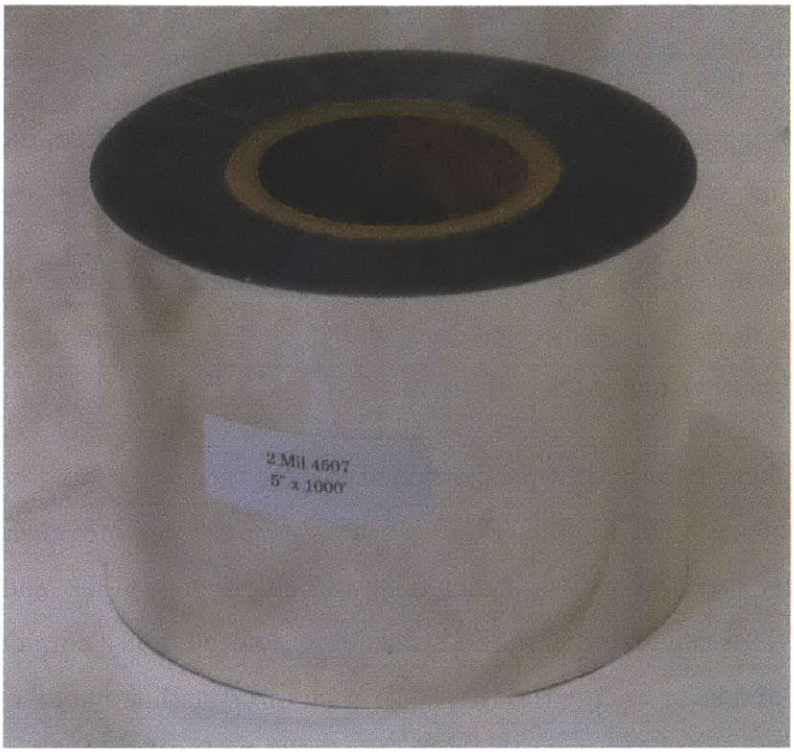

Figure 2.34: Roll of 500 feet of 5" wide, 0.002" thick Hostaphan 4507 PET film on a 3" ID wound paper core

Nominally, the PET web will be stretched taut and flat throughout the machine. One of the most common causes for defects in roll-to-roll processes is a wrinkled web. Wrinkled webs can present for a variety of reasons, and the web-handling industry has developed many methods of dealing with this problem. On such a small scale narrow-web machine, though, web wrinkling should not be an issue so long as there is sufficient web tension. Most web-handling experts recommend a tension of approximately 1 PLI/mil for PET. This is 1 pound of tension per linear inch of web width per mil of thickness. For a 5" wide, 0.002" thick web, this translates to a desired web tension of 10 pounds. Note that the specification of 1 PLI/mil is equivalent to an applied normal stress in the web of 1000 psi. Many suppliers specify a yield strength for PET of around 10,000 psi, so the nominal handling tension of 10% of that value is reasonable.

The Hostaphan 4507 film is "print treated" to promote ink adhesion, though it is unknown what process or material they use to treat or coat the film. It was measured with a set of dyne pens to have a surface energy of 42 dynes/cm^2. These test are shown in Figure 2.35. Many flexography inks are formulated for substrates with surface energies between 38 and 42 dynes/cm^2. In order to use such inks, it would be best to corona treat the PET film before printing to boost its surface energy.

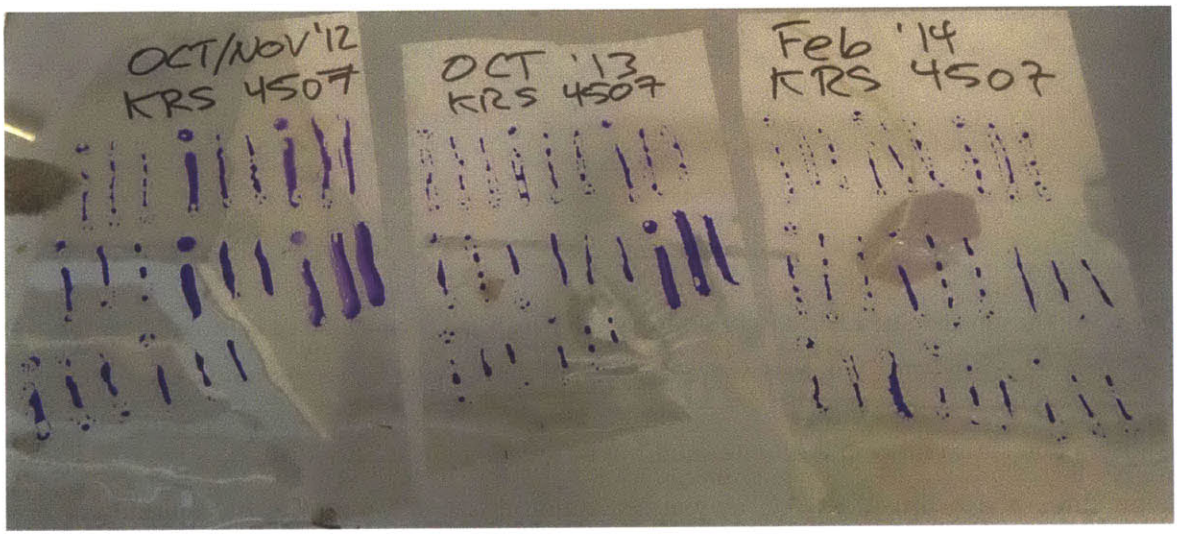

Figure 2.35: Surface energy measurements of PET film using a set of standardized Dyne Pens. Each marker in the set has an ink that is specifically formulated to have the stated surface energy. By testing which pens are able to wet the PET film surface and which pens are not, it is possible to discern the surface energy of the PET film.

2.4.5 Unwind and Rewind

The unwind and rewind stands were purchased from Double E company. They are the CLEV12-TBA 3" diameter cantilevered expanding shaft chucks manufactured by International Expanding Shafts S.R.L. These chucks allow for the quick changing of material rolls through a mechanically expanding shaft. When torque is applied to the material roll, numerous steel balls expand radially outwards and engage the inner surface of the material core. This locks the material roll in a self-centering fashion and allows for torque transfer from the shaft to the web. The back of the chuck has a spindle that has been machined with a drive shaft bore and broached internal keyseat to match that of the specified motor gearbox. One of these safety chucks is pictured in Figure 2.36.

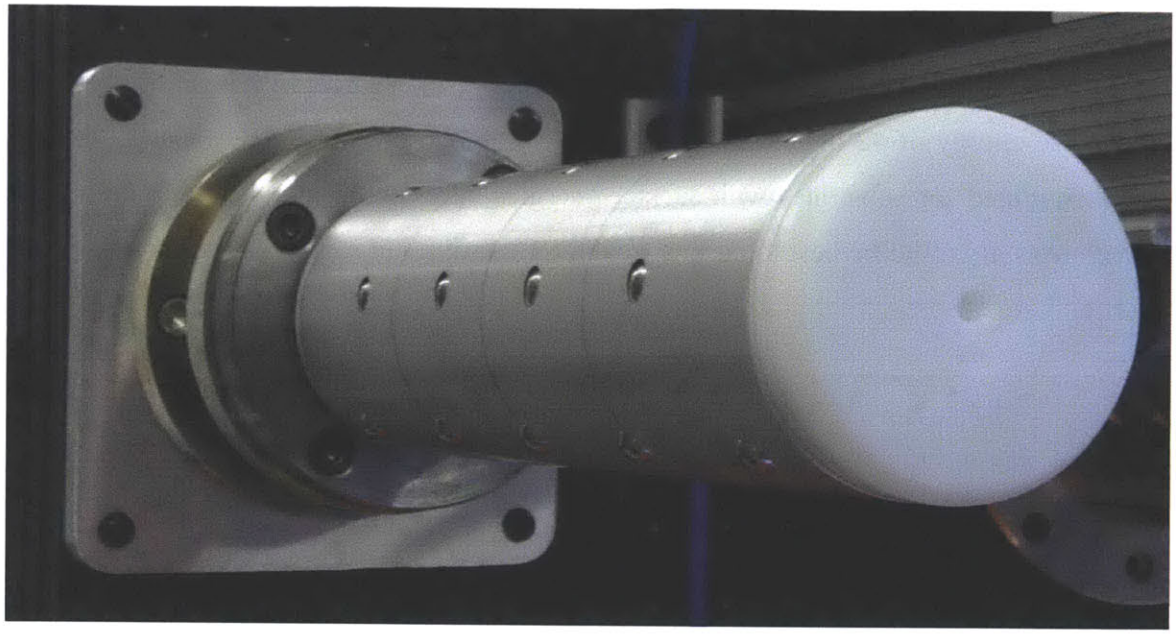

Figure 2.36: The unwind and rewind reels are expanding-shaft safety chucks. The balls visible in this roller expand outward to securely grip the material roll core for torque transfer

The motors chosen to drive the unwind and rewind reels are the Sure Servo SVL-202. These are 230 volt three-phase brushless AC driven servomotors rated for 200 watts continuous power. They are the low inertia model, with an integrated 2500 line count encoder which gives 10000 counts per revolution. The rated continuous torque is 5.7 lb-in, while the maximum rated torque is 16.9 lb-in. The rated continuous speed is 3000 rpm, with the max speed being 5000 rpm.

These servomotors are driven by the Sure Servo SVA-2040 motor drivers. This AC motor driver is rated for 400 watts continuous power and is matched to the SVL-202 motors. The motor driver can be operated in position control, velocity control, or torque control modes.

The mating gearbox is the Neugart PLE60 with a 32:1 gear ratio. These high-efficiency planetary gearboxes are rated for 390 lb-in of torque. They directly mate with the driveshaft and face of the SVL-202 motors. The keyed output shaft of the gearbox mates with the machined spindle of the unwind and rewind chucks. The motor-gearbox combination is diagrammed in Figure 2.37.

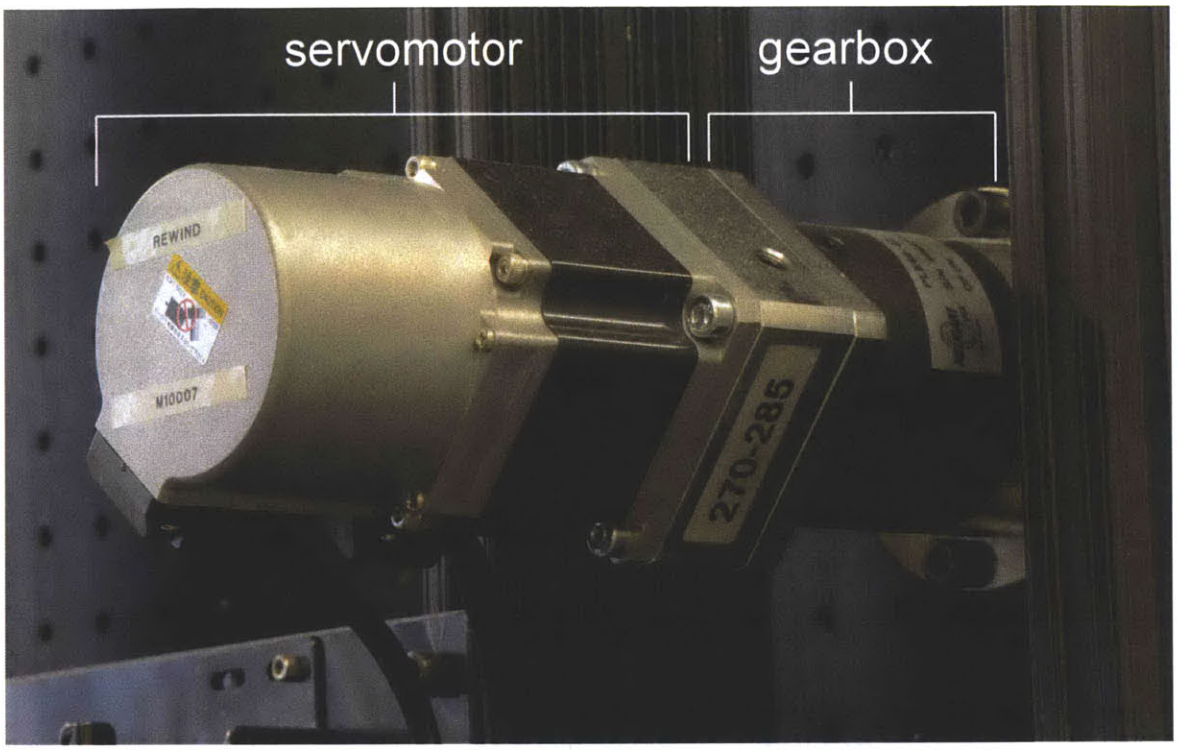

Figure 2.37: The servomotor and gearbox that are used to drive the unwind and rewind rolls

The torque-speed curve for the SVL-202 motor is flat from the point of maximum continuous speed to the point of maximum continuous torque. Therefore, the combination of the gearbox, servomotor, and motor driver gives each safety chuck a rated speed of 93.75 rpm at a torque of 182 lb-in (20.5 N-m). For a chuck with an empty material core, this allows for 14.7 in/s (0.37 m/s) web speed at 122 lbs of web tension. For the largest material roll that the machine is designed for, a 9" OD, the motor and gearbox specs allow for 44.2 in/s (1.1 m/s) web speed at 40.5 lbs (180 N) of web tension. However, in a full production run, the entire amount of web material will transfer from the unwind reel to the rewind reel. This means that only the lesser of each of the web speed and tension values can be reliably achieved, giving a maximum feasibly sustainable web speed of 14.7 in/s (0.37 m/s) at a web tension of 40.5 lbs (180 N).

2.4.6 Idler Rolls

Two idler rolls were provided by Componex Corporation. They are the WINertia Standard Lightweight Aluminum Dead Shaft Idler Rollers. These are the 3 x 2 Lite WINertia model, which is a 3.070" OD idler roll rotating on a 1" steel dead shaft that runs through the center of

the roll. The total indicated runout is specified to be 0.0005" per foot, and they are balanced for web speeds up to 2000 feet per minute. A photo of one of the idler rolls is presented in Figure 2.38

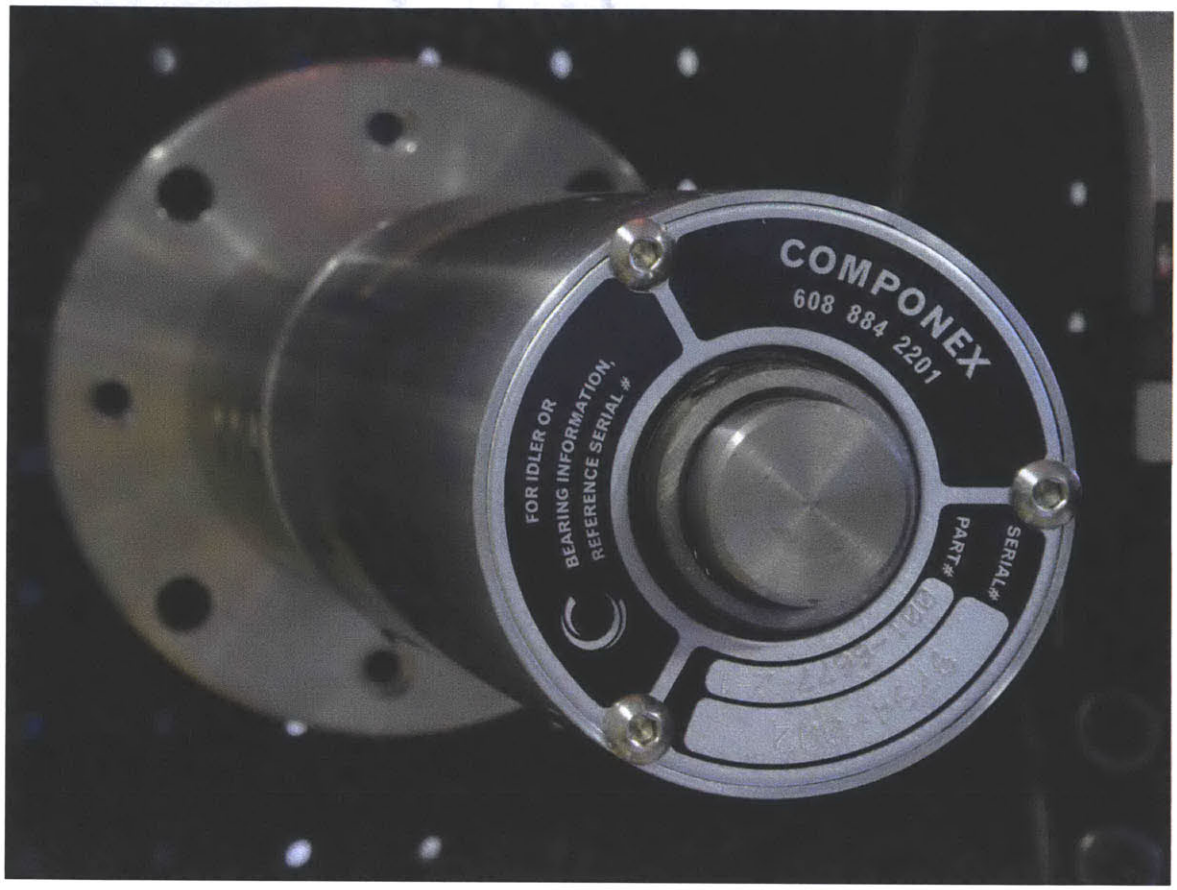

Figure 2.38: One of the Componex dead shaft idler rolls

The idler rolls came with the dead shaft protruding from one end. In order to mount these as cantilevered rolls, a cantilever mount had to be machined. A clamp was designed for the idler roll's dead shaft, and this was attached to a face-mounting flange with bolt-hole patterns that match the hole spacing on the optical breadboard backplane. This allows the idler rolls to be easily moved on the backplane and mounted in a variety of places. With easily movable idlers, experiments can be run for a variety of different impression cylinder wrap angles.

The idler roll cantilever mounts were machined out of aluminum. The first revision was designed to be monolithic, and made from a solid piece of aluminum. The second revision used two separate pieces of aluminum. The dead shaft clamp and the flange mount were machined

independently, and then bolted together to form the cantilever mount. These two idler roll mounts are shown in Figure 2.39.

Figure 2.39: Idler rolls in flange-mounted clamps. The left mount is made from billet aluminum, while the right mount is a two-piece clamp and flange design.

2.4.7 Web Sensing

One of the benefits of having idler rolls in the system is that they can be easily instrumented. A cantilever mount could be designed to have integrated strain gauges that measure the force on the roll. Knowing both the web's resultant force and wrap angle on the roll allows for the calculation of a real-time high-bandwidth measurement of the web tension. This is commonly done in the industry, and there are even many off-the-shelf solutions for cantilever mounts with integrated load cells, or even fully packaged cantilevered load cell idler rolls and mounts. A diagram of how the resultant force on a load cell might be calculated is diagrammed in Figure 2.40.

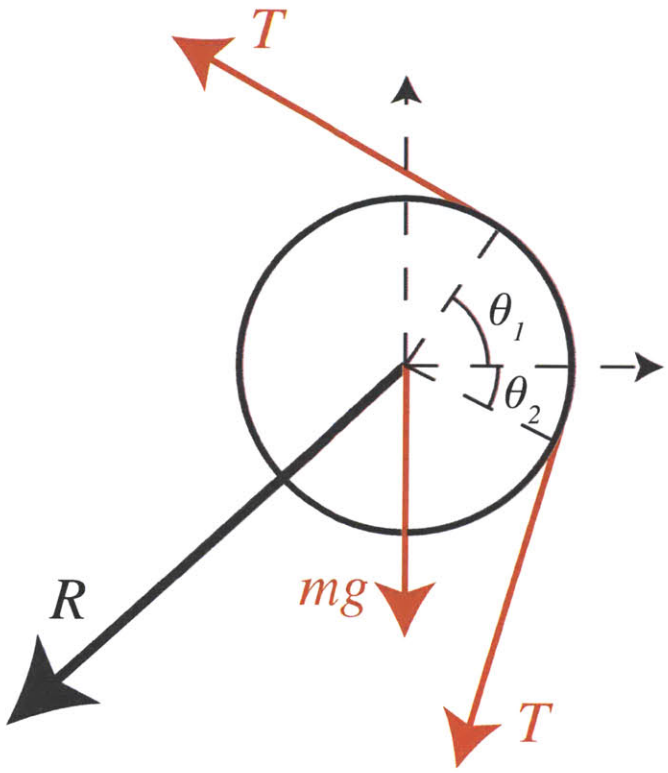

Figure 2.40: Diagram of web tension sensing with idler roll load cells

The machine is not currently equipped with any active tension measurement, other than the indirect tension control via motor torque. This method was deemed to give steady enough tension for initial experiments, as the process should not be highly sensitive to tension so long as the web is sufficiently taut and tracking well. Further improvements to the machine should include the making or purchase of a load cell idler roll that can give detailed tension

measurements and feed these back into the web-handling control loop so that it can be controlled for a specific constant tension value.

Another way to instrument the idler roll is with an encoder to use it to measure web speed. By equipping the idler roll with a rotary optical encoder, the angle of the idler roll can be easily measured. With timing, it is possible to measure the rotational speed of the idler roll, and therefore, with the radius of the idler known, the linear speed of the web. The process is highly sensitive to varying web speeds, so one of the idler rolls was modified to have a rotary optical encoder. A standoff mount was designed and machined for the US Digital DISK-2 transmissive rotary encoder disk. This 2" diameter, 0.007" thick Mylar polyester disc has an optical quadrature track with 2500 counts per revolution. Another mount was designed and machined for the US Digital EM1 Transmissive Optical Encoder Module. This encoder read-head is carefully aligned to the encoder disk and outputs the quadrature signal from the spinning disk as a digital signal. A close-up photo of the idler roll encoder disk is shown in Figure 2.41.

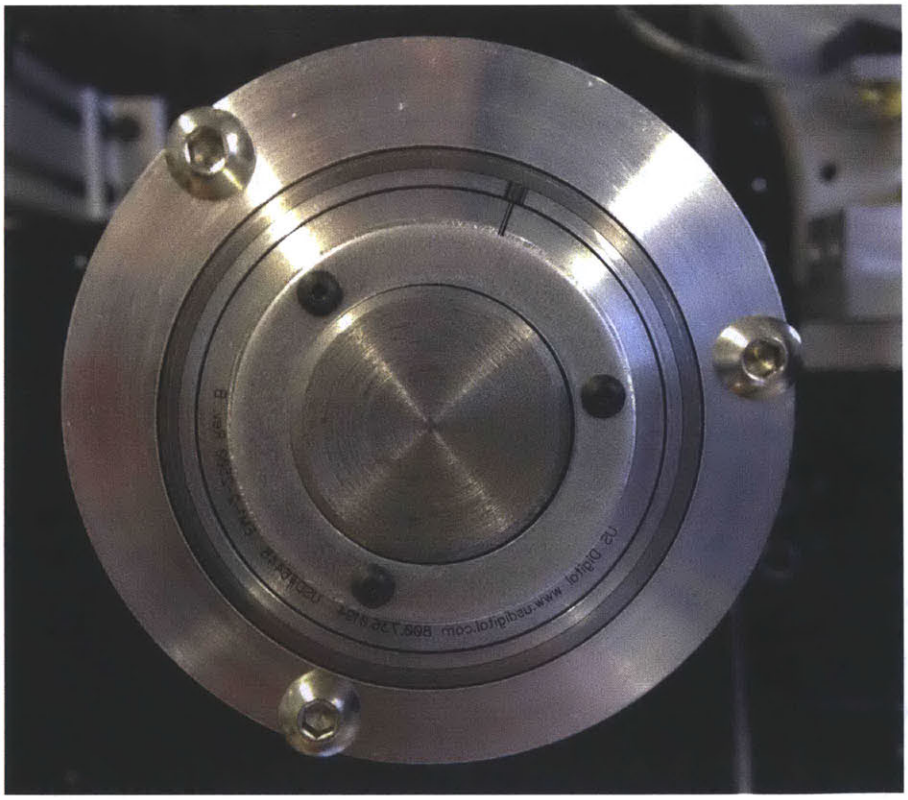

Figure 2.41: The rotary optical encoder disk mounted on the custom machined idler roll faceplate standoff. The encoder read-head (not pictured) gives 2500 counts of quadrature per rotation of the idler roll.

Using a quadrature decoder and counter allows for the accurate tracking of the idler roll's rotation, and therefore the web's movement. The National Instruments 9401 8 Channel 5V TTL High-Speed Bidirectional Digital I/O Module is used to acquire these digital signals. This module interfaces with the National Instruments CompactDAQ system. One of the CompactDAQ's four onboard high-speed counters is used to count the quadrature coming from the rotary optical encoder. Through LabView, it is possible to know the position of the idler, and therefore web, at all times. With millisecond timing, it is possible to calculate the idler roll's rotational speed and therefore the web's linear speed.

2.4.8 Steering

The need for a steering roll was investigated, so that the substrate could be actively controlled to have good tracking and little transverse direction movement. Talking to people with decades of experience in the web-handling industry from multiple companies indicated that a steering roll would not be necessary, though. On such a small system with so few rolls, the web should not require any active steering. Instead, just a careful alignment of all the rolls prior to running the machine should be enough to guarantee consistent web tracking without any significant wandering. Steering stations are bulky and expensive if bought off the shelf, require entry and exit idler rolls, and introduce tension gradients across the web. For these reasons, it was decided that the first revision of the machine should not include an active steering roller, but that the web should be closely observed for transverse direction movement so as to determine whether steering will be needed in future revisions.

2.5 Electronics and Software

Nill detailed the design of the electronics and software his Master's thesis [40]. Whereas many research machines have electrical boxes that look like cobwebs and rats nests of disorganized wires, this machine's electrical components and installation were intended to be as professional as possible. As with an industrial machine, applicable National Electrical Codes were strictly adhered to, and electrical best practices were followed. The robust electrical system architecture, neat installation, and thorough documentation of all the electrical components and connections enable this machine to perform with high reliability and allow for easy troubleshooting.

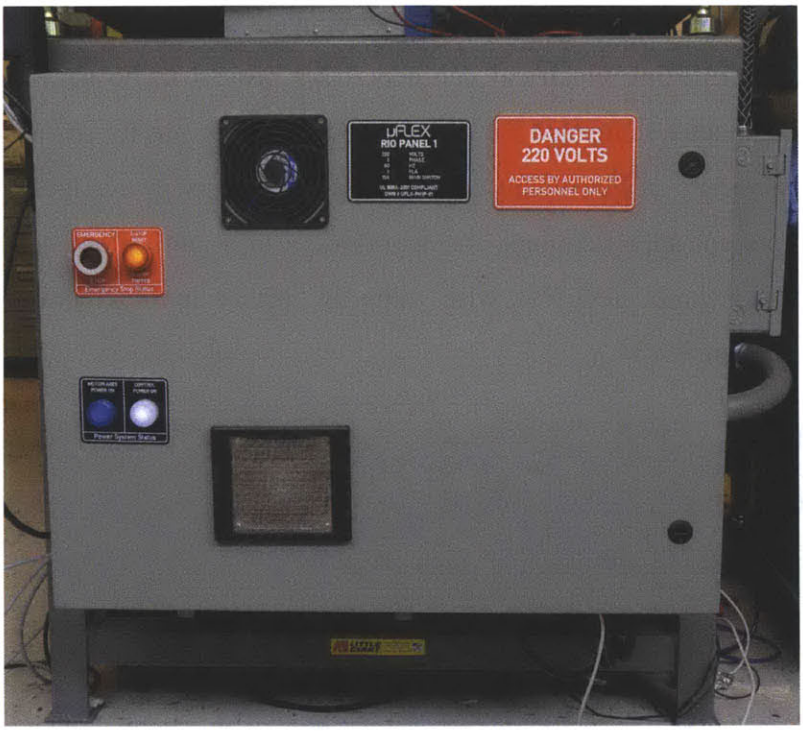

Figure 2.42: The electrical cabinet, closed

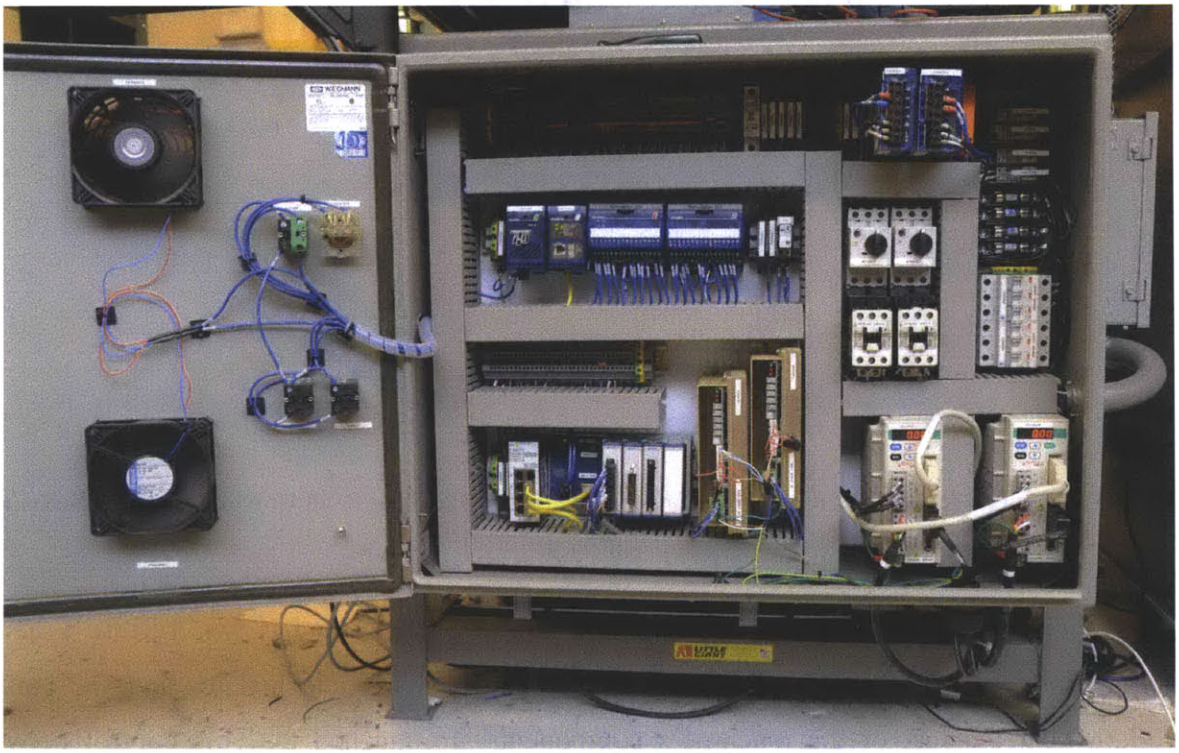

Figure 2.43: The electrical cabinet, open. A full description of the components pictured is available in [40]

The adherence to industry standards allows for the replication of the machine by any contractor reasonably skilled in outfitting electrical cabinets. This proved to be necessary when a near-duplicate electrical cabinet was needed for a replicate machine made for the project collaborators at the King Faud University of Petroleum and Minerals. With readily available blueprints, wiring diagrams, and component specifications, the work was easily outsourced to a contractor, who was able to build the same electrical with minimal further involvement or guidance. This machine is shown in Figure 2.44.

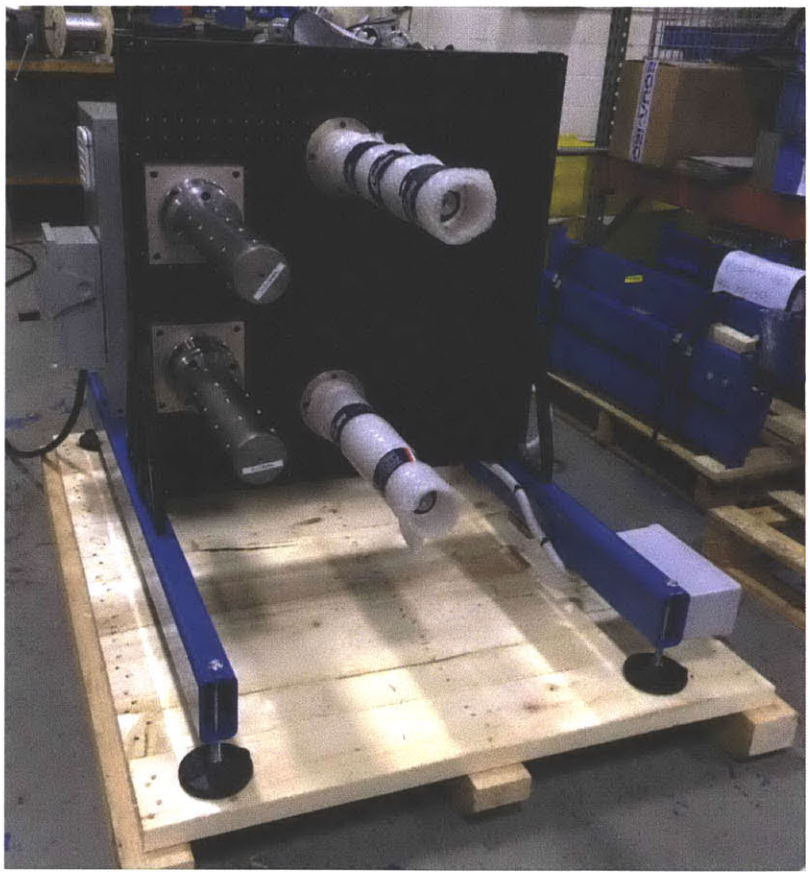

Figure 2.44: The near-replicate machine, built by contractors for the King Faud University of Petroleum and Minerals.

The machine is controlled with LabView running on a PC. This PC has two TCP/IP Ethernet networks: the camera network, which the inspection camera is attached to, and the control network, which the rest of the machine's components are attached to. This control network interfaces with a National Instruments CompactDAQ system. The CompactDAQ provides +/- 10V DAC outputs for the web-handling motor drivers and for the print head's voice coil

amplifiers. As well, 24V digital inputs are interfaced with the HMI terminal, the three E-stop switches, and the air pressure transducer. A 24V digital output controls the air supply solenoid valve. Finally, high-speed 10 MHz digital inputs and counters are used for the print head position encoders, as well as the idler roll rotary encoder for the web.

Bench top power supplies are used to power the 5V linear and rotary encoder interfaces. As well, a bench top power supply is used to provide current to the UV LED flashlights that cause the stamp to fluoresce.

The user interacts with the machine via the human-machine interface (HMI). The HMI consists of a computer monitor, keyboard, mouse, and control panel mounted on a swing arm at standing height. This is shown in Figure 2.45.

Figure 2.45: The human machine interface (HMI) terminal

CHAPTER

3

MACHINE CHARACTERIZATION

The roll-to-roll microcontact printing machine was manufactured in-house. The machine was built to specification, assembled, and connected to the building's high-voltage mains and air supply. A photo of the completed machine is shown in Figure 3.1.

Before research on roll-to-roll microcontact printing process could commence, the machine was characterized to ensure that each component meets the design requirements. Special consideration was given to investigating any non-idealities that could prevent the printing process from achieving the precision it requires. This chapter details that investigation and the characterization of each of the machine components.

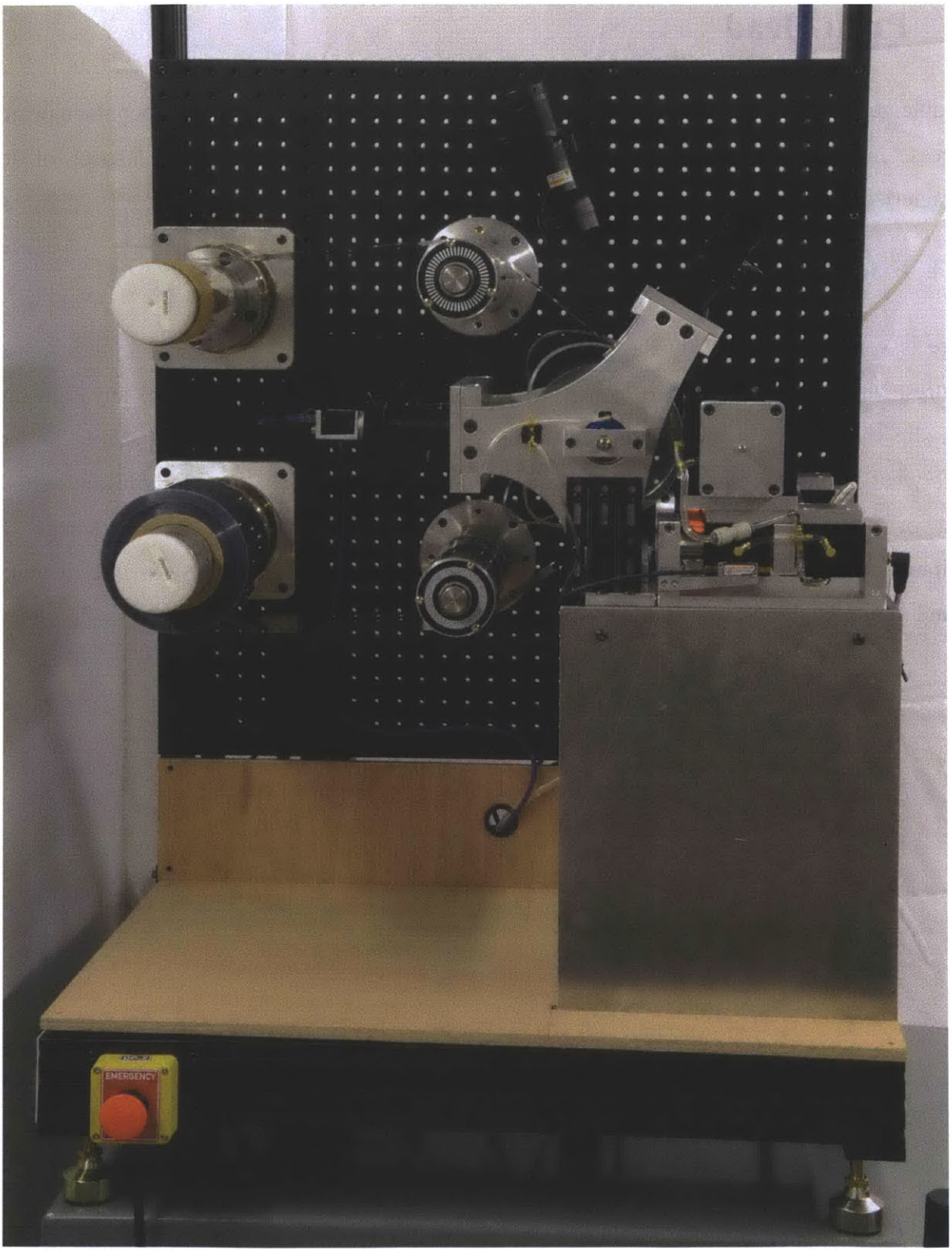

Figure 3.1: The completed roll-to-roll microcontact printing machine

3.1 Print Head

Reliable performance of the print head is critical to the success of the microcontact printing process. In order to ensure that the print head works as designed, each aspect of it is characterized.

3.1.1 Friction

There is very little friction in the print head assembly because of the use of air bearings and flexures. More importantly, there is not any noticeable stiction. The presence of any significant stick-slip motion could present difficulty for the print head, as it needs to be able to move reliably in the micron and sub-micron range. When the stage is floating without any actuator input or physical disturbances, the encoders report sub-micron random movements and oscillations from the stage. This could be due to the hiss of the air supply, or due to general ground motion and mechanical vibrations from the environment.

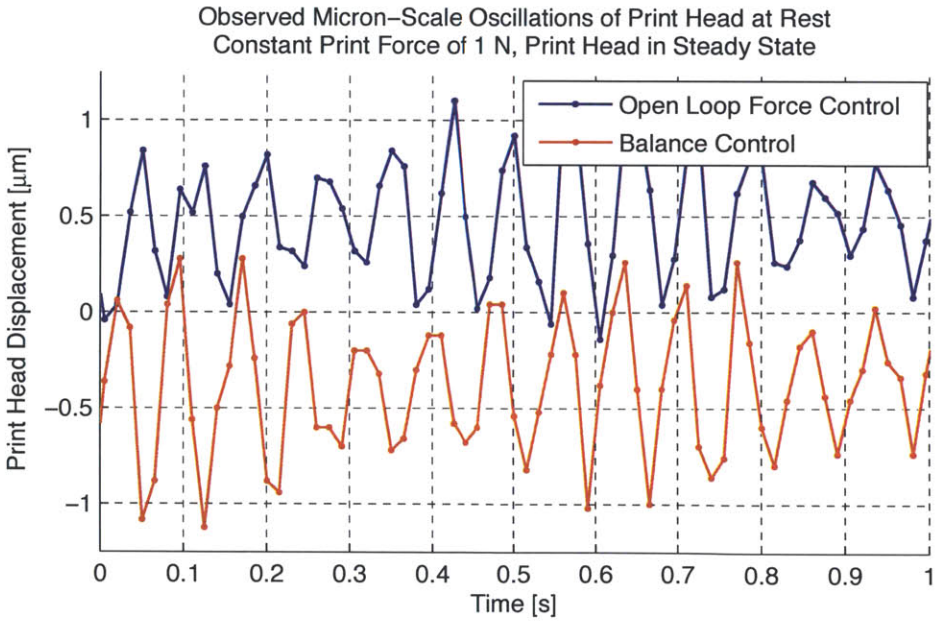

Figure 3.2: Print head displacement oscillations at rest: The stamp is gently pressed up against the stationary impression cylinder with a print force of 1 N and allowed to come to rest. The micron-scale oscillations are persistent and independent of the controller being used. It is hypothesized that these oscillations are due to vibrations from the ground that are transmitted through the machine structure.

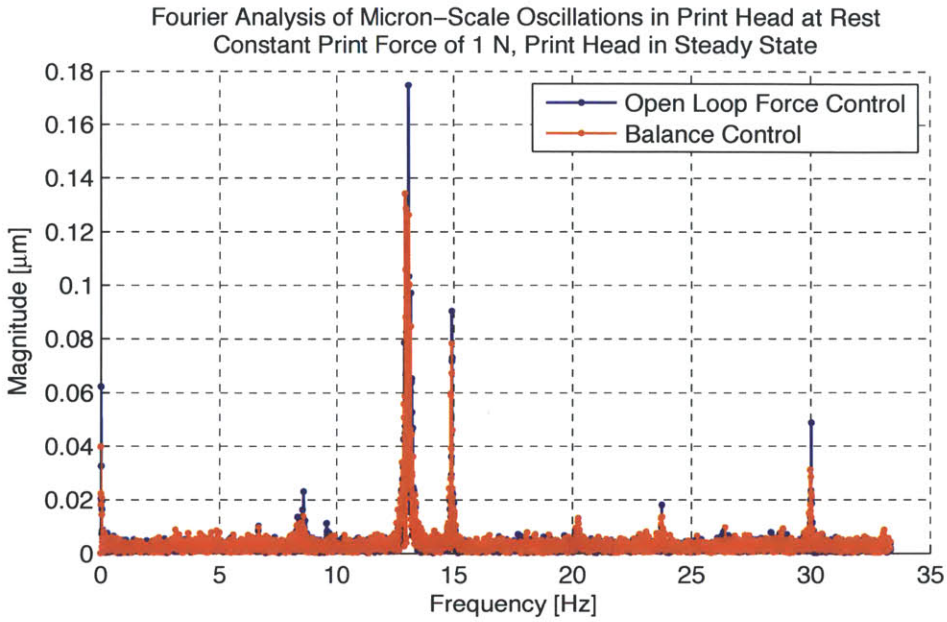

Figure 3.3: Print head displacement oscillations at rest: A frequency domain analysis is performed for the oscillations visible in Figure 3.2. The oscillations are comprised of a strong 13 Hz signal, in addition to a 15 Hz and 30 Hz signals. The 30 Hz mode is likely a harmonic of the 15 Hz mode.

The cause of these oscillations is unknown, but it is hypothesized that they are a natural movement due to the hiss of the air bearings, or more likely, that the vibrations from the ground are transmitted through the machine structure to the print head. In this iteration of the machine, only simple vibration absorbing rubber feet were used on the machine. For sub-micron scale printing with future revisions of the machine, an optics grade vibration isolation table will be necessary.

With such little friction in the print head, even small forces and disturbances can be noticed. The print head is very sensitive to the angle of the machine, so leveling feet on the frame are used in conjunction with a Starrett machinist's level to ensure that the print platform is as horizontal as possible. Similarly, one of the largest sources of error in the applied print force comes from the stiffness of the hoses that carry air to the print head's bearings. Compliant air hoses made from soft materials were used, and they are positioned in such a way that they are inciting the most minimal disturbance possible on the print stage. However, a more precise and robust solution to this problem will need to be implemented in order to ensure that the print head is not affected by the finite stiffness of these hoses.

The spring-mass system of print head has a significant resonance, and due to the low friction of the air bearings, it is a lightly damped mode. This slewing mode presents clearly at 5 Hz and does not quickly damp out.

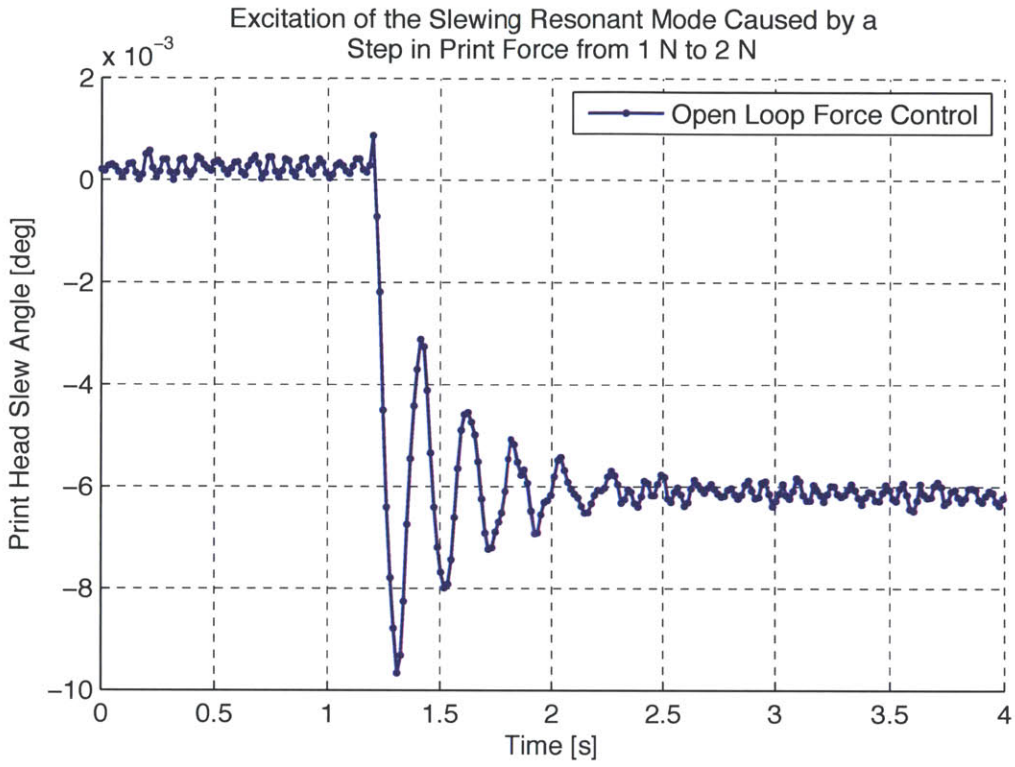

Figure 3.4: Open loop force control: A step in print force excites the resonant slewing mode of the print head, which is only lightly damped. These oscillations present at 5 Hz.

Unfortunately, this mode is close to the expected frequency of disturbances that might arise from an eccentric stamp when printing at speed. One easy low-cost potential improvement would be to replace the solid stainless steel print roll with a centerless ground thin-wall tube. This would significantly decrease the mass of the print head and therefore push the resonance of the slewing mode further above the operating range. Other modifications could be made to further decrease the mass of the printhead, which would similarly help separate the slewing mode resonance from the expected disturbances. As well, this would help to increase the bandwidth of the stage.

3.1.2 Voice Coils

The linear amplifier supplied with the voice coils requires tuning and balancing before it can be used. Following the instructions provided with the voice coil, the amplifier was tuned to map the +/- 10-volt output signal from the DAC to the full available +/- 24-volt supply for the amplifier. The amplifier was balanced so that a reference voltage of zero had zero voltage output to the coils. The gain of the amplifier was measured as the output voltage divided by the reference voltage.

Once the amplifier was properly tuned, the motor constant of the voice coils was checked and verified. This was done using a hand-held digital force gauge. Various forces were commanded through the LabView script, and the resulting force at each coil was measured. The measured force was always within 5% of the commanded force, confirming the specified motor constant and overall system transfer function.

3.2 Impression Assembly

The impression assembly is second only to the print head in importance. It was thoroughly inspected to ensure that its mechanical and optical properties were as expected.

3.2.1 Stiffness

The impression cylinder serves as the datum for both the web-handling and the printing process. All components in the machine are aligned to this master roll. For this reason, the roll must be held firmly in place by its bearings. As well, this roll serves as the impression cylinder for the microcontact printing process, so it must not deform or move significantly when it experiences the forces due to printing and any potential disturbances.

The six radial air bearings used to encapsulate the impression cylinder have a rated stiffness of 22 N/micron at their ideal load of 156 N. When the bearings are all brought into contact with the cylinder and preloaded, their stiffnesses add like springs in parallel. Altogether, the cylinder is expected to have a stiffness of 66 N/μm in the print direction and 82 N/μm in the vertical direction. The addition of a tensioned web will compress the air film of the back bearings in the

impression assembly, which is shown to increase stiffness. Expected print forces are on the order of 5 N total, which will result in negligible deflection of the print roll compared to the 5-10 μm height of the cast PDMS features. As the cast features get smaller and approach 1 μm, the ideal print force will also decrease.

The cylinder is held laterally by two opposing flat round 40mm-diameter air puck bearings. The effective stiffness of the cylinder in this transverse direction is calculated to be twice the 28 N/μm stiffness rating of each of these bearings.

3.2.2 Friction

The impression cylinder is held in place with air bearings. Because a thin film of air is developed between the bearings and the cylinder surface, there is no mechanical contact with the cylinder to create stiction. This non-contact solution eliminates stick-slip phenomena and gives nearly zero friction. In practice, there is some viscous friction from the shear of the air film, though it is orders of magnitude less than conventional roller element bearings. Another great advantage of the air bearings is that the movement is smooth and silent, as there is no contact between roller elements like in a conventional bearing. This is important for precision printing of micron-scale features which can be sensitive to contact noise.

The impression cylinder rotates with very little resistance. This is important because any resistive torque from friction will result in unequal tensions in the web on either side of the impression roll. This creates a tension gradient across the length of the web that is in contact with the impression cylinder. The tension gradient leads to a stress and strain gradient in the web material. This results in the web stretching or contracting as it moves over the surface of the impression cylinder. The stick-slip phenomena that might result from this could cause noise that would be significant when printing micron scale features with narrow process windows. As well, if the web is stretching or contracting in the region that is in contact with the stamp, the stamp features will be deformed in this process.

3.3 Stamp

The stamp is characterized to determine its uniformity and topology. In order to develop a model and a controller that will maintain conformal contact, it is helpful to know the scale of any asperities to the stamp's geometry. In order to measure the magnitude of the deformations and eccentricities in the stamp, the following experiment is performed.

The print head is used to press the stamp directly against the impression cylinder with a constant print force of 4 N. The impression cylinder is then driven at a constant speed, and the stamp allowed to rotate. Throughout the course of a full rotation, the displacement of the print head is measured. Since a constant force condition is imposed, if there is a thick section of the stamp, then the print head should naturally displace away from the impression cylinder in order to allow for this section to pass through. These tests are performed at low web speeds to decrease the effects of any dynamics. Figure 3.5 shows that the displacement of the print head is repeatable on the wavelength of the stamp's circumference, giving good confidence that these displacements are a measurement of the stamp topology.

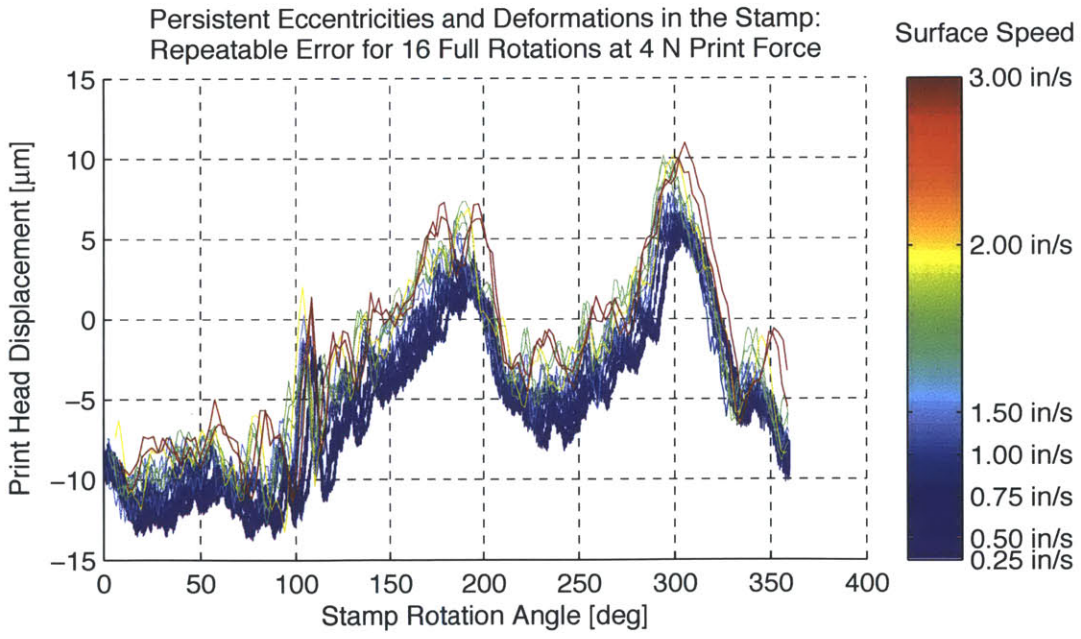

Figure 3.5: Characterization of the stamp: The stamp is pressed directly against the rotating impression cylinder with a constant print force of 4 N. As the rolls rotate, the print head tracks any disturbances in the contact region. These disturbances are shown to be repeatable on the fundamental wavelength of the print

roll's rotation, independent of the web speed. The cause of these significant variations in stamp topology is unknown.

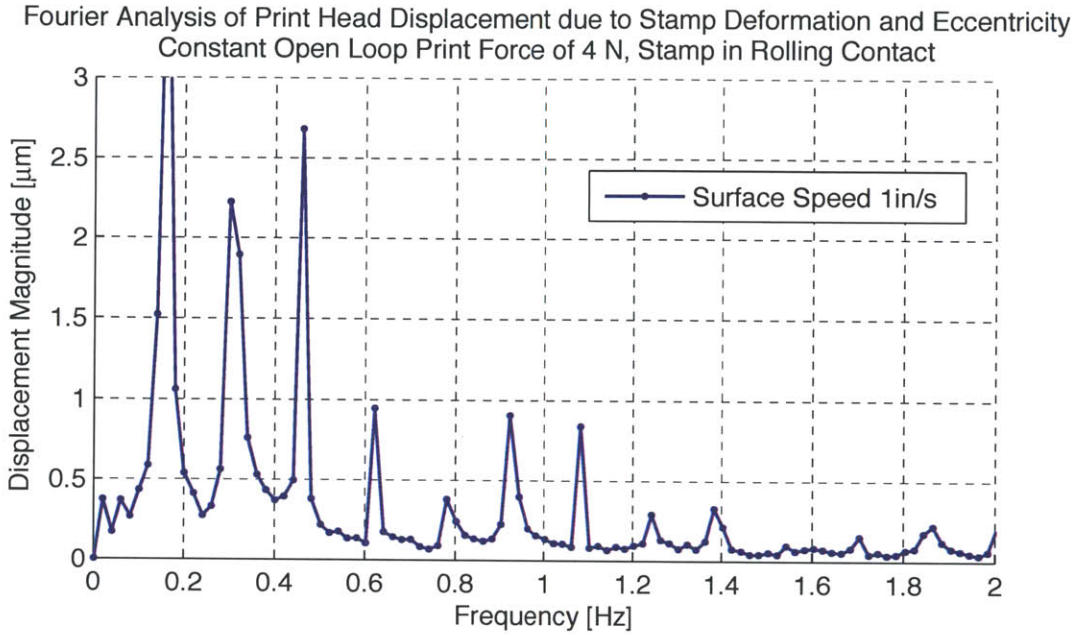

Figure 3.6: Characterization of the stamp: A Fourier analysis of the print head movement in Figure 3.5. This frequency spectrum directly scales with the surface speed.

Figure 3.6 shows a Fourier analysis of the stamp topology presented in Figure 3.5 for the 1 in/s equivalent web speed. This frequency component of this spectrum has been shown to directly scale with the web speed, while the magnitude remains consistent.

At a rolling contact surface speed of 1 in/s, this spectral analysis shows significant frequency content near 1 Hz. With the current camera, which has a 10 Hz frame-rate, these disturbances will be difficult to compensate. However, because the frequency spectrum scales with web speed, it is expected that upgrading to a 100 Hz or higher frame-rate camera will enable the controller to compensate for the disturbances that are expected at up to 10 Hz for web speeds of 10 in/s.

3.4 Sensing

The *in-situ* inspection of the print contact region provides the unique opportunity to visualize what is occurring in the stamp-substrate contact region in real time. However, due to the

transparent nature of the both glass impression cylinder and the PDMS stamp, it proved to be difficult to discern what was occurring in this region. The casting of a special multilayer stamp served to address this problem and enable the camera to make valuable measurements of the occurrences in the contact region.

3.4.1 Stamp

The traditional clear formulation PDMS did not present enough contrast to the camera for any measurements or inferences to be made about the stamp-substrate interaction. In order to increase the contrast of the stamp while also increasing the amount of signal available to the camera, Nietner details the casting of a fluorescent stamp that illuminates the contact region brightly when flooded in ultraviolet light [42]. Using the centrifugal casting machine developed by Petrzelka [19], Nietner is able to cast a cylindrical PDMS stamp that is doped with fluorescein powder. Though the doped PDMS brightly fluoresces in ultraviolet light and presents a strong signal to the camera, the fluorescein powder is noticed to have significant effects on the mechanical properties of the stamp. Most notably, the doped PDMS is stiffer than the pure PDMS formulation. This increased stiffness decreases the stamp's ability to make conformal contact. As well, the fluorescein powder was found to migrate to the surface of the stamp during the centrifugal casting process, which caused the normally smooth PDMS stamp to take on a rough surface texture. This poses a significant obstacle to the replication of small features with a fluorescein-doped stamp.

In order to create a stamp that has both the beneficial material properties of a pure PDMS stamp with the fluorescent properties of the fluorescein-doped PDMS, Nietner casts a graded multi-layer stamp. The stamp is comprised of a thick fluorescent PDMS backing layer with a thin pure PDMS feature layer. A microscope image of the layered stamp is shown in Figure 3.7.

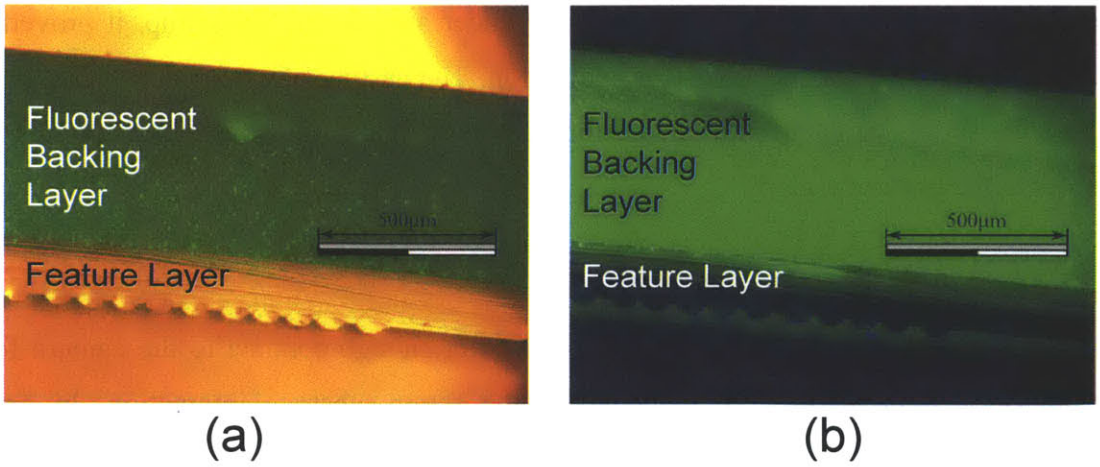

Figure 3.7: Multi-layer fluorescein-doped stamps: Microscope images of thin cross-sectional slices of the dual-layer stamp reveal functionally graded layers. The fluorescent backing layer is thick and heavily doped with fluorescein powder so that it fluoresces brightly for the camera to see. The feature layer is made of pure PDMS so that it retains all the functional surface properties of the material, while also allowing the light from the fluorescent backing to pass through: (a) the stamp in normal light (b) the stamp in the dark, flooded with UV light

These fluorescent dual-layer stamps are used exclusively when the *in-situ* visualization of the contact region is desired.

3.4.2 Optics

The optical properties of the impression cylinder are crucial to the success of the *in-situ* contact sensing. The details of the system optics can be found in Scott Nill's Master's thesis [40]. A video camera is mounted to look through the rear of the impression cylinder to the contact region. It is possible to discern the region where contact is made between the glass cylinder and the cylindrical PDMS stamp surface. With the camera fully zoomed, it is possible to distinguish individual stamp features on the order of 10 μm. The contrast and clarity of these images are heavily dependent on the lighting conditions, though. Various light sources and placements were used to achieve the best visual signal-to-noise ratio.

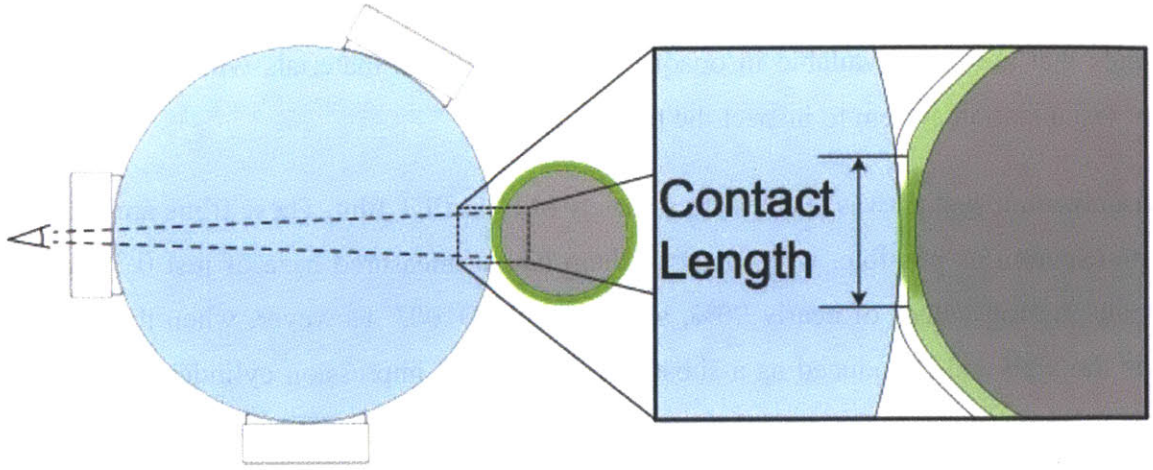

Figure 3.8: Web speed controller: The speed of the web is measured for a 2 in/s set point with the controller disabled and enabled. The web speed controller does not effectively reduce the standard deviation in web speed, but the integral term does help to reduce the mean error. The average speed without the controller was 1.988 in/s, where as the average speed with the controller enabled was 2.000 in/s.

In order to achieve greater contrast, special two-layer PDMS stamps were cast. The backing layer of these stamps is doped with a fluorescein powder that glows when the stamp is exposed to ultraviolet light. Flooded with two UV light sources, the stamp is then brought into contact with the impression cylinder. The fluorescent light coming from the stamp is able to easily travel through the region where contact is made with the impression cylinder to the camera on the other side. The use of these functional stamps with this lighting technique has been shown to greatly increase image contrast for the camera.

The cylindrical impression cylinder presents itself as a lens to the camera. This lens causes vertical distortion to the image, but in the horizontal direction the image remains true. However, the PDMS stamp only makes contact with the impression cylinder in a very narrow strip along the equator of the lens. In this region, close to the centerline of the lens, there is little distortion to the image. Still, the optics of a cylindrical lens are well understood and could be accounted for in the post-processing of the camera's video stream. This will be especially important if the camera is used to make any absolute measurements of contact length or feature spacing.

The ability to visualize the contact region is contingent on the impression cylinder being optically clear, but any substrate used must also be transparent. Many industries and processes

use webs made from transparent materials, but there exist plenty of products made from substrates that are only available in opaque materials. These materials will not allow for the current visualization system to inspect the print region.

The visualization system was tested with a variety of clear PET film. These films are designed to be as transparent as possible, with many of them having measured haze of just 0.3% and total light transmission values of nearly 90%, as per ASTM D1003. However, when these films are used as the web and introduced as a substrate between the impression cylinder and the stamp, they significantly degrade the optical signal available to the camera. The contact region becomes cloudy non-uniform. Looking closely at the PET film wrapped onto the impression cylinder, it is possible to discern colorful contours throughout the surface. It is possible that, due to the surface roughness of the PET film, it does make complete contact with the surface of the glass cylinder, and the shallow gaps between the two cause the iridescent reflections. The clouding of the contact region worsens the signal-to-noise ratio for the camera, making a clean measurement of contact more difficult to acquire. It is possible that special low surface roughness PET will improve the imaging results, but the exact reasons for this effect should be further investigated.

3.5 Web-handling

3.5.1 Speed

The web speed is controlled using the motor driver's speed controller. A reference voltage of between -10 volts and 10 volts from the DAC sets the reference rotational speed of the rewind reel's motor. The maximum motor speed was set to 1500 RPM, which is half the specified maximum continuous motor speed. This mode allows for better speed resolution. With the 32:1 gearbox, the unwind reel is therefore limited to just under 47 RPM.

The linear web speed depends on both the rotational speed and the diameter of the rewind reel. If a constant motor rotational speed is commanded, the linear speed of the web will increase as material winds onto the rewind reel and its diameter increases. The maximum speed of 47 RPM allows for a maximum web speed of 7.36 in/s (0.18 m/s) with an empty rewind reel, up to 22.1 in/s (0.56 m/s) with a full rewind reel. These maximum speeds can be doubled by changing the motor's control mode, but at the expense of resolution.

Accurate control for constant speed was determined to be critical to the printing process, due to the passively driven print roll's sensitivity to varying web speeds. Industry often uses the rotational speed of the motor along with the ultrasonically measured radius of the roll to determine and control the linear web speed. However, the ultrasonic sensors that are used for the roll diameter measurements are quite expensive and give noisy measurements, so a cheaper and more accurate measure of speed was desired for this research. In place of this method, one of the idler rolls in the system was outfitted with a 2500-count rotary quadrature encoder. This encoder allows for the measurement of 0.144 degrees of idler roll rotation, or 3.77 thou of linear web movement. With millisecond timing, it is possible to discern roll velocity from the position encoder's ticks, and then use this as feedback for a speed controller.

In order to control for constant web speed, a feedforward controller was implemented. When the LabView code starts, the user initializes the script with the measured diameter of the material on the rewind roll. Using this measurement and the desired web speed, the script is able calculate the appropriate reference voltage for the motor's rotation. At each iteration of the control loop, the measured web speed from the idler roll's rotary encoder is integrated over time. This allows for tracking how much material has passed through the machine, as well as tracking the diameter of the rewind roll at any given moment. The feedforward term uses this estimated diameter on the next iteration to command the appropriate motor speed necessary to maintain constant web speed.

The feedforward controller alone gives great performance, provided an accurate measurement of the rewind roll's diameter is taken. However, over time, the estimated diameter of the roll can drift from the actual. In order to account for any drift or other inaccuracies with the open-loop feedforward controller, a feedback term was added to the controller. A PI controller was implemented around the idler roll's measured web speed. With the combination of the feedforward and feedback terms in the controller, the web-handling system is able to reliably move at a constant speed for the entire length of a roll. The performance of this system is shown in Figure 3.9.

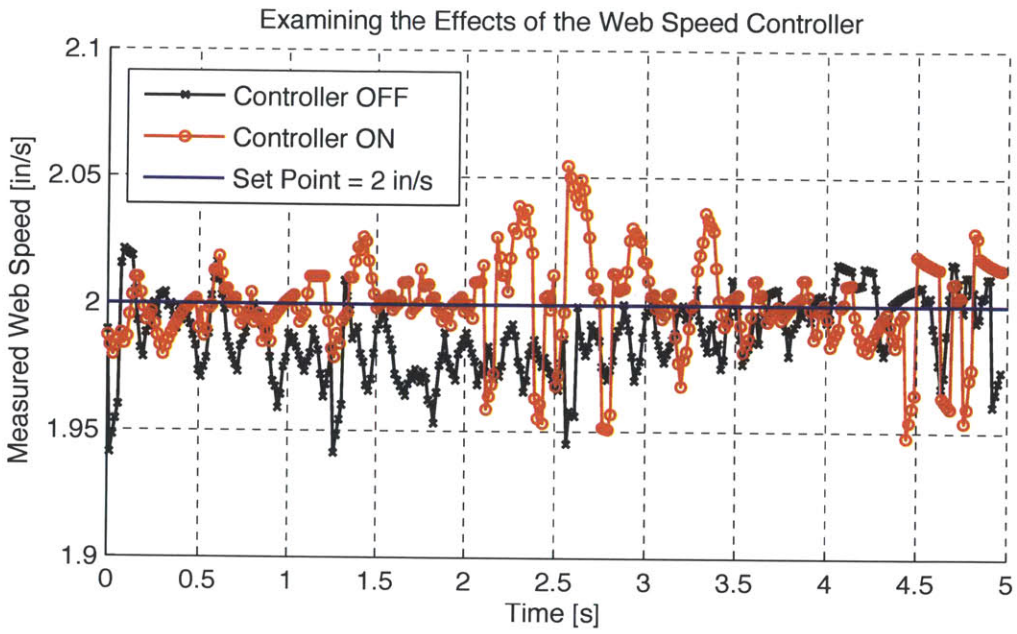

Figure 3.9: Web speed controller: The speed of the web is measured for a 2 in/s set point with the controller disabled and enabled. The web speed controller does not effectively reduce the standard deviation in web speed, but the integral term does help to reduce the mean error. The average speed without the controller was 1.988 in/s, where as the average speed with the controller enabled was 2.000 in/s.

3.5.2 Tension

The tension in the web is set by the unwind reel's torque-controlled motor. The motor is rated for a maximum continuous torque of 5.7 lb-in, though the driver is scaled to 25% of that, as the full torque is not needed for the PET substrate and limiting the maximum has the benefit of improving the resolution. A reference voltage from the DAC of -10 volts to +10 volts sets the desired torque in this range. At the output of the 32:1 gearbox, the unwind and rewind reels can achieve 182.4 lb-in of torque. Controlling for a constant torque will result in steadily increasing web tension as the machine runs, due to the decreasing diameter of the unwind roll as material leaves it. At the beginning of a run, with a full unwind roll, a web tension of 40.5 lbs can be achieved. By the end of the run, when the unwind roll is mostly empty, a tension of 121.6 lbs can be achieved.

Considering the industry recommended standard of 1 PLI/mil (pound of tension per linear inch width per thousandth inch thickness of material), this minimum tension allows for running a 5" wide web up to 0.008" thick.

At low web speeds of less than 0.5 in/s, significant cogging is noticeable in the unwind reel's motion. The unsteady motion of the unwind reel could cause tension and speed fluctuations in the web, which would negatively impact printing performance. The cause for this cogging is uncertain, but it might need to be resolved for reliable low-speed printing.

3.5.3 Tracking

For best printing results, the web should run straight through the machine with minimal transverse direction movement. In order to ensure that this would happen, the rolls were carefully aligned with each other to have parallel axes. This was accomplished with the use of a Starrett 98-6 precision machinists level, which allowed for the rolls to be leveled with the ground at a angular precision of 0.005" per foot. Thin plastic shims were used between the roll flanges and the backplane to adjust the vertical angle of the roll. Then, PI Tape was used to ensure that the rolls were all sufficiently parallel with each other in the horizontal plane. This precision diameter tape is made of stainless steel and allows for measurements that are repeatable to within a thousandth of an inch. For non-extensible web materials like aluminum foil, it is recommended that the rolls be level and tram to within 0.001" per foot of length. However, for extensible materials like PET, there are relaxed requirements on alignment.

Another helpful method to ensure good web tracking is to ensure that the web is fed straight through the machine. By setting up the machine with a straight web path, it is possible to prevent significant drift in the transverse direction to web movement. A simple gauge was laser-cut to help with this task. The unwind, rewind, and idler rolls were marked with a Sharpie at the desired inboard and outboard edges of the web. When the material roll is loaded onto the unwind reel and the web is manually fed over all the rolls to the rewind reel, special care is taken to make sure that it is aligned with these markings.

With the roll and web alignments performed, the machine is started up. Tension is increased on the web, and then it is slowly ramped up to speed. If the web is properly aligned, it should not

wander or drift, but rather track straight through the machine and rewind cleanly into a roll. If this is verified to be the case, then the machine can be operated as normal.

CHAPTER

4

PRINT HEAD MODELING

In order to better understand the microcontact printing process and achieve high-speed patterning, the stamp-substrate interaction must be modeled. An accurate model allows for an effective print head controller to be designed, which is necessary to ensure conformal contact. The development of the print head and stamp model is detailed in this chapter.

4.1 Roll-to-Plate Contact Model

Understanding stamp behavior is crucial to the formation of a printing model. The use of PDMS as a stamp material results in some non-trivial dynamics because of its viscoelastic behavior and high surface energy. However, even first-order understanding of the contact mechanics will help greatly in developing a realistic model of the stamp-substrate interaction.

Petrzelka studied the contact mechanics in a roll-to-plate microcontact printing machine [19]. The mechanics of the roll-to-roll stamp interaction present in this machine are expected to differ from Petrzelka's findings. However, a sufficiently large radius impression roll can be approximated as a flat plate by taking its radius to infinity. Therefore, in the case of a large ratio of impression roll diameter to print roll diameter, the roll-to-plate contact mechanics developed by Petrzelka will be sufficiently accurate. A depiction of roll-to-plate and roll-to-roll contact is presented in Figure 4.1.

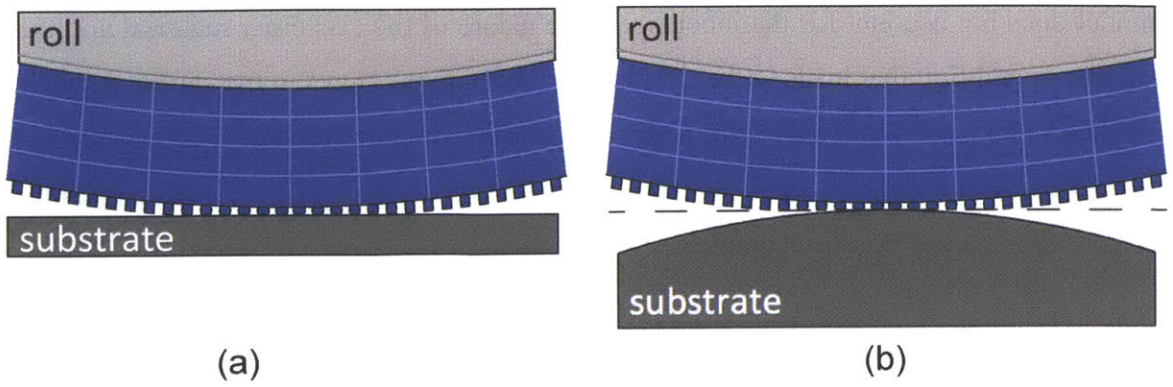

Figure 4.1: Stamp-substrate interaction: (a) roll-to-plate contact, modeled by Petrzelka, will differ significantly from (b) roll-to-roll contact, except in the case of a comparatively large impression roll

4.2 Roll-to-Roll Contact Model

If the roll-to-plate model cannot accurately approximate for roll-to-roll contact behavior, such as with small diameter impression cylinders, a suitable model must be developed. One of the primary uses of a roll-to-roll mechanics model is to accurately predict the force-displacement relationship of the stamp.

The roll-to-roll model is developed using first-order approximations of the contact behavior. The stamp is modeled as a row of parallel springs. Each of these springs is compressed by the amount of interference in that column between the stamp and the substrate. The linear stiffness of the springs is derived from the elastic modulus of PDMS. This linear model is justified by the small displacements that are expected. The force in each spring is integrated to give the total print force for each level of displacement. A depiction of this model is shown in Figure 4.2.

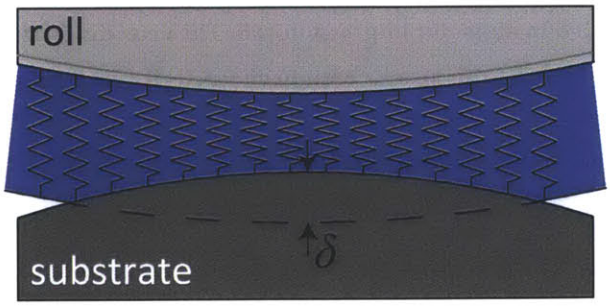

Figure 4.2: Roll-to-roll contact model: The stamp-substrate interaction is modeled as a row of compressed springs. The force in each of these springs is integrated over the contact length, and then multiplied by the contact width to achieve the total print force.

This model does not account for the incompressible nature of the elastomer material and the no-slip boundary condition that leads to the development of high pressures in the stamp. As well, the high surface energy of PDMS results in a significant work of adhesion. Petrzelka discusses how leaving this effect unaccounted for in a model will cause the contact length to be underestimated and the contact forces to be overestimated.

A sample load-unload experiment on a featureless stamp is shown in Figure 4.3. This is used to characterize the stamp and test the accuracy of the roll-to-roll model.

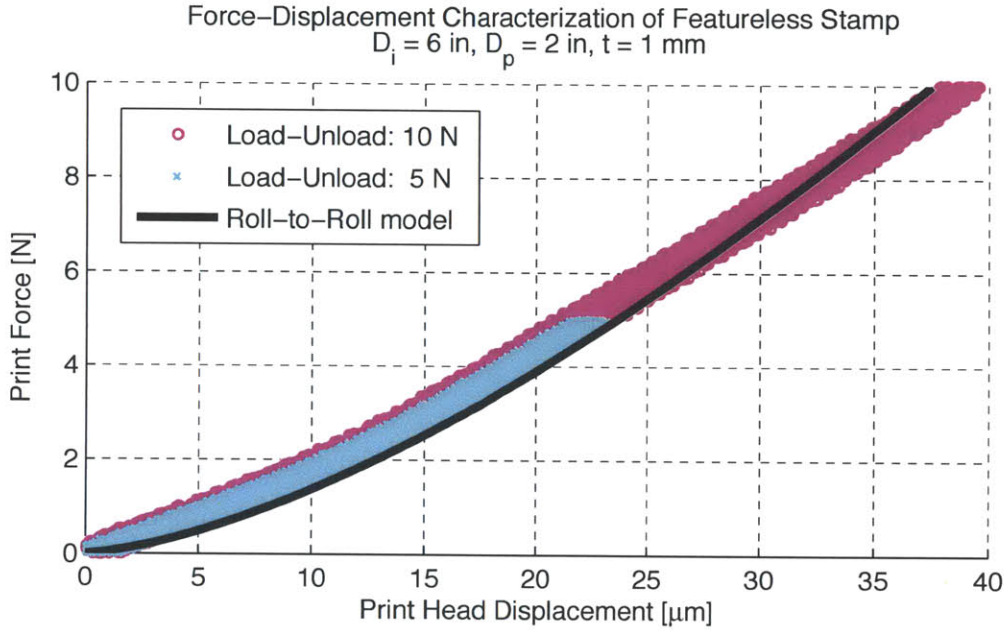

Figure 4.3: Roll-to-roll contact model: A featureless stamp is brought into direct contact with the impression roll. The print force is slowly ramped up to a maximum and back down to zero over the course of 75 seconds. This plot shows the resulting force-displacement curves for a 1 mm thick cylindrical stamp on a 2 in diameter print roll, pressed up against a 6 in diameter impression roll. The empirical data seems to match the model. This force-displacement test can also be used to characterize each stamp before printing.

Though many approximations and linearization that were made in the development of the roll-to-roll contact model, it seems to well describe the data for small displacements. Similar load-unload tests were used to verify the model's prediction of contact length, which is calculated as simply the length of stamp-substrate interference. The contact length sensor, detailed in 5.3.1, is used to measure the stamp-substrate contact length during the force ramp, and this is plotted against the print head's displacement in Figure 4.4.

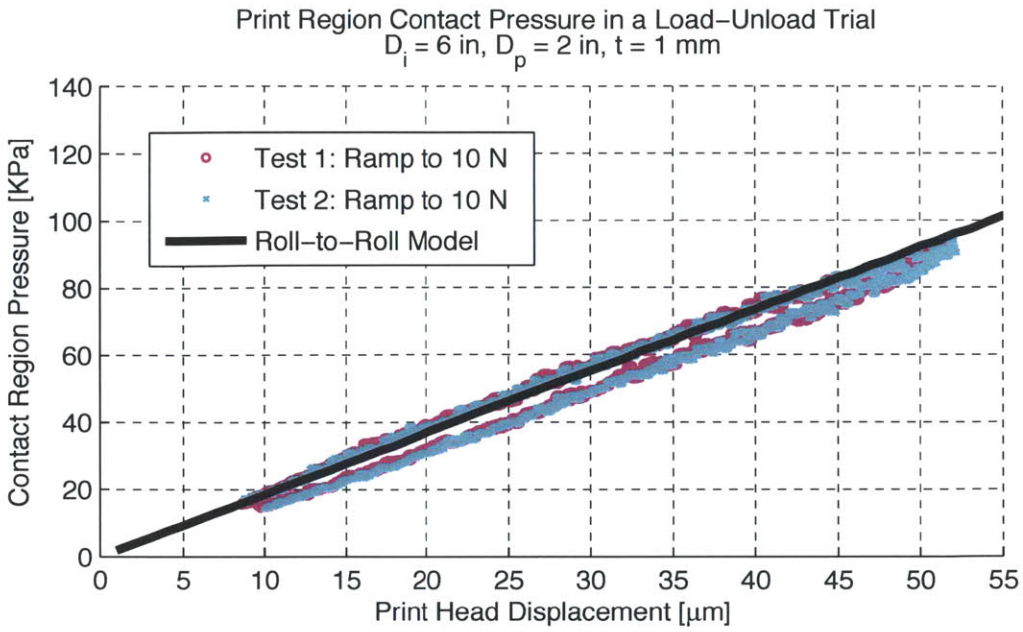

Figure 4.4: Roll-to-roll contact model: The pressure in the contact region is plotted against the displacement of the print head. The pressure is calculated using the applied force, the stamp width, and the measured contact length.

The roll-to-roll contact model accurately predicts the contact length of the stamp throughout the load-unload trial. Note that the experiment did not investigate the behavior of the stamp at contact pressures below 20 KPa. This is because the current sensor algorithms have difficulty measuring the stamp balance and contact length at low print pressures, so the load-unload test started with a print force pre-load of 1 N. The relationship between contact length and roll displacement is not expected to remain linear in this region of small displacement like the simplified model suggests. At print forces of less than 1 N, the surface energy of the stamp will likely dominate, and this behavior is not described in the current roll-to-roll contact model. For low-pressure printing, which could be useful for stamps with delicate features or complex geometry, a more accurate roll-to-roll contact model will have to be developed.

4.3 One-D.O.F. Print Head Model

A simple one-degree-of-freedom model was created for the interaction between the print head and the impression cylinder. This model assumes that the impression cylinder is rigid and ground to a perfect cylinder. The print head is a modeled as a frictionless spring-mass-damper system,

attached to the impression cylinder ground. A contextual diagrammatic simplification of the stamp is shown in Figure 4.5, while the model of the system is depicted in Figure 4.6.

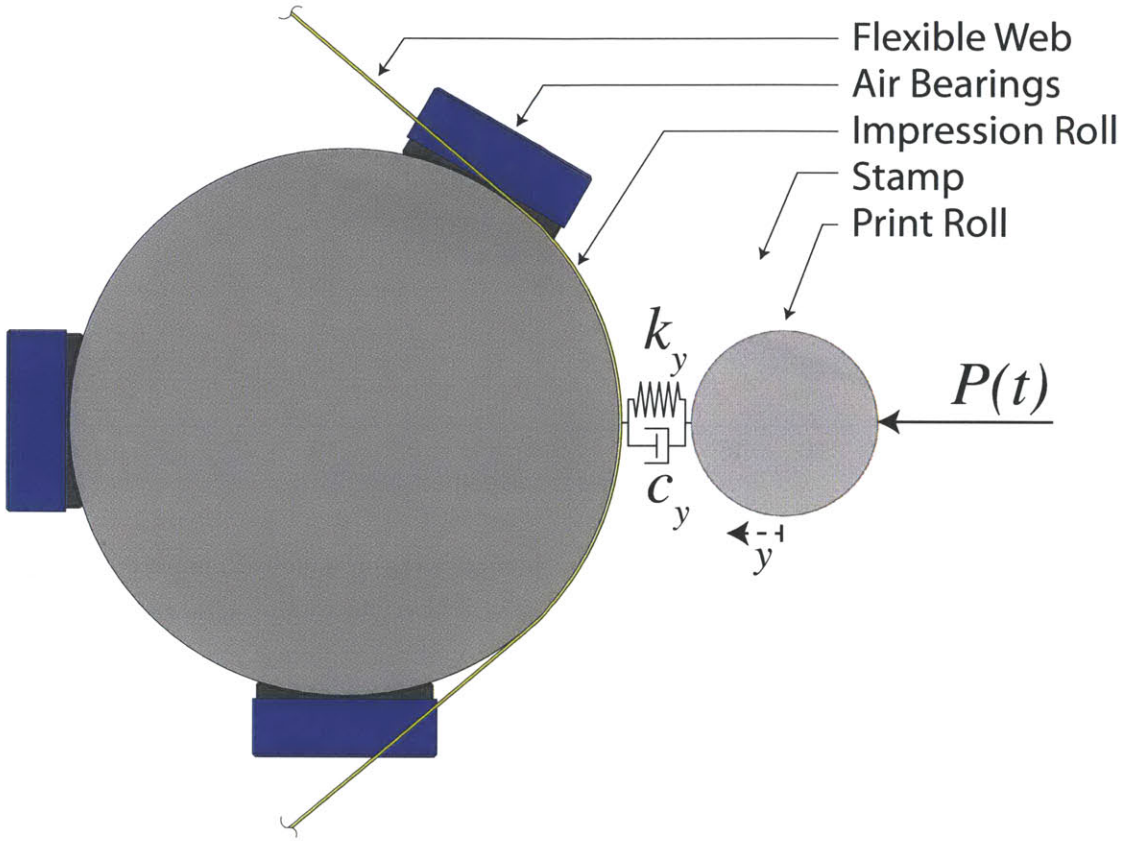

Figure 4.5: One-D.O.F. print head model: This diagram of the print roll–impression roll interaction shows the modeled simplification of the stamp as a linear spring-damper

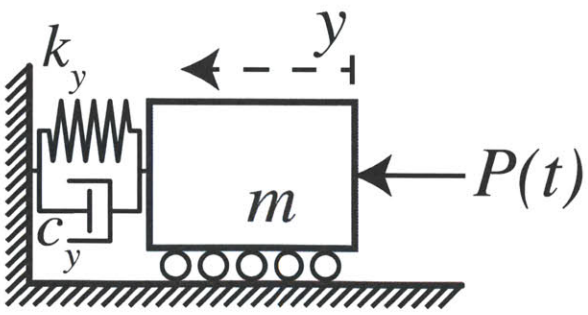

Figure 4.6: One-D.O.F. print head model: The print interaction is modeled as a simple spring-mass-damper system with a time-varying print force applied to it.

It is known from the stamp model and characterization that the thin PDMS layer does not act as a linear spring and damper. However, this model's first-order approximation still gives some helpful insights. As well, this linearization is found to be sufficiently accurate in the case of small displacements about a constant print force.

The equation of motion for the print head is shown in Equation (4.1).

$$m\ddot{y} + c_y\dot{y} + k_y y = P \tag{4.1}$$

The Laplace transform of this equation gives the transfer function from applied print force P to print head motion y. This is shown in Equation (4.2).

$$\frac{Y}{P} = \frac{1}{ms^2 + c_y s + k_y} \tag{4.2}$$

The one-degree-of-freedom model provides a good first order estimate of the system's displacement response to stamp or substrate asperities. It also provides an estimate of the mechanical resonance due to the stiffness of the stamp. Oscillations in the y direction are expected to have the natural frequency calculated Equation (4.3).

$$\omega_{n,y} = \sqrt{\frac{k_y}{m}} \tag{4.3}$$

Though the stiffness of the stamp is not expected to be linear as described, its stiffness can be linearized about a set point. The force-displacement curve in Figure 4.3 shows the stamp to have a stiffness of about 300,000 N/m at a print force of 4 N. Equation (4.3) gives a natural frequency of 22 Hz for the mechanical resonance in the y direction at that print force.

The 1-D.O.F. model is limited in that it does not describe the print head's angular slewing motion. The one-D.O.F. model is extended into a two-D.O.F. model in order to accurately portray the behavior of both degrees of freedom of the print head.

4.4 Two-D.O.F. Print Head Model

The print head has two actuated degrees of freedom, as shown in Figure 4.7: displacement in the y direction, and angular slew ψ about the z axis. A two-degree-of-freedom model is created to describe the motion of these axes.

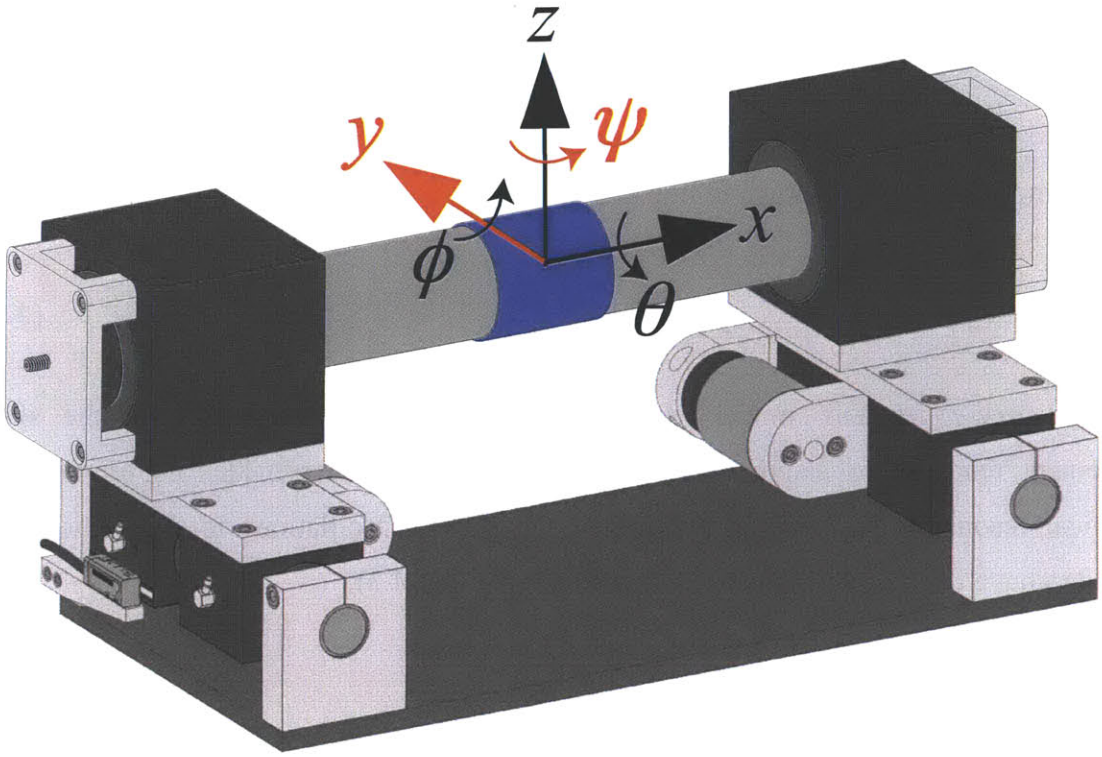

Figure 4.7: Two-D.O.F. print head model: The print head is able to move along linear guide rods in the y direction, and slewing bearings on either side allow for angular slew ψ about the z axis

Flexural bearings were used in the print head to allow it to slew, which enables the print head to correct for any taper in the stamp or misalignment with the impression cylinder. These slewing bearings were designed to be rotational flexures because of their lack of friction and high degree of repeatability. However, these flexures present as a rotational spring with a finite stiffness. It is important to include these flexures in any model of the print head because of the resonance that their stiffness incurs.

In the 2-D.O.F. print head model, the PDMS stamp is modeled as a row of parallel linear spring-dampers. The applied force from the voice coils is modeled as passing through a point mass on either end of the print roll. This model is depicted in Figure 4.8.

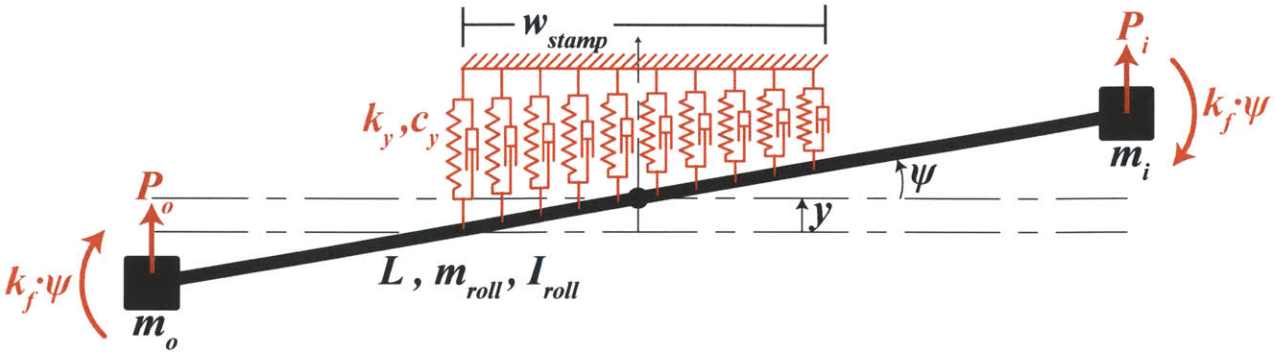

Figure 4.8: Two-D.O.F. print head model: The print roll is modeled as a rigid rod with length L, mass m_{roll}, and rotational inertia about the center I_{roll}. At each end of the print roll is a point mass, denoted m_o and m_i for outboard and inboard. Voice coil forces P_o and P_i act on these masses in the positive y direction, and the rotational flexures impart a resistive torque of k_f times the slew angle ψ. The stamp is modeled as a row of linear spring-dampers with coefficients k_y and c_y.

The model in Figure 4.8 can be simplified by viewing the stamp as just two spring-dampers, separated by the stamp width. Figure 4.9 illustrates this simplification.

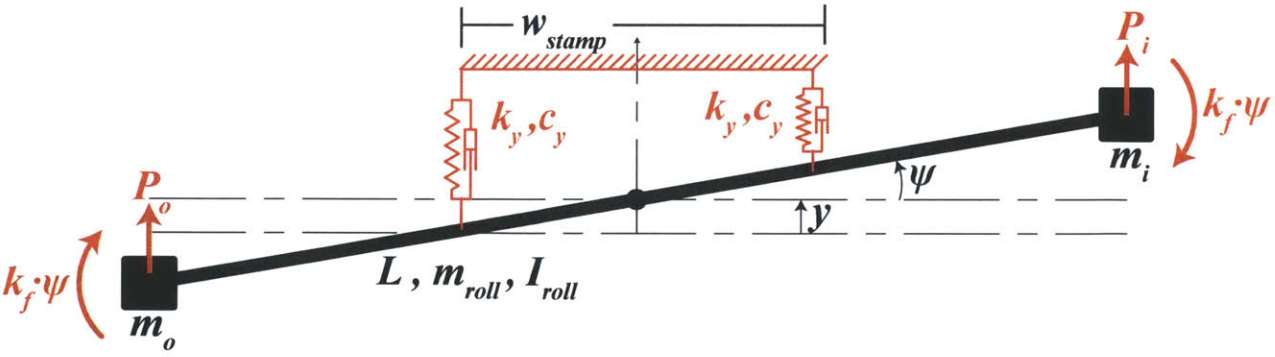

Figure 4.9: Two-D.O.F. print head model: The model of the stamp is simplified to two parallel linear spring-dampers with coefficients k_y and c_y, separated by the stamp width w_{stamp}.

The model illustrated in Figure 4.9 can accurately describe the print head dynamics. However, the degrees-of-freedom y and ψ are strongly coupled by the voice coil forces P_o and P_i and the stamp reaction forces. It is possible to decouple these degrees of freedom via a coordinate

transformation. The sum of the two voice coil forces is taken as the print force, P. The difference in the forces times half the distance between them $(P_i - P_o) \times L/2$ is taken as the print torque, Q.

The degrees of freedom are also decoupled from the stamp by transforming the two parallel spring-dampers into a linear spring damper and a rotational spring damper. Though it is suspected that the stamp may actually present some coupling of the two degrees of freedom, this first-order approximation greatly simplifies the model. These transforms result in a decoupled system with a force actuator affecting only y, and a torque actuator affecting only ψ, as illustrated in Figure 4.10

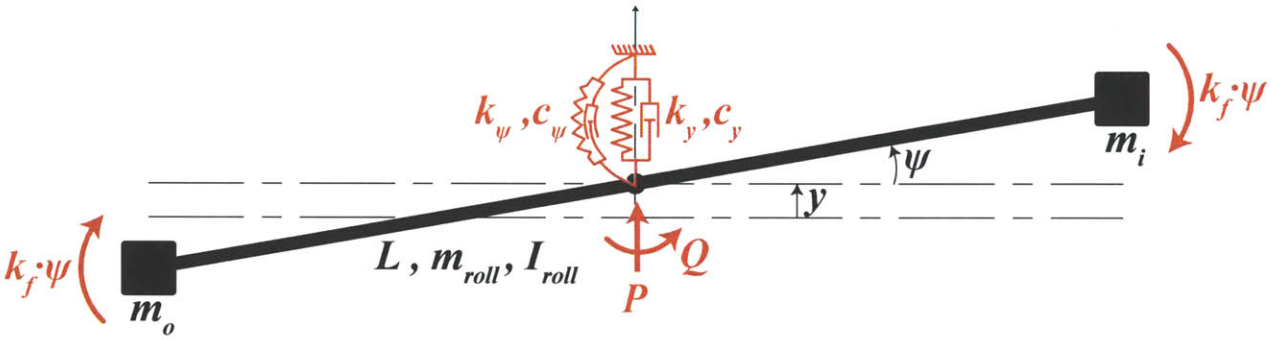

Figure 4.10: Two-D.O.F. print head model: Using a coordinate transform, the model is simplified further to decouple the degrees of freedom. The total printing force $P_i + P_o$ is denoted as P, acting on the center of the rod in the positive y direction. The difference in voice coil forces times half the distance between them $(P_i - P_o) \times L/2$ is the print torque denoted as Q. The stamp is modeled as a linear spring-damper with coefficients k_y and c_y and as a rotational spring-damper with coefficients k_ψ and c_ψ.

This final decoupled two-D.O.F. model is able to accurately predict the dynamics of the print head using two independent equations. However, it is important to recognize the assumptions that are made in the formation of this model. The stamp likely has some coupling effect that should be investigated. As well, the stamp interaction is not expected to be linear as modeled. While it is easy to measure the linear force-displacement relationship of the stamp and linearize about the expected print force, it is not so easy to estimate or measure the linear damping coefficient or either of the rotational spring-damper coefficients. Finally, though the print head's air bearings and flexures provide little friction, the total damping is non-negligible. For the purpose of this analysis, the print stage damping is lumped into the stamp's linear and rotational damping.

Though many assumptions are made in this model, it is expected to give good predictions of the print head behavior in the case of small angles and displacements. The equations of motion are presented in Equations (4.4) and (4.5) where the print force P and print torque Q are defined in Equations (4.6) and (4.7).

$$(m_{roll} + m_o + m_i)\ddot{y} + c_y\dot{y} + k_y y = P \tag{4.4}$$

$$(I_{roll} + \tfrac{1}{4}m_o L^2 + \tfrac{1}{4}m_i L^2)\ddot{\psi} + c_\psi\dot{\psi} + (k_\psi + 2k_f)\psi = Q \tag{4.5}$$

$$P = P_o + P_i \tag{4.6}$$

$$Q = (P_i - P_o)\tfrac{L}{2} \tag{4.7}$$

Taking the Laplace transform of the equations of gives the transfer functions from force to displacement and from torque to slew angle, shown in Equations (4.8) and (4.9).

$$\frac{Y}{P} = \frac{1}{(m_{roll} + m_o + m_i)s^2 + c_y s + k_y} \tag{4.8}$$

$$\frac{\Psi}{Q} = \frac{1}{(I_{roll} + \tfrac{1}{4}m_o L^2 + \tfrac{1}{4}m_i L^2)s^2 + c_\psi s + (k_\psi + 2k_f)} \tag{4.9}$$

These transfer functions provide valuable insights into the dynamics of the print head. Most notably, this two-D.O.F. model of the print head provides information about the angular slewing resonant mode of the print head. This mode presents mainly because of the rotational stiffness of the flexures, which is expected to be orders of magnitude greater than that of the stamp. Equation (4.10) describes the natural frequency of this resonance.

$$\omega_{n,\psi} = \sqrt{\frac{k_\psi + 2k_f}{I_{roll} + \tfrac{1}{4}m_o L^2 + \tfrac{1}{4}m_i L^2}} \tag{4.10}$$

Using Equation (4.10), the natural frequency of the slewing mode is calculated to be 2.62 Hz. Because of the low frequency of this mode, special consideration will have to be taken in order to avoid exciting it. The current 10 Hz frame-rate of the camera presents a significant bottleneck that will make it difficult to control for the resonance. It is recommended that a faster camera be

used control for this resonance. However, in future modifications to the machine, the slewing flexure should be replaced with a slewing bearing that does not have a rotational stiffness. This removes the slewing resonance from the system entirely and allow for a more robust printing process.

Now that a model of the system has been formed, it is possible to design a controller for the print head.

CHAPTER

5

CONTACT CONTROL

The success of the high-speed roll-to-roll microcontact printing process is contingent upon the implementation of a controller that is able to maintain conformal contact between the stamp and the substrate. The need for such a controller was demonstrated by Stagnaro [26] and Baldesi [38], who showed that manual adjustment of the print head would not suffice for more delicate stamps with smaller features. Petrzelka implemented an impedance controller in a precision parallel kinematic stage for roll-to-plate printing [19]. This work demonstrated the utility of being able to actively control the force on the print head and, indirectly, the stamp contact pressure. As well, Petrzelka pioneered a novel *in-situ* inspection technique, which resulted in visual data about the contact region that could be used as feedback for process control.

These ideas are synthesized in this chapter, and a control architecture is developed to make use of *in-situ* visualization of the contact region to control for both the "balance" and contact pressure in the print region. These two controllers run in parallel, and they map nicely to the two decoupled degrees of freedom of the print head. The measured balance of the print head is used as feedback to control the applied print torque Q, which incites rotation ψ about the z axis. The measured contact length of the stamp is a surrogate for the contact pressure, and is used as feedback to control the applied print force P, which moves the print head in the positive y direction.

Unfortunately, the bandwidth of the controllers is limited by the available camera's frame-rate of 10 Hz. This bottleneck prevents the designed controllers from being able to compensate for any disturbances with frequency content greater than 1 Hz. It is warned in Gene Franklin's *Feedback Control of Dynamic Systems* that a controller sampling rate of only $5\omega_n$ rarely results in a stable controller, and that only mediocre performance can be expected from a controller sampling rate of $10\omega_n$ [43]. It is recommended that the controller have a sampling rate of $>20\omega_n$ for reasonable

results and $>30\omega_n$ for good performance. With a camera frame-rate of only 10 Hz, it is only expected that the controllers presented in this chapter be able to compensate for disturbances on the order of 0.5 Hz or less. However, the upgrade to a faster frame-rate camera will enable these controllers to compensate for faster disturbances and therefore enable successful printing at higher web speeds.

5.1 Open-Loop Force Control

The print head is equipped with a voice coil on each side. These actuators are used to apply the commanded amount of force on each side of the stage. In the most basic control scheme, the print head can be actuated open-loop, with no feedback of force or position. This serves to be extraordinarily useful in basic control of the print head, and is the building block for the closed-loop controllers.

5.1.1 Controller Design

Commanding a current to the voice coils results in a force being applied on either side of the print head. The magnitude of this force relative to the applied current is characterized by the motor constant of 29.56 N/amp. The voice coils are designed to have this parameter remain as constant as possible throughout their specified travel. Though the DAC, linear amplifier, and voice coil each have associated dynamics, the time constants for each of these are orders of magnitude faster than the operating range of the print head. Therefore, the transfer functions for these components can be modeled as simple gains. Knowing these parameters, the entire transfer function from DAC output voltage to applied print force is calculated and coded into the LabView script. With just open-loop control of the voice coils, it is possible to precisely control the applied print force on the substrate. The block diagram of the system is shown in Figure 5.1.

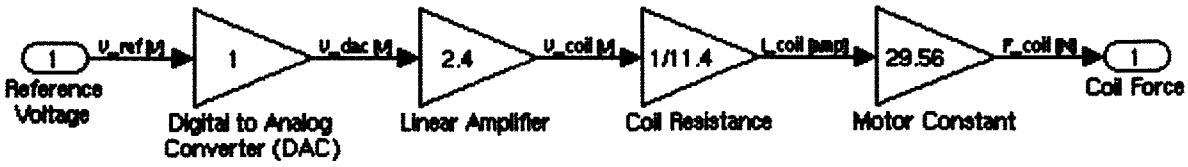

Figure 5.1: Open-loop force control block diagram: The dynamics of the DAC, linear amplifier, and voice coil are orders of magnitude faster than the bandwidth of the system, allowing these components to be accurately modeled as simple gains. Knowing these gains, it is possible to accurately command the desired force.

In order to match the two-D.O.F. model of the print head, a coordinate transform is applied to the voice coil outputs. Instead of acting as parallel force actuators separated by distance L, they are used as a linear force actuator and a rotational torque actuator, both acting through the center of the print head. This is achieved by transforming the desired print force P and print torque Q to the voice coil forces P_i and P_o. Equations (5.1) and (5.2) show this transformation.

$$P_i = \frac{Q}{L} + \frac{P}{2} \tag{5.1}$$

$$P_o = \frac{-Q}{L} + \frac{P}{2} \tag{5.2}$$

The ability to command the voice coils as independent force and torque actuator is critical to the success of the closed-loop balance and contact controllers detailed in Sections 5.2 and 5.3.

5.1.2 Performance

Using the voice coils open-loop allows for reliable command of force and torque on the print head. Given a uniform stamp with no significant asperities, this method will yield constant contact force. If the stamp is not uniform, or the surface asperities are significant, the print head will displace to track these disturbances. However, printing with open-loop force control is found not to yield balanced contact pressure across the width of the contact region in the case of a tapered stamp or any machine misalignment. Therefore, without feedback, open-loop control does not guarantee the even distribution of pressure throughout the contact region.

5.2 Balance Control

In order to achieve conformal contact between the stamp and the substrate, a uniform printing pressure across the width of the stamp is desired. Simple force control of the print head is not a robust method to ensure an evenly distributed force throughout the width of the contact region. This is especially apparent when the stamp and substrate are rotating, and the various defects in the stamp cause the print roll to oscillate from side to side.

Direct control the stamp-substrate interaction will enable the print head to correct for these steady state or time-varying disturbances, which is critical to the microcontact printing process, as the successful transfer of patterns is a function of conformal contact. This section details the design of a balance controller that is able to achieve uniform print pressure across the entire width of the stamp, which will help to enable conformal contact.

5.2.1 Sensor Design

The balance controller makes use of the *in-situ* visualization of the contact region, as detailed in [40]. A fluorescein-doped stamp, as described by [42], is illuminated with ultraviolet light and brought into contact with the impression cylinder. Where the fluorescent stamp makes contact with the cylinder, it glows brightly to the camera. The image from the camera is thresholded, and the horizontal center of gravity of all the illuminated pixels is calculated. For an evenly balanced stamp, this center of gravity will be in the middle of the frame. If the stamp is out of balance and making more intense contact on one side than the other, the weighted average of the thresholded pixels will report how far off the center of gravity is from the middle of the frame. This measurement of balance is reported on a scale from -1 to 1, with zero being a perfectly balanced stamp.

This real-time measurement of balance is used as feedback for the controller. In most every printing situation, an even balance is desired, so the controller is designed to drive the balance measurement to zero. In order to properly design this controller, it is necessary to know the balance sensor's transfer function from the visual balance measurement to the actual stage angle. In order to determine this, a calibration experiment was performed.

The print head was brought into contact with the impression cylinder with a constant total force. Using open-loop control, the torque on the stage was manually adjusted until the stamp had an even distribution of contact along its width and the balance measurement read zero. At this point, the print head's position encoders were tared and set to zero. With constant print force, the torque on the print head was slowly ramped from one extreme to the other and back, causing the print head to slew. During these torque ramps, the visual inspection system calculated the balance measurement at each time step and the print head position encoders measured the slew angle of the print stage. This quasi-static test showed the relationship between the balance measurement and the stage slew angle. The results from the highest print force and lowest print force tests are compared in Figure 5.2

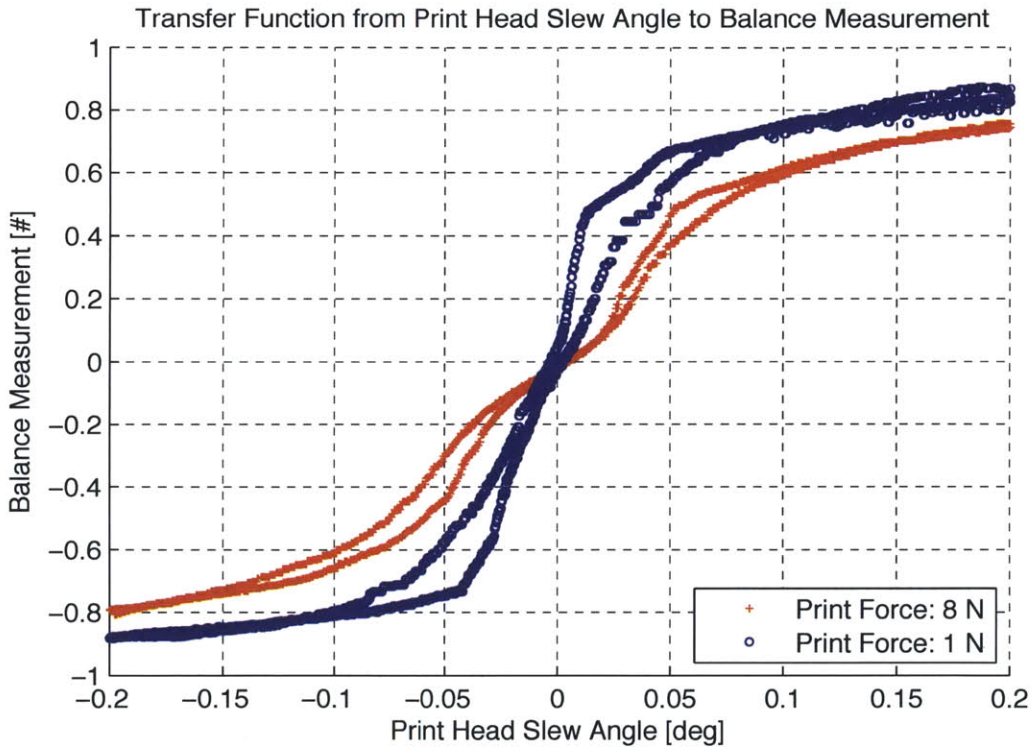

Figure 5.2: Stamp balance controller sensor calibration: An experiment was performed to determine the relationship between balance measurement and print head slew angle. Though relatively linear at small angles and small print forces, the transfer function is shown to not be independent of print force for the current balance measurement algorithm.

The relationship between balance measurement and stage angle is nearly linear in the small angle range for low print forces. However, there is significant hysteresis, and for larger print forces, the

function turns into an S-curve. This balance measurement is computed at the 10 Hz frame-rate of the camera. This is an order of magnitude faster than the expected system bandwidth, so for a first order approximation, the sensor can be modeled as a time-invariant gain.

The sensor gain is determined by linearizing about the origin for a 4 N print force. This is shown to be an appropriate amount of force for printing with similar sized setups in [18], [19]. Linearizing about the balance point for this print force, a gain of 10.5 balance/degree slewing angle is used as the sensor gain for the design of the balance controller.

In future improvements to the controller, the calibration curve could be either parameterized or programmed in as a lookup table if the linear range is exceeded. In order to further increase the robustness of the controller, the sensor's balance calculation algorithm should be reworked to give consistent balance measurements over a large range of print forces.

5.2.2 Controller Design

A discrete implementation of a PID controller was used to keep the print stage properly balanced. A block diagram of the system is shown in Figure 5.3.

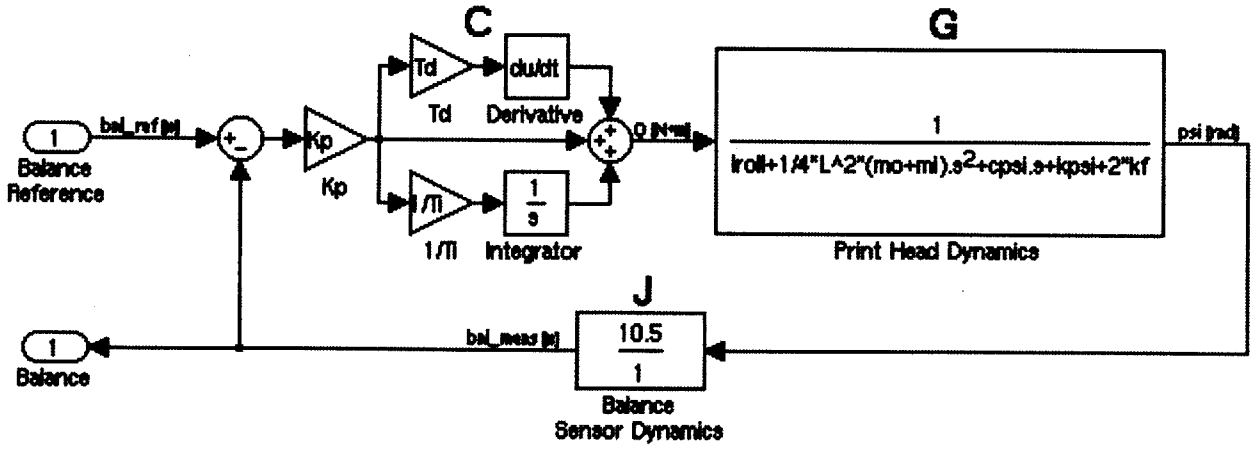

Figure 5.3: Stamp balance controller block diagram: The PID controller used in the balance controller is labeled C. The dynamics of the print head are displayed in the transfer function G. The dynamics of the sensor, which is modeled as a simple gain, are labeled as J.

The controller was tuned using the Ziegler-Nichols method [43]. However, implementing the prescribed ZN gains did not result in a stable controller. This is likely because the significant

noise in the balance measurement is amplified by the derivative term. The heavy filtering required of the balance measurement would introduce significant phase delay and put the system at the margins of stability. Instead, the derivative term was significantly decreased and the remaining proportional and integral gains were manually tuned to achieve a controller that gives a good mix of fast response and robust stability. The resulting controller has the ability to recover from significant disturbances and rarely causes the system to become unstable. The gains that are found to give this performance are $K_p = 1.125$, $T_d = 0.01$, $T_i = 0.5$.

5.2.3 Performance

The balance controller is shown to reliably maintain an even contact pressure across print region. It was tested using an unfeatured cylindrical stamp. The stamp is brought into direct contact with the impression cylinder and the balance controller is enabled. The balance controller has proven to be robust for print forces as low as 0.125 N and as high as 60 N, and is able to track zero with minimal steady state error. This is confirmed visually by either looking at the camera feed or through the back of the impression cylinder. An evenly balanced print roll presents a brightly glowing patch with constant length throughout the entire width of the stamp.

The balance controller was used in order to ensure that the load applied to the stamp was evenly distributed throughout the duration of the load-unload trials used in 4.2. These trials are used to characterize the stamp's force-displacement and contact length-displacement behavior, and accurate results require a balanced distribution of print pressure. Figure 5.4 shows that the stage remained within 2% of the ideal balanced pressure distribution throughout the 75-second long trials, even with a constantly changing print force.

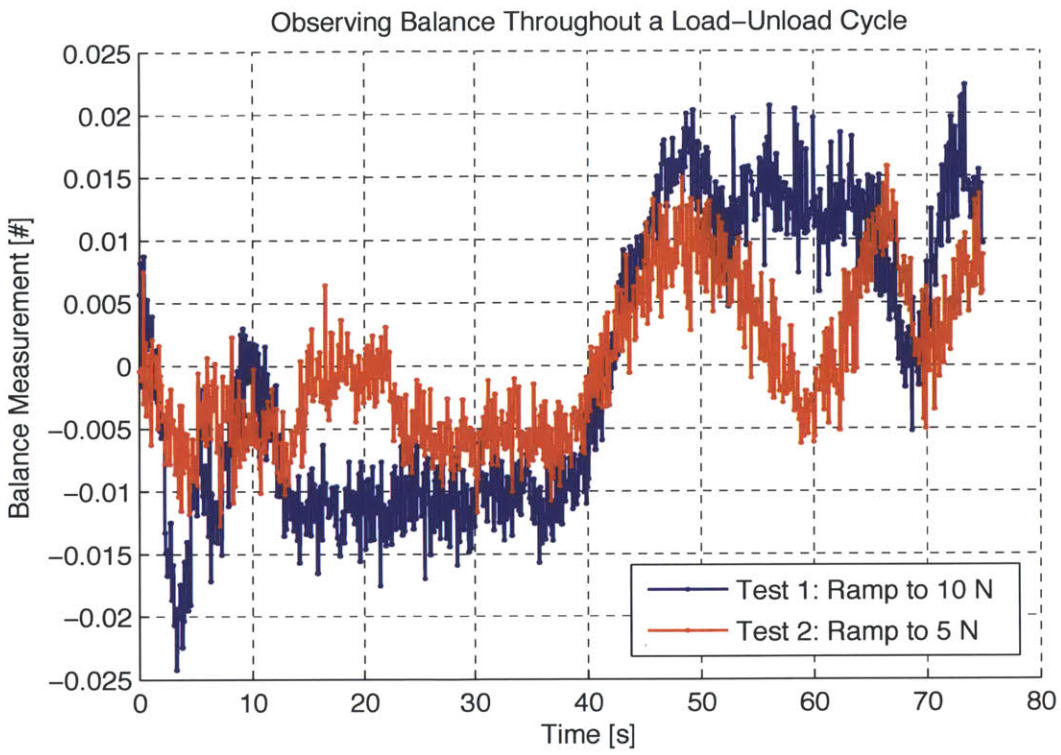

Figure 5.4: Characterization of the stamp: In order for the load-unload tests to give an accurate force-displacement curve for the stamp, it is necessary that the stamp be properly balanced throughout the experiment. This plot shows that, during the 75 second long force ramp experiments, the print stage never deviates more than 2% from perfect balance. It is unknown what causes the shift in both trials at the 40 second mark.

Figure 5.5 shows the controller's response to a step in reference balance from -0.1 to +0.1 while the stamp is in stationary (non-rolling) contact. Though it is rare that any balance other than 0 will be desired in a printing situation, this response is helpful in characterizing the response of the controller.

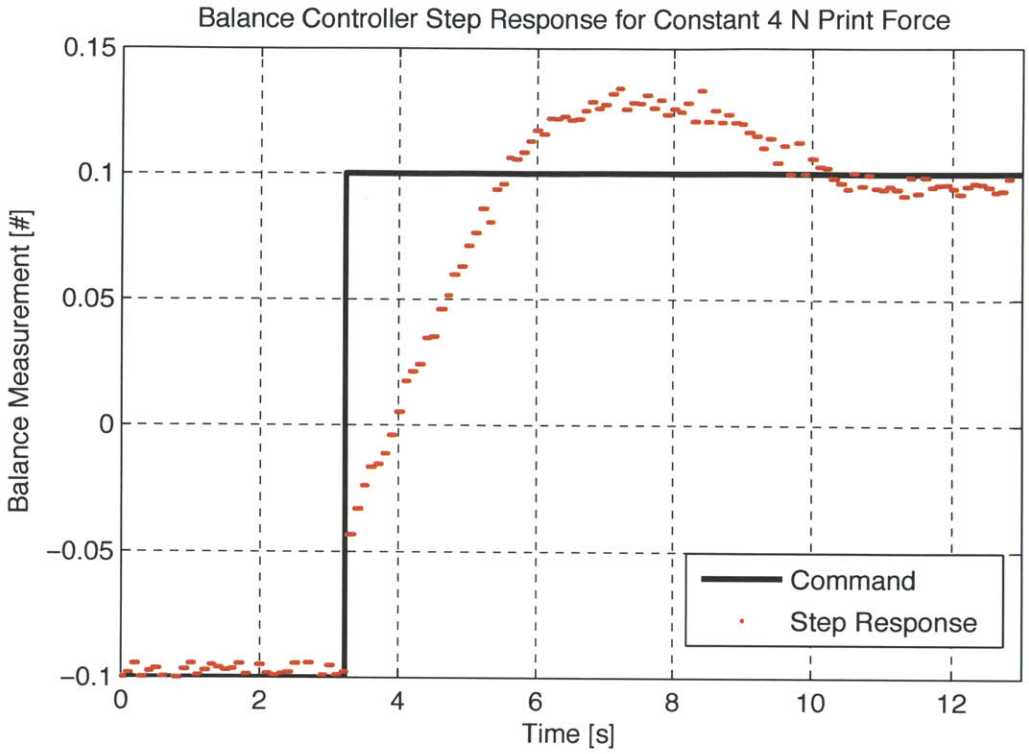

Figure 5.5: Stamp balance controller step response: The response takes 8 seconds to settle to the commanded value because of the slow sampling speed of the camera.

Figure 5.7 and Figure 5.6 show how the balance controller recovers from an impulse disturbance, simulated by forcefully flicking the print head with a finger. With the print head in just open-loop force controller, there remains a significant steady-state error after the disturbance. With the balance controller enabled, the print head returns to an even balance after the disturbance. These tests were also performed in stationary contact.

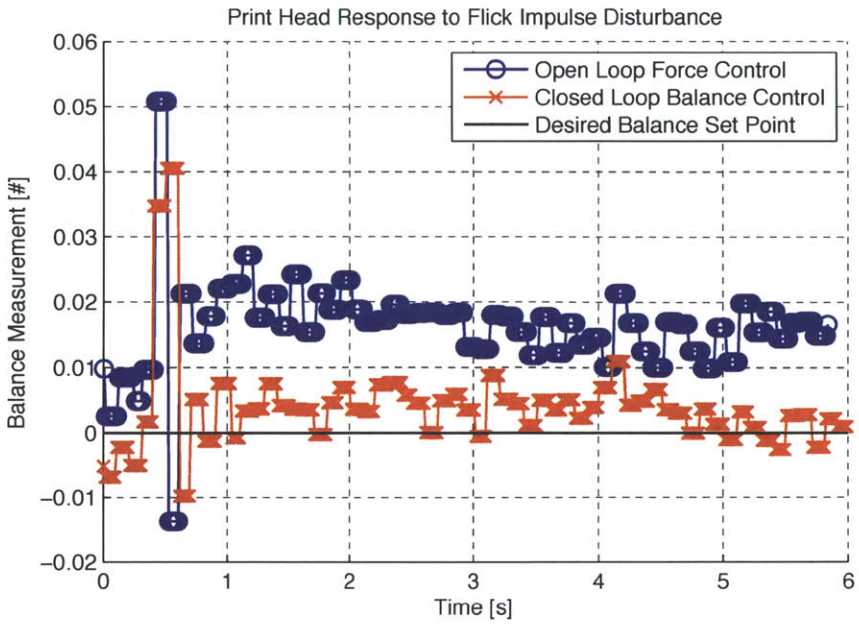

Figure 5.6: Stamp balance controller: Shown here is the disturbance response. The print head returns to balance with the balance controller enabled, while there is significant steady-state error if the controller is disabled.

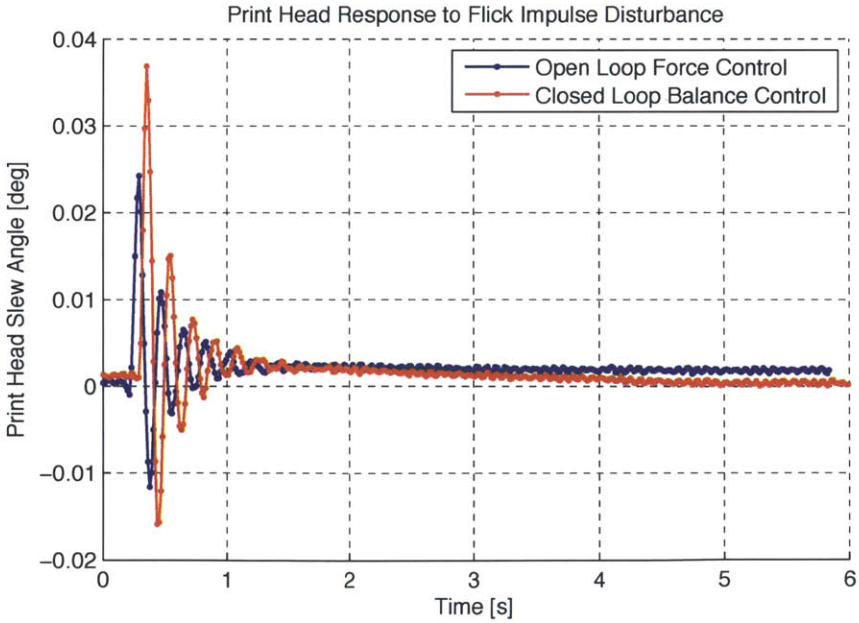

Figure 5.7: Stamp balance controller disturbance response: The impulse disturbance caused by flicking the print roll excites the slewing resonant mode, which is slow to die out. Note that the balance controller is eventually able to achieve balance, albeit slowly, while the open-loop test never returns to zero.

The angular slewing resonance of the print head is easily excited by the impulse disturbance, and is not quickly damped out This is a result of the inherently low mechanical damping in the system and the inability to use significant derivative action in the controller. The slow return to steady state is from the weak integral term, but this cannot be much increased without more damping.

In order to better understand the slewing mode, a spectral analysis was performed. Figure 5.8 shows the Fourier analysis of both the print head displacement and the print head slew angle.

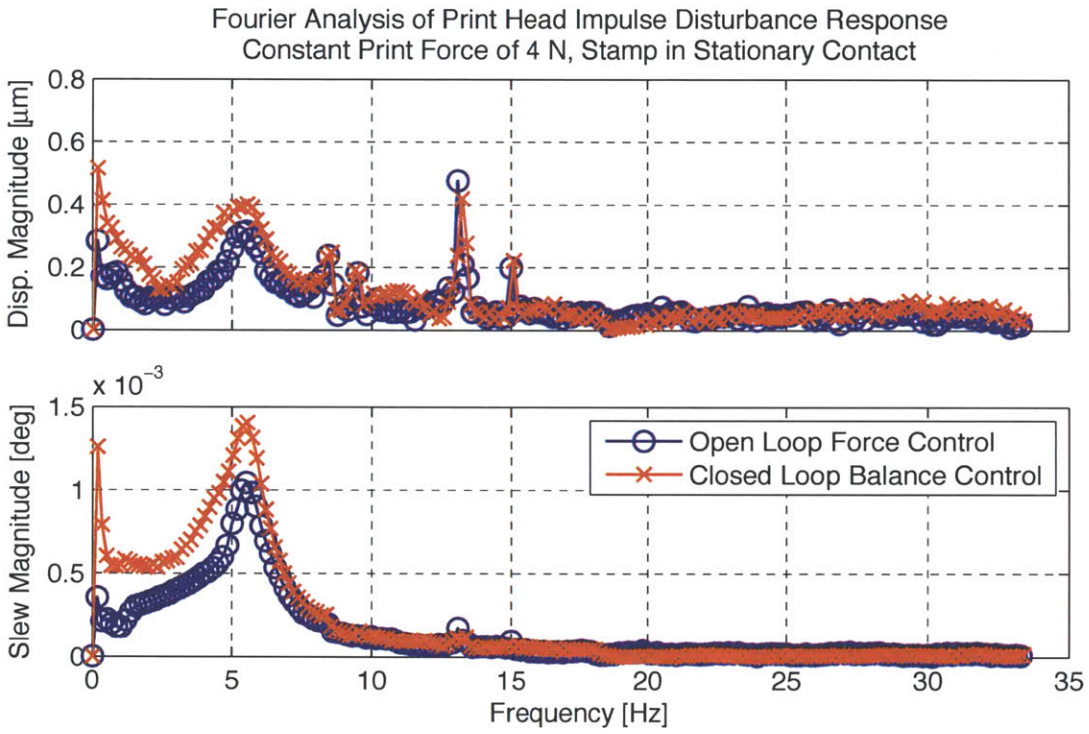

Figure 5.8: Stamp balance controller disturbance response: The spectral analysis of the print head's angular ψ movement in the bottom plot shows the slewing mode resonance at 5.5 Hz. The top plot shows the spectral analysis of the y direction movement, with resonances at 13 Hz and 15 Hz. The source of these y direction resonances is unknown.

The purpose of the balance controller is to enable an evenly balanced pressure during printing. The balance controller is intended to work while the stamp is in rolling contact. For the ideal case, the mechanics of balance for rolling contact are the same as for stationary contact. However, the stamp has been found to have various deformations and eccentricities, so the balance controller will have to actively work to cancel these out while in rolling contact.

The balance controller has been tested in direct contact with the rotating impression cylinder for equivalent web speeds between 0.125 in/s and 1 in/s. In this range, it is able to noticeably decrease the amount of variation in balance compared to trials with the controller disabled. As well, the balance controller ensures little mean error. One of the rolling contact trials is shown in Figure 5.9.

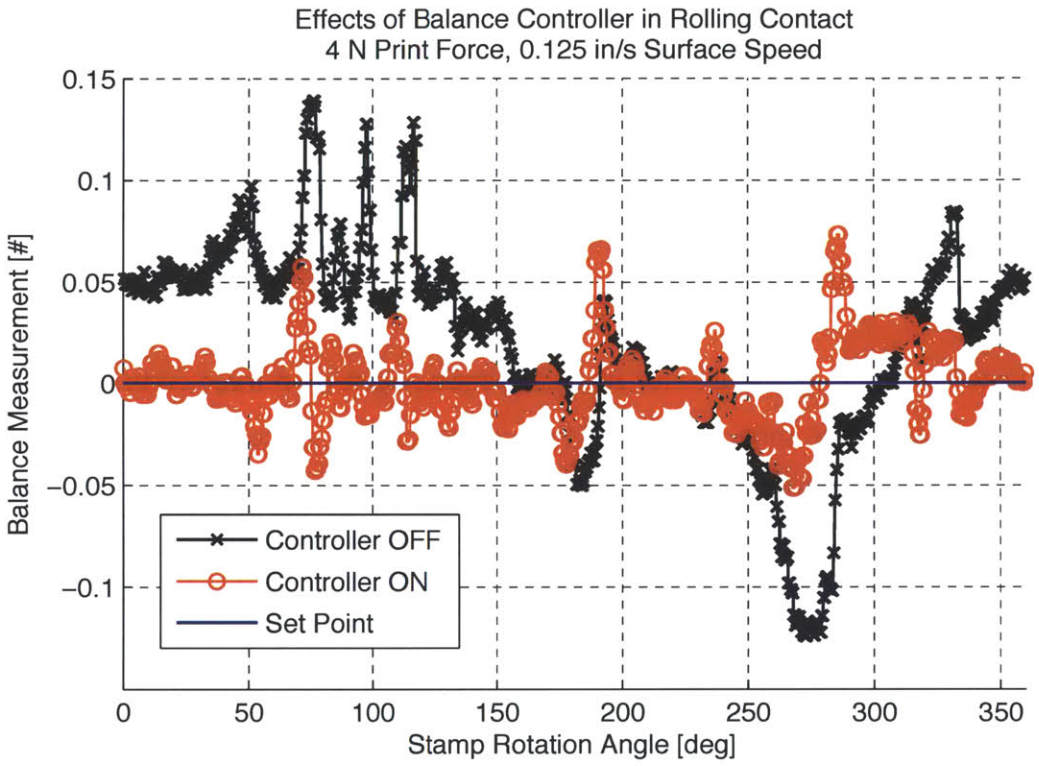

Figure 5.9: Stamp balance controller: The balance controller is tested in the case of rolling contact. A featureless cylindrical stamp was pressed directly against the impression cylinder with a constant print force of 4 N. The balance was measured for one full rotation with the balance controller disabled and for one full rotation with the balance controller enabled. The use of the balance controller is shown to help the print head compensate for disturbances and track the set point of zero, which is an evenly balanced stamp. The standard deviation of balance without controller is 0.050, while the use of the controller decreases it to 0.019. The mean error without the controller is 0.021, while the controller brings the mean error to just 0.001. However, a statistical analysis for significance was not performed.

Though a test for statistical significance was not performed, the balance controller appears to compensate for disturbances and stamp deformations in rolling contact at low web speeds. There is a repeatable improvement in both the standard deviation of balance and the mean error from

the set point for web speeds up to 1 in/s. At higher speeds, the frequency content of disturbances due to the rolling stamp contact is too high for the controller to successfully compensate for. The standard deviation of balance in the 1 in/s to 4 in/s web speed trials is not better with the controller enabled than with it disabled. However, even at these higher speeds, the use of the controller still results in better tracking of the set point, and therefore a lower mean error.

The ability of the controller to keep the print head balanced while running a web will be critical to the success of continuous high-rate microcontact printing. Though tested only with an unfeatured stamp, the controller is expected to work with stamps of most any geometry, so long as the features are mostly symmetrically distributed about the center.

5.3 Contact Control

For an unfeatured stamp in the absence of disturbances, open-loop force control will suffice in achieving consistent print force. With the balance controller successfully implemented, it is possible to ensure that this print force is evenly distributed along the width of the contact region. However, these controllers do not allow for the determination of print pressure. For a featured stamp with varying geometry along its circumference, or in the case of an eccentric stamp and other unexpected disturbances, the success of a precision printing process will depend on the ability of the controller to actively maintain the ideal contact pressure.

5.3.1 Sensor Design

The contact controller, like the balance controller, is designed around the feedback from the visual inspection technique. The camera is used to measure the stamp-substrate contact length. This is possible because the region of contact between the stamp and the substrate fluoresces brightly. Using an edge-finding algorithm to determine the position of the high-contrast horizontal edges of the stamp contact, it is possible to measure the distance between them. This distance is the contact length. The sensor measurements are all done in camera pixels, but a printed scale was used to calibrate the sensor to output the measured contact length in mm. More details on the image processing algorithms used to determine the contact length measurement are found in [40].

The relationship between print head displacement and stamp contact length is a function of contact mechanics. The roll-to-roll contact model developed in 4.2 is not found to accurately describe the observed behavior. This is likely due to the non-linear effects of the high surface energy of the PDMS stamp and the resulting significant work of adhesion. Though a model should be developed to describe this behavior, it is possible to use empirical data from the experimental setup to determine how contact length scales with print head displacement. A quasi-static force ramp was used to determine this relationship, and is shown in Figure 5.10.

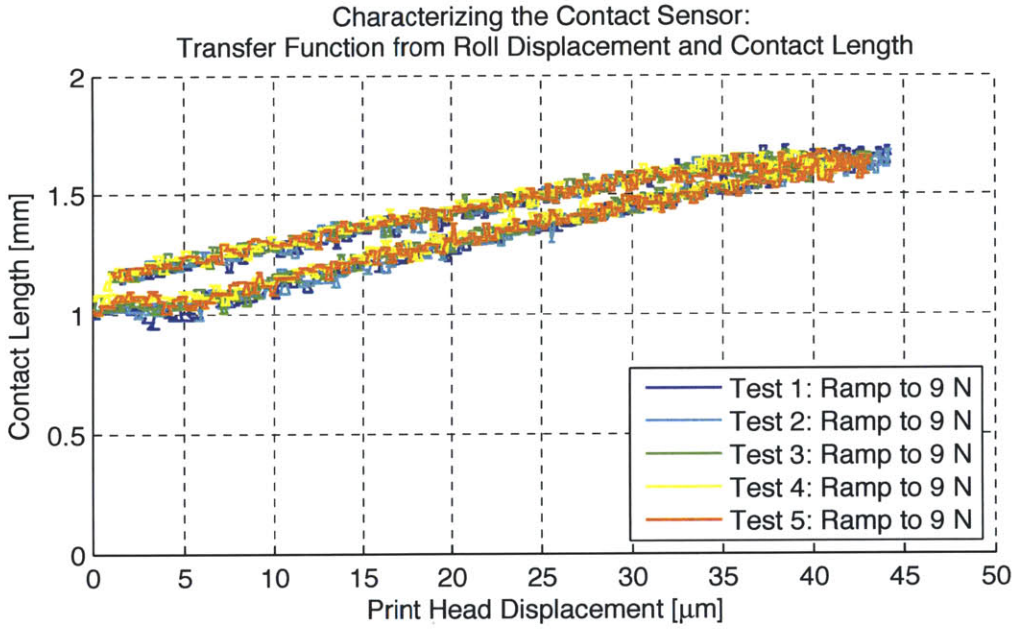

Figure 5.10: Stamp contact controller: A force ramp was used to characterize the relationship between print head displacement and stamp-substrate contact length. Note that even at zero measured print roll displacement, there is a significant measurable contact length of nearly 1 mm. This is likely due to the high surface energy of the stamp, as it naturally snaps down to the substrate surface even in the absence of external forces.

The transfer function from print head displacement to stamp contact length shows hysteresis, but is very linear. The dynamics of the stamp are expected to be much faster than the controller bandwidth, so the stamp behavior can be modeled as a simple gain of 0.0153 mm of contact length per micron of print head displacement.

The contact length sensor calculations are computed at the 10 Hz camera frame rate. Because this is an order of magnitude faster than the controllable 1 Hz operating range, the sensor is not

modeled to have any dynamics. As detailed in [40], the contact length sensor's pixel measurements are calibrated and reported in mm contact length, so the sensor appears as simply a unity gain in the system block diagram shown in Figure 5.11.

5.3.2 Controller Design

Inspired by the successful results of the balance controller, the contact controller was implemented in much the same manner. The block diagram for the system is shown in Figure 5.11.

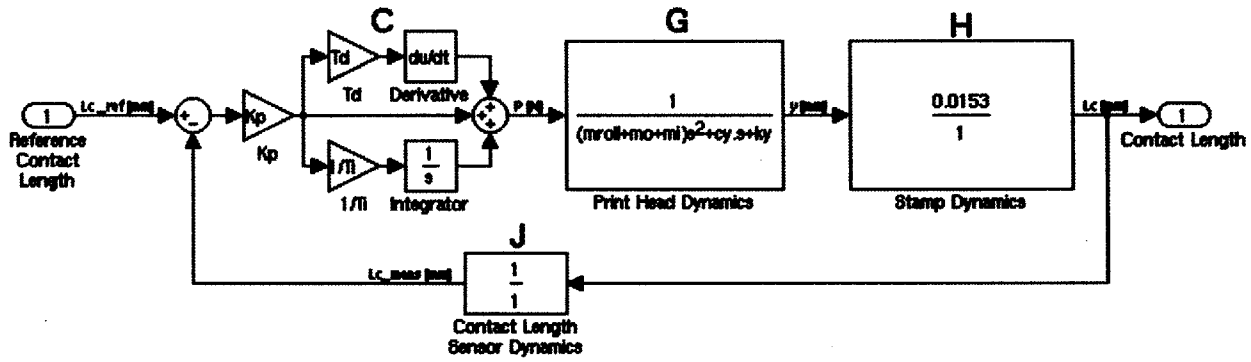

Figure 5.11: Stamp contact controller: Block diagram of the system

A discrete implementation of a PID controller was coded in LabView. The controller was manually tuned, loosely based on the method of Ziegler-Nichols [43]. The noise in the contact-length measurement is amplified by the derivative term, so the majority of the control effort is dominated by the proportional and integral gains. A robust, stable controller was achieved with gains of $K_p = 20$, $T_d = 0.01$, $T_i = 1$.

5.3.3 Performance

The contact controller is independent of the balance controller. However, it operates best when the balance controller is also enabled in parallel. This is because of the way the contact sensing algorithm was developed, as it relies on an evenly balanced stamp to perform the horizontal edge finding. As well, the contact controller works best when the balance controller is also running because these two degrees of freedom are not entirely decoupled like the simplified 2-D.O.F. print head model suggests. Rather, changes in print force and contact length are seen to effect

changes in the balance of the print head. Eventually, a MIMO controller will have to be designed to be able to properly control for this behavior, as the two independent SISO controllers are found to sometimes interact with each other, resulting in sub-optimal performance.

The print head is shown to be able to control for a wide range of contact length set points, though it is difficult to maintain a contact length of less than 0.5 mm, as the high surface energy of the PDMS causes snap-down adhesion of the stamp to the impression cylinder.

The controller is stable and robust to moderate disturbances. Shown in Figure 5.12 is the response to a step in commanded contact length.

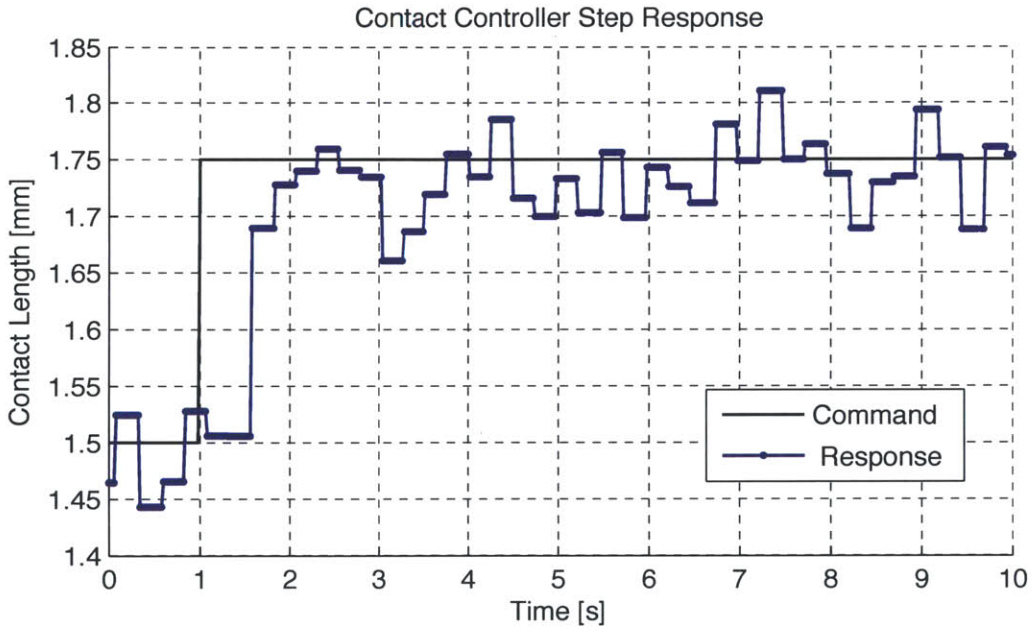

Figure 5.12: Stamp contact controller: Shown is the contact controller's response to a 0.25 mm step in reference command. The significant noise makes accurate measurement difficult, but the rise time appears to be on the order of 1.5 seconds. The controller exhibits little if any overshoot.

With a faster frame-rate camera, the contact controller's slow rise time of about 1.5 seconds could be improved. As well, a lower noise measurement of contact length would allow for a more aggressive controller to be tuned, due to the increased ability to rely on the derivative term.

The contact controller was tested with both a stationary impression cylinder and one moving at equivalent web speeds of 0.12 in/s to 0.5 in/s. The trials at slower surface speeds showed the

controller's ability to improve the consistency of contact. Figure 5.13 shows these effects in a rolling contact experiment, though the results were not analyzed for significance using statistical methods.

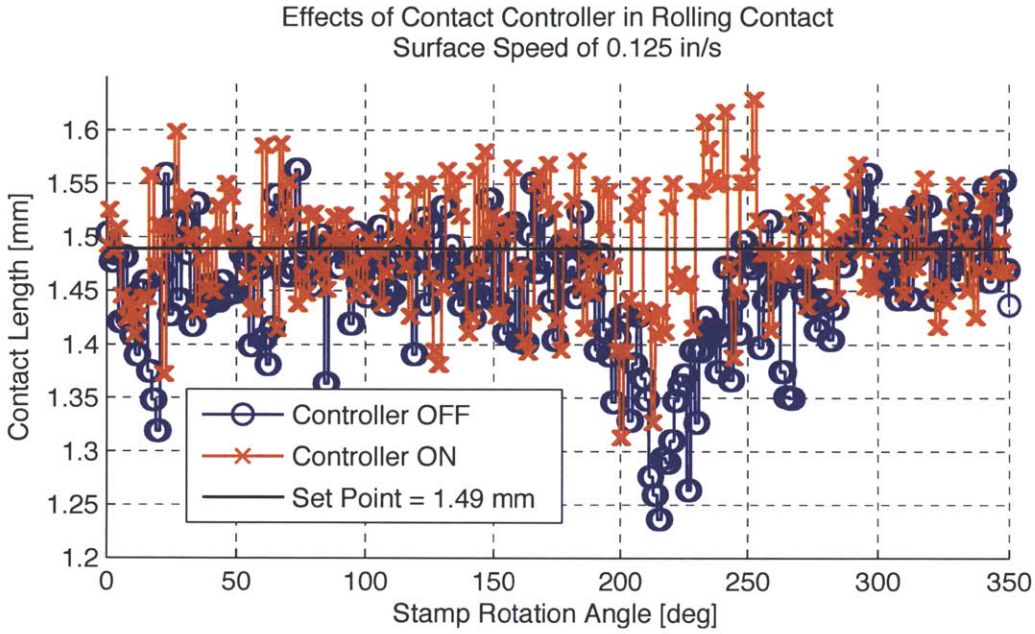

Figure 5.13: Stamp contact controller: The stamp is brought into contact with the impression cylinder, rotating at a surface speed of 0.125 in/s. The trial with the controller disabled shows a significant disturbance at the 220 degree mark in the stamp's rotation, probably due to a stamp deformation. The measurement of contact length for the trial with the enabled contact controller does not show this same dip, though, as the contact controller is able to compensate for it and maintain a more consistent contact pressure.

Though the controller is shown to compensate for disturbances at web speeds of 0.125 in/s to 0.25 in/s, it is not effective at higher speeds, for which the frequency content of the disturbances is on the order of the controller's bandwidth. In order to allow for faster web speeds, the controller bandwidth must be increased. With a fast enough camera and the use of a real-time controller or FPGA, it is conceivable that such a contact controller could be used to achieve consistent print pressure and conformal contact for web speeds of many feet per second.

CHAPTER

6

CONCLUSION

This thesis details the creation of a precision controllable machine for roll-to-roll microcontact printing. This pilot machine serves as the test bed for researching how microcontact printing can be developed into a high-rate manufacturing process with the ability to print micron-scale features onto flexible substrates at web speeds of meters per second.

6.1 Contributions

The focus of this thesis was on the design of a precision roll-to-roll microcontact printing machine and the control of that machine. Specifically, special consideration was given to the design and control of the print head. The precision of the print head's movement and actuation is critical to the success of the roll-to-roll microcontact printing process, so a near-frictionless high-bandwidth controllable positioning stage was designed. Two control schemes for regulating stamp contact pressure were demonstrated. The open-loop force controller allows for setting a constant force on the print head, while a closed-loop controller was developed around real-time *in-situ* contact visualization and control of the print pressure. Such a control architecture shows promise for being able to adjust the force on the print head in order to compensate for eccentricities and disturbances in the system. This was demonstrated at web speeds of up to 1 in/s, with disturbances of frequency content up to 1 Hz. The print head has the mechanical bandwidth, however, to track disturbances of 50 μm amplitude at up to 50 Hz, which could potentially be achieved if the system is upgraded with a faster frame-rate camera and real time controller or FPGA.

As well, a model of the roll-to-roll contact mechanics of the stamp was developed and shown to accurately describe the stamp behavior. This use and further development of this model will be instrumental in the ability to design a controller that is able to compensate for disturbances in the

system. A robust controller will prove to be crucial as printing speeds are scaled up to many feet per second.

6.2 Next Steps

In this thesis, a pilot-scale machine was used to show the potential for precision roll-to-roll microcontact printing and a novel form of process control was demonstrated. However, this is just the starting point; there is still much research to be done. In order to successfully scale this process into a large-area high-rate manufacturing method, there needs to be a better understanding of the factors at play. Though this thesis was largely empirical, the ability to scale up microcontact printing is contingent upon the development of an accurate model of the roll-to-roll contact mechanics. This research machine will help to validate such a model, which will eventually serve to guide the design of the cylindrical stamps and future iterations of the printing machine. As well, with a better understanding of the print interaction and contact mechanics, a more effective controller can be designed. Because of the sensitive nature of PDMS stamps with micron-sized features, the development of a robust contact controller will also be critical to the success of the manufacturing method.

The roll-to-roll printing machine detailed in this thesis will serve as the platform for this further research. It was designed to allow for many future experiments, modifications, and additions. As the printing process is better understood, individual components can be changed or upgraded to suit the needs of the researcher. For example, it has become clear through the experiments in this research that the bandwidth of the controller needs to be improved. Currently, this is limited by both the contact sensing camera's 10 Hz frame-rate and the speed of Labview's software-timed loops. A faster frame-rate camera, in conjunction with a real time controller, will enable the balance and contact controllers to more quickly respond to disturbances and keep constant contact pressure even at higher web speeds.

6.3 Future Challenges

It will be a challenge to successfully achieve continuous microcontact printing on meter-wide webs at meters-per-second web speeds, due to the fundamental scale of the problem. Trying to print features that are only microns wide or tall over the entire width of a meter-wide web is a

challenge that scales six orders of magnitude. In order to achieve such a feat, the components, sensors, and actuators of the full-scale machine must be precise enough to maintain the ideal contact pressure within an incredibly narrow process window. Research into how this process window may be expanded is presented in Petrzelka's thesis [19]. Further research into how to make the microcontact printing more robust will help improve the odds that it can be turned into a real manufacturing method.

6.4 Outlook

There are many emerging technologies, such as flexible electronic displays, that require high-speed, high-resolution, and large-area patterning. Current forms of press printing and nanofab are not suited to the manufacturing needs of these new devices. If production of these devices is to ramp up to meet the expected demand in the near future, new manufacturing processes must be developed. Microcontact printing is one of these promising methods that could help to enable the high-speed and economic manufacturing of devices that require large-area, high-resolution patterning. There are still many challenges that must be addressed before the process can be performed at this scale, but with the right research, it can be achieved. It is my hope that the pilot-scale machine designed in this thesis will be used by future researchers to investigate and tackle those challenges in the effort to prove microcontact printing as a viable manufacturing process.

REFERENCES

[1] A. Kumar and G. Whitesides, "Features of Gold Having Micrometer to Centimeter Dimensions Can Be Formed Through a Combination of Stamping with an Elastomeric Stamp and an Alkanethiol Ink Followed by Chemical Etching," *Appl. Phys. Lett.*, vol. 63, no. 14, pp. 2002–2004, Oct. 1993.

[2] A. Kumar, H. A. Biebuyck, and G. M. Whitesides, "Patterning Self-Assembled Monolayers: Applications in Materials Science," *Langmuir*, vol. 10, no. 5, pp. 1498–1511, May 1994.

[3] H. A. Biebuyck, N. B. Larsen, E. Delamarche, and B. Michel, "Lithography beyond light: Microcontact printing with monolayer resists," *IBM J. Res. Dev.*, vol. 41, no. 1.2, pp. 159–170, Jan. 1997.

[4] A. Perl, D. N. Reinhoudt, and J. Huskens, "Microcontact Printing: Limitations and Achievements," *Adv. Mater.*, vol. 21, no. 22, pp. 2257–2268, 2009.

[5] A. P. Quist, E. Pavlovic, and S. Oscarsson, "Recent advances in microcontact printing," *Anal. Bioanal. Chem.*, vol. 381, no. 3, pp. 591–600, Feb. 2005.

[6] C. D. Bain, E. B. Troughton, Y. T. Tao, J. Evall, G. M. Whitesides, and R. G. Nuzzo, "Formation of monolayer films by the spontaneous assembly of organic thiols from solution onto gold," *J. Am. Chem. Soc.*, vol. 111, no. 1, pp. 321–335, Jan. 1989.

[7] J. A. Helmuth, H. Schmid, R. Stutz, A. Stemmer, and H. Wolf, "High-Speed Microcontact Printing," *J. Am. Chem. Soc.*, vol. 128, no. 29, pp. 9296–9297, Jul. 2006.

[8] T. E. Balmer, H. Schmid, R. Stutz, E. Delamarche, B. Michel, N. D. Spencer, and H. Wolf, "Diffusion of Alkanethiols in PDMS and Its Implications on Microcontact Printing (μCP)," *Langmuir*, vol. 21, no. 2, pp. 622–632, Jan. 2005.

[9] M. Geissler, H. Wolf, R. Stutz, E. Delamarche, U.-W. Grummt, B. Michel, and A. Bietsch, "Fabrication of Metal Nanowires Using Microcontact Printing," *Langmuir*, vol. 19, no. 15, pp. 6301–6311, Jul. 2003.

[10] A. G. Lopez and H. G. Craighead, "Subwavelength Surface-Relief Gratings Fabricated by Microcontact Printing of Self-Assembled Monolayers," *Appl. Opt.*, vol. 40, no. 13, pp. 2068–2075, May 2001.

[11] E. Delamarche, J. Vichiconti, S. A. Hall, M. Geissler, W. Graham, B. Michel, and R. Nunes, "Electroless Deposition of Cu on Glass and Patterning with Microcontact Printing," *Langmuir*, vol. 19, no. 17, pp. 6567–6569, Aug. 2003.

[12] N. L. Jeon, R. G. Nuzzo, Y. Xia, M. Mrksich, and G. M. Whitesides, "Patterned self-assembled monolayers formed by microcontact printing direct selective metalization by chemical vapor deposition on planar and nonplanar substrates," *Langmuir*, vol. 11, no. 8, pp. 3024–3026, Aug. 1995.

[13] Tae Hyun Park, Young Min Kim, Young Wook Park, Jin Hwan Choi, Jin-Wook Jeong, Kyung Cheol Choi, and Byeong-Kwon Ju, "Self-assembled microarray of organic light-emitting diodes using a self-assembled monolayer by microcontact printing," *Appl. Phys. Lett.*, vol. 95, no. 11, p. 113310, Sep. 2009.

[14] L. B. Goetting, T. Deng, and G. M. Whitesides, "Microcontact Printing of Alkanephosphonic Acids on Aluminum: Pattern Transfer by Wet Chemical Etching," *Langmuir*, vol. 15, no. 4, pp. 1182–1191, Feb. 1999.

[15] A. G. Koutsioubas, N. Spiliopoulos, D. L. Anastassopoulos, A. A. Vradis, and G. D. Priftis, "Formation of alkane-phosphonic acid self-assembled monolayers on alumina: an in situ SPR study," *Surf. Interface Anal.*, vol. 41, no. 11, pp. 897–903, Nov. 2009.
[16] J. C. Love, L. A. Estroff, J. K. Kriebel, R. G. Nuzzo, and G. M. Whitesides, "Self-Assembled Monolayers of Thiolates on Metals as a Form of Nanotechnology," *Chem. Rev.*, vol. 105, no. 4, pp. 1103–1170, Apr. 2005.
[17] T. Kaufmann and B. J. Ravoo, "Stamps, inks and substrates: polymers in microcontact printing," *Polym. Chem.*, vol. 1, no. 4, pp. 371–387, May 2010.
[18] M. Hale, *Manufacturing conductive patterns on polymeric substrates : development of a microcontact printing process / by Melinda Hale.* c2013., 2013.
[19] J. E. Petrzelka, *Contact region fidelity, sensitivity, and control in roll-based soft lithography / by Joseph Edward Petrzelka.* c2012., 2012.
[20] C. Y. Hui, A. Jagota, Y. Y. Lin, and E. J. Kramer, "Constraints on Microcontact Printing Imposed by Stamp Deformation," *Langmuir*, vol. 18, no. 4, pp. 1394–1407, Feb. 2002.
[21] J. N. Lee, C. Park, and G. M. Whitesides, "Solvent Compatibility of Poly(dimethylsiloxane)-Based Microfluidic Devices," *Anal. Chem.*, vol. 75, no. 23, pp. 6544–6554, Dec. 2003.
[22] Y. Xia, D. Qin, and G. M. Whitesides, "Microcontact printing with a cylindrical rolling stamp: A practical step toward automatic manufacturing of patterns with submicrometer-sized features," *Adv. Mater.*, vol. 8, no. 12, pp. 1015–1017, 1996.
[23] J. A. Rogers, Z. Bao, A. Makhija, and P. Braun, "Printing Process Suitable for Reel-to-Reel Production of High-Performance Organic Transistors and Circuits," *Adv. Mater.*, vol. 11, no. 9, pp. 741–745, Jun. 1999.
[24] Z. Bao, A. Makhjita, and J. A. Rogers, "High-resolution method for patterning a substrate with micro-printing," US6736985 B1, 18-May-2004.
[25] H. H. Lee, E. Menard, N. G. Tassi, J. A. Rogers, and G. B. Blanchet, "Large Area Microcontact Printing Presses for Plastic Electronics," *MRS Online Proc. Libr.*, vol. 846, p. null–null, 2004.
[26] A. Stagnaro, *Design and development of a roll-to-roll machine for continuous high-speed microcontact printing / by Adam Stagnaro.* c2008., 2008.
[27] C. A. Datar, *Design and development of high precision elastomeric-stamp wrapping system for roll-to-roll multi-layer microcontact printing / by Charudatta Achyut Datar.* c2009., 2009.
[28] E. Delamarche, H. Schmid, B. Michel, and H. Biebuyck, "Stability of molded polydimethylsiloxane microstructures," *Adv. Mater.*, vol. 9, no. 9, pp. 741–746, Jan. 1997.
[29] P. Roca-Cusachs, F. Rico, E. Martínez, J. Toset, R. Farré, and D. Navajas, "Stability of Microfabricated High Aspect Ratio Structures in Poly(dimethylsiloxane)," *Langmuir*, vol. 21, no. 12, pp. 5542–5548, Jun. 2005.
[30] K. G. Sharp, G. S. Blackman, N. J. Glassmaker, A. Jagota, and C.-Y. Hui, "Effect of Stamp Deformation on the Quality of Microcontact Printing: Theory and Experiment," *Langmuir*, vol. 20, no. 15, pp. 6430–6438, Jul. 2004.
[31] H. Schmid and B. Michel, "Siloxane Polymers for High-Resolution, High-Accuracy Soft Lithography," *Macromolecules*, vol. 33, no. 8, pp. 3042–3049, Apr. 2000.
[32] K. M. Choi and J. A. Rogers, "A Photocurable Poly(dimethylsiloxane) Chemistry Designed for Soft Lithographic Molding and Printing in the Nanometer Regime," *J. Am. Chem. Soc.*, vol. 125, no. 14, pp. 4060–4061, Apr. 2003.

[33] D. Trimbach, K. Feldman, N. D. Spencer, D. J. Broer, and C. W. M. Bastiaansen, "Block Copolymer Thermoplastic Elastomers for Microcontact Printing," *Langmuir*, vol. 19, no. 26, pp. 10957–10961, Dec. 2003.
[34] A. M. Kendale, *Automation of soft lithographic microcontact printing / by Amar Maruti Kendale*. c2002., 2002.
[35] T. Burgin, V.-E. Choong, and G. Maracas, "Large Area Submicrometer Contact Printing Using a Contact Aligner," *Langmuir*, vol. 16, no. 12, pp. 5371–5375, Jun. 2000.
[36] A. M. Kendale and D. L. Trumper, "Microcontact printing," US7665983 B2, 23-Feb-2010.
[37] A. M. Kendale and D. L. Trumper, "Microcontact printing," US7117790 B2, 10-Oct-2006.
[38] P. Baldesi, *Design and development of high precision five-axis positioning system for roll-to-roll multi-layer microcontact printing / by Paolo Baldesi*. c2009., 2009.
[39] C. Acar and A. Shkel, *MEMS Vibratory Gyroscopes: Structural Approaches to Improve Robustness*. Springer, 2008.
[40] S. Nill, "Integrated Hardware, Software, and Sensor Design for Control of a Scalable, Continuous Roll-to-Roll Microcontact Printing Process," Master of Science, Massachusetts Institute of Technology, Cambridge, MA, 2014.
[41] J. John, Y. Tang, J. P. Rothstein, J. J. Watkins, and K. R. Carter, "Large-area, continuous roll-to-roll nanoimprinting with PFPE composite molds," *Nanotechnology*, vol. 24, no. 50, p. 505307, Dec. 2013.
[42] L. Nietner, "A Direct-Write Thick-Film Lithography Process for Multi-Parameter Control of Tooling in Continuous Roll-to-Roll Microcontact Printing," Master of Science, Massachusetts Institute of Technology, Cambridge, MA, 2014.
[43] G. F. Franklin, J. D. Powell, and A. Emami-Naeini, *Feedback Control of Dynamic Systems*, 6 edition. Upper Saddle River N.J.: Prentice Hall, 2009.